SYNTHESIS AND CHARACTERIZATION OF 10GDC, 10GDC/CeO_2, 10GDC/Y_2O_3 AND 10GDC/Yb_2O_3 COMPOSITES

by

ŞÜKRÜ CEYLAN

THESIS SUBMITTED TO
THE GRADUATE SCHOOL OF NATURAL AND APPLIED SCIENCES
OF
THE ABANT İZZET BAYSAL UNIVERSITY
IN PARTIAL FULFILLMENT OF THE REQUIREMENTS FOR THE DEGREE
OF
MASTER OF SCIENCE
IN
THE DEPARTMENT OF CHEMISTRY

APRIL 2014

Approval of the Graduate School of Natural and Applied Sciences

Prof. Dr. Yaşar DÜRÜST
Director

I certify that this thesis satisfies all the requirements as a thesis for the degree of Master of Science.

Prof. Dr. Nedime DÜRÜST
Head of Department

This is to certify that we have read this thesis and that in our opinion it is fully adequate, in scope and quality, as a thesis for the degree of Master of Science.

Prof. Dr. Ayşe MORKAN
Supervisor

Prof. Dr. Aivaras Kareiva
Co-supervisor

Examining Committee Members

1- Prof. Dr. Ayşe MORKAN .....

2- Prof. Dr. Ceyhan KAYRAN .....

3- Assist. Prof. Dr. Bahadır ALTINTAŞ .....

ABSTRACT

SYNTHESIS AND CHARACTERIZATION OF 10GDC, 10GDC/CeO_2, 10GDC/Y_2O_3 AND 10GDC/Yb_2O_3 COMPOSITES

CEYLAN, Şükrü
Master of Science, Department of Chemistry
Supervisor: Prof. Dr. Ayşe MORKAN
Co-Supervisor: Prof. Dr. Aivaras Kareiva

April 2014, 95 pages

In this study, 10 mol % gadolinium doped ceria was taken as a basic compound and new compositions with additional amounts of CeO_2, Y_2O_3 and Yb_2O_3 in various ratios were prepared using sol-gel combustion synthesis technique. For comparison, all compounds were also synthesized by solid state reaction method. The annealing conditions (temperature and heating time) were identical for both synthesis routes.

For the characterization of synthesized products, infrared (IR) spectroscopy, X-ray powder diffraction (XRD), energy-dispersive X-ray spectroscopy (EDX) and scanning electron microscopy (SEM) were used. It was demonstrated that single-phase compounds synthesized by sol-gel combustion technique were obtained

independent on the amount of CeO_2, Y_2O_3 and Yb_2O_3 while in the case of solid-state reaction synthesis route the mixture of oxides was obtained.

IR results showed that the final products of the sol-gel combustion technique after heating at 800 ^oC have identical bands compared to each other and rare earth oxides. XRD results showed that the sol-gel combustion products were single phase compounds with no additional phase; however, the solid state products have additional diffraction lines belonging to Gd_2O_3, Y_2O_3 and Yb_2O_3. SEM results showed that the morphology of particles does not depend on the nature and amount of addition of rare-earth oxide. EDX results were in a good agreement with nominal compositions of elements.

Keywords: GDC, fuel cells, composite, sol-gel, solid state.

ÖZET

10GDC, 10GDC/CeO_2, 10GDC/Y_2O_3 VE 10GDC/Yb_2O_3 KOMPOZİTLERİNİN SENTEZİ VE KARAKTERİZASYONU

CEYLAN, Şükrü
Yüksek Lisans, Kimya Bölümü
Tez Danışmanı: Prof. Dr. Ayşe MORKAN
Yardımcı Tez Danışmanı: Prof. Dr. Aivaras KAREIVA

Nisan 2014, 95 sayfa

Bu çalışmada, %10 mol Gadolinyum katkılanmış seryum temel bileşik olarak saptanmış ve bunun değişen oranlarda ek miktarda CeO_2, Y_2O_3 ve Yb_2O_3 eklenmesiyle oluşan kompozitleri, Sol-Jel Yakma Sentez tekniğiyle hazırlanmıştır. Karşılaştırma yapmak amacıyla, tüm bu bileşikler ayrıca katı hal sentez yoluyla da elde edilmiştir. Tavlama koşulları (sıcaklık ve ısıtma süresi) iki sentez yöntemi için de aynıdır.

Sentezlenen örneklerin karakterizasyonu için Kızılötesi spektrumu (FTIR), X-ışını toz kırınımı (XRD), Enerji dağılımlı X-ışını spektrumu (EDX) ve Tarama

elektron mikroskobu (SEM) teknikleri kullanılmıştır. Yapılan analizler sol-jel tekniğiyle hazırlanan bileşiklerin tek faz bileşik olduğu ve eklenen CeO_2, Y_2O_3 ve Yb_2O_3 miktarına bağlı olmadığı, ancak katı hal tekniğiyle oksit karışımı elde edildiği görülmüştür.

IR çalışmaları, sol jel tekniğiyle sentezlenen ürünlerin 800 ^oC sıcaklıkta ısıtılmalarından sonra elde edilen kızılötesi spektrumlarının diğerleriyle ve oksit karışıma ait olanlarla çok benzer sonuçlar verdiğini göstermiştir. XRD sonuçları sol-jel tekniğiyle hazırlanan örneklerin ek faz içermeyen tek-faz bileşikler olduğunu, ancak katı hal yöntemiyle sentezlenen örneklerin XRD spektrumlarında Gd_2O_3, Y_2O_3 ve Yb_2O_3 fazlarının da ayrıca bulunduğu görülmüştür. SEM sonuçları, parçacıkların morfolojik yapısının eklenen oksitlerin miktarına ya da yapısına bağlı olmadığı görülmüştür. EDX sonuçları, elementlerin sayısal bileşimini doğrular niteliktedir.

Anahtar Kelimeler: GDC, yakıt hücreleri, kompozit, sol-jel, katı hal

ACKNOWLEDGEMENTS

I would like to express my deepest gratitude to Professor Ayşe MORKAN, my supervisor, for her encouragement, professional guidance and helpful suggestions during the time of this study. I appreciate very much her decision as believing in me and always standing by my side.

I would also like to express my much gratitude to Professor Aivaras KAREIVA, my co-supervisor, and his PhD student Skirmante Butkute, my former lab-mate in Vilnius University Chemistry Department for their encouragements, providing me the required equipments and chemicals, and their contributions to my study during the time I studied in Vilnius University, Lithuania. His laboratory team has also helped me much and I appreciate their help too. I am also thankful to Erasmus Foundation for giving me the chance to study abroad.

I would like to thank to Rıdvan MENDİ, for his financial and and intellectual supports, believing in me all the time, and standing by my side.

Honorable mention goes to my parents, Sefer CEYLAN and Güler CEYLAN, my brothers and sisters, Zeynep CEYLAN, Hüseyin CEYLAN, Ali CEYLAN, Musa CEYLAN and Fatma CEYLAN, for their understandings and supports during the time I studied. I could not have done this study without the mentioned people above.

LIST OF ABBREVIATIONS

XRD	X-ray Powder Diffraction
FTIR	Fourier-Transform Infrared Spectroscopy
SEM	Scanning Electron Microscopy
EDX	Energy Dispersive X-ray Analysis
ICDD	International Centre For Diffraction Data
GDC	Gadolinia-Doped Ceria

TABLE OF CONTENTS

LIST OF TABLES

LIST OF FIGURES

CHAPTER I

INTRODUCTION

1.1. GENERAL REVIEW ON MATERIAL SCIENCE

Material science has always been one of the most important branches of science throughout the human history. In our everyday lives, we can see the influence of materials like housing, electronics, vehicles, clothing, food production etc. During the history, the production and improvement of materials have led to the advancement and development of societies. It starts from the first days of humans and still continues to develop.

In past, there were a few materials that humans could obtain naturally like wood, stone, clay, leather. As the time past, they started to discover ways to make new materials that had advanced advantages over the natural ones. Moreover, they also discovered that some materials can be processed by heat and additions of other materials to change its properties as desired. So lately scientist started to understand the chemical structures of materials and its dependence on the properties. That led scientists to discover thousands of materials needed for the specific uses like superconductors, very light aircraft body parts, etc [1].

1.1.1. Classification of Materials

Materials can be classified into 5 main groups as Metals (Alloys), Ceramics, Polymers, Semiconductors and Composites.

- **Metallic materials (Alloys)**

An alloy is a metal that contains addition of one or more metals or non-metals. Generally, metals have good electrical and thermal conductivity. Alloys have relatively higher strength, stiffness, ductility or formability. They are specifically useful in structural or strength-requiring applications such as conducting wires, structural steel parts for buildings, etc [2].

- **Ceramic materials**

A ceramic can be defined as an article or coating made of inorganic and non-metallic solid produced by heating at temperatures sufficient to cause sintering, solid-state reactions, bonding, or conversion partially or wholly to the glassy state. Ceramics are used in a wide range such as structural products, refractories, whitewares and technical products [3].

- **Polymeric materials**

The polymers are prepared by a process known as polymerization, involving the chemical combination of many small units known as monomers. Polymers are types of electrical and thermal insulators. They are used almost in all parts of our daily life as all kinds of plastics or plastic-containing-materials such as clothes, toys, car parts, etc [4].

- **Semiconductors**

A semiconductor is a material of which the electrical conductivity is between that of an insulator and a conductor. Semiconductors are usually used as transistors, diodes etc. [2].

- **Composites**

Composites are the materials that have the purpose of blending the properties of different materials. A good example for this kind of materials is fiberglass, which is made by dispersing glass fibers in a polymer matrix [2].

1.1.2. Composite Materials

A composite material can be defined as a combination of two or more materials that results in better properties than those of the individual components used alone. In contrast to metallic alloys, each material retains its separate chemical, physical, and mechanical properties. The two main constituents are a reinforcement and a matrix. The main advantages of composite materials are their high strength and stiffness, combined with low density, when compared with bulk materials, allowing for a weight reduction in the finished part.

The reinforcing phase provides the strength and stiffness. In most cases, the reinforcement is harder, stronger, and stiffer than the matrix. The reinforcement is usually a fiber or a particulate. Particulate composites have dimensions that are approximately equal in all directions. They may be spherical, platelets, or any other regular or irregular geometry. Particulate composites tend to be much weaker and less stiff than continuous fiber composites, but they are usually much less expensive.

Particulate reinforced composites usually contain less reinforcement (up to 40 to 50 volume percent) due to processing difficulties and brittleness. For electrolyte and electrode composites, reinforcing phase provides some of the followings: strength, stiffness, electronic conductivity, ionic conductivity, resistance to high temperatures, resistance to decomposition, etc.

The continuous phase is the matrix, which is a polymer, metal, or ceramic. Polymers have low strength and stiffness, metals have intermediate strength and stiffness but high ductility, and ceramics have high strength and stiffness but are brittle. The matrix (continuous phase) performs several critical functions, including maintaining the fibers in the proper orientation and spacing and protecting them from abrasion and the environment. In polymer and metal matrix composites that form a strong bond between the fiber and the matrix, the matrix transmits loads from the matrix to the fibers through shear loading at the interface. In ceramic matrix composites, the objective is often to increase the toughness rather than the strength and stiffness; therefore, a low interfacial strength bond is desirable [5].

1.2. FUEL CELLS

1.2.1. General Review of Fuel Cells

In 1962, there had been a revolution in the energy research. Westinghouse Electric Corporation scientists (now Siemens Westinghouse), for the first time, demonstrated the applicability of providing electricity from a device they called a "solid electrolyte fuel cell" [6]. From that time, there has been an intense interest in researching and development of fuel cell technology.

A fuel cell can be defined as a battery-like system that can convert the chemical energy of a fuel and an oxidant to electrical energy continuously by a process involving an essentially unvarying electrode-electrolyte system [7]. In Figure 1.1, the operation principle and the basic elements of a fuel cell with a proton-conducting electrolyte are depicted.

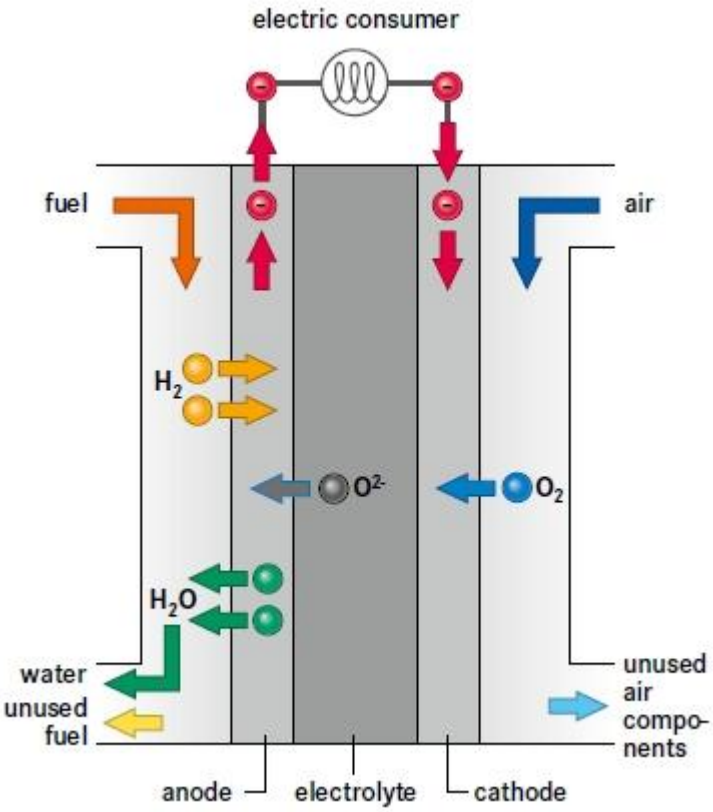

Figure 1.1 Operation principle of a fuel cell [8]

There are three main elements as the anode, the cathode and the electrolyte. H_2, as the fuel here, is provided to the anode so that the anode releases electrons as a result of being oxidized, and those electrons would perform the electrical work. Then the electrons pass to the cathode, leading to reduction of the oxygen into water at the electrode/electrolyte interface. The protons from the anode make it to the cathode

through the electrolyte medium. In order to be permeable to gas, both anode and cathode should be porous [9].

1.2.2. Types of Fuel Cells

Fuel cells can be classified according to the electrolyte used as ion conductor medium. Amongst those, Direct Methanol Fuel Cell (DMFC) is an exception being identified by the fuel used in it.

- **Alkaline Fuel Cells (AFC)**

The electrolyte in AFCs is an aqueous solution of potassium hydroxide (KOH). The ions carried by the alkaline electrolyte are OH^- forming water at the anode electrode. Although it has advantages like having a low cost electrolyte as KOH and being mechanically rechargeable, it has disadvantages like having pure H_2 as the only suitable fuel, and hydroxide electrolyte having great tendency to formation of carbonate ions from carbon dioxide. [10-11]

- **Proton Exchange Membrane Fuel Cells (PEMFC)**

PEMFCs use a polymer membrane, perfluorosulfonic acid, as the electrolyte, and because the electrolyte is an acid, hydrogen ions (H^+) are the ions that are transported in the process. Due to that fact, hydrogen is the fuel supplied to the system and oxygen or air is the oxidant.

PEMFCs have many disadvantages like requirement of expensive catalysts due to having acidic electrolyte. Also H_2O management at the polymer membrane is essential because the membrane should be humid in order to conduct ions [12]. Also

having high cost electrolyte and pure H_2 as a suitable fuel are the problems faced with PEMFCs [11].

- **Direct-Methanol Fuel Cells (DMFC)**

DMFCs use trifluoromethane sulfonic acid or a proton exchange membrane as electrolyte. Methanol is used as the fuel and directly supplied to the cell. It is advantageous that Methanol is liquid and can be stored and dispensed easily. However, DMFCs show lower efficiency in comparison with other fuel cells.

- **Phosphoric Acid Fuel Cells (PAFC)**

In PAFCs, phosphoric acid (H_3PO_4) is used as electrolyte in a liquid form. The electrolyte is acidic and conducts hydrogen ions. Despite having advantages like low operating temperature, low cost of the electrolyte and high fuel efficiency, it has disadvantages like electrode having low conductivity, high-cost catalysts, etc.

- **Molten Carbonate Fuel Cells (MCFC)**

In MCFCS, lithium potassium carbonate or lithium sodium carbonate are used to conduct carbonate (CO_3^{2-}) ions. CO_2 should be supplied at cathode to form CO_3^{2-} with oxygen. Catalysts in MCFC are low cost due to fast electron kinetics and low poisoning sensitivity. However, CO_2 supply needs a complex system and electrolyte is very sensitive to corrosion.

- **Solid Oxide Fuel Cells (SOFC)**

In SOFCs, a ceramic membrane is used for the conduction of ions at temperatures above 600 ^oC. There are two types of SOFC as intermediate temperature SOFC (IT-SOFC) and high temperature SOFC (HT-SOFC). IT-SOFCs

operate in the range of 600-800 ^{o}C, using ceria-doped rare earth (e.g. gadolinium) electrolytes. HT-SOFCs use yttrium stabilized zirconia (YSZ) and operate in the range of 1000-1200^{o}C.

HT-SOFC has the disadvantage of working at high temperature as the materials would degrade faster.

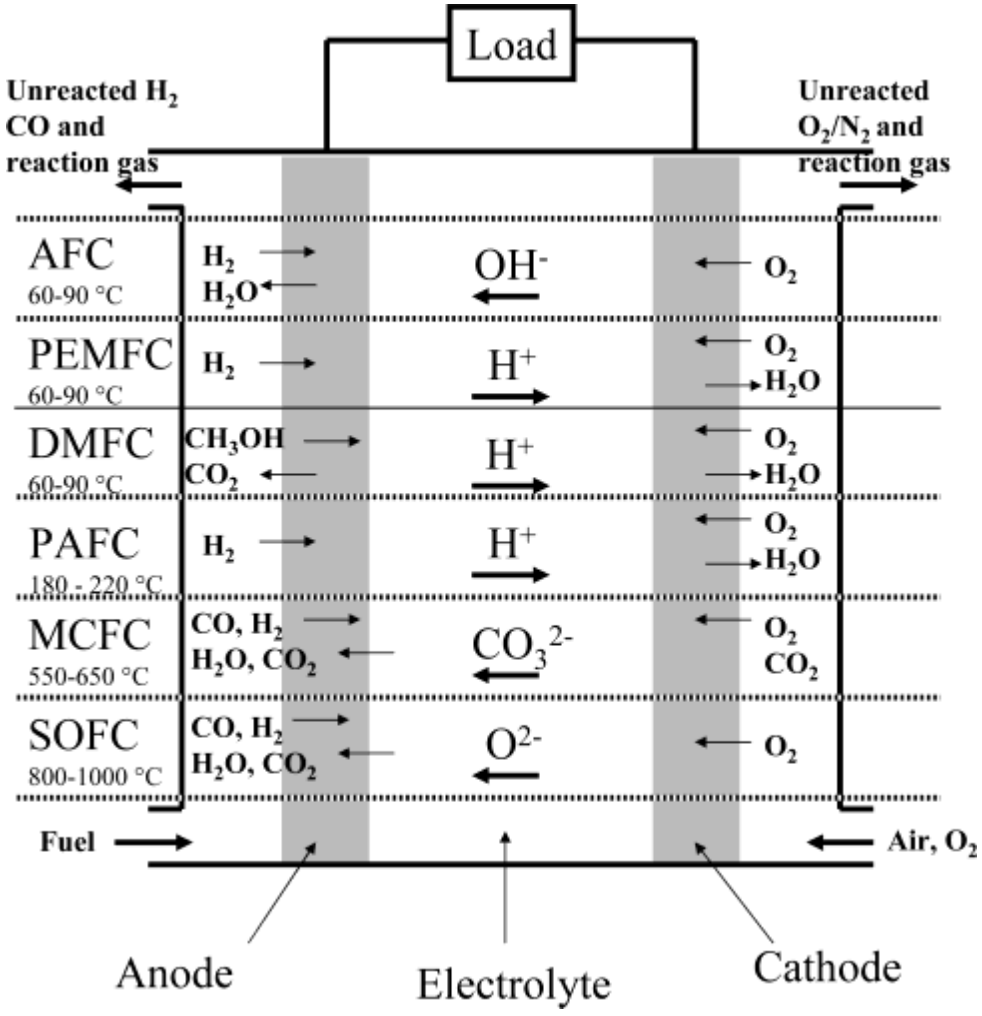

Figure 1.2 Summary of the operating temperatures, reactions and processes that occur in the various fuel cell systems [11]

1.2.3. Solid Oxide Fuel Cells

Due to the increase in energy usage demands in the world, it is necessary to find cleaner and more efficient energy resources to reduce the dependence in the

fossil fuels. Fuel Cells, especially “Solid Oxide Fuel Cells”, are one of the useful candidates for the solution of this issue as The Solid Oxide Fuel Cells are expected to supply a highly efficient power generator system for future applications [13-14].

A solid oxide fuel cell (SOFC) is an electrochemical energy conversion device that produces electricity directly from oxidizing a fuel. The principle of operation of a solid-oxide fuel cell (SOFC) is given in Figure 1.3. In a solid oxide fuel cell, oxygen ions react with the fuel, either hydrogen (H_2) or methane (CH_4), generating an electrical current (e) and minimal waste products (water and some CO_2) at the anode. Oxygen molecules are dissociated and charged, replenishing reacted oxygen ions at the anode through the electrolyte at the cathode [16].

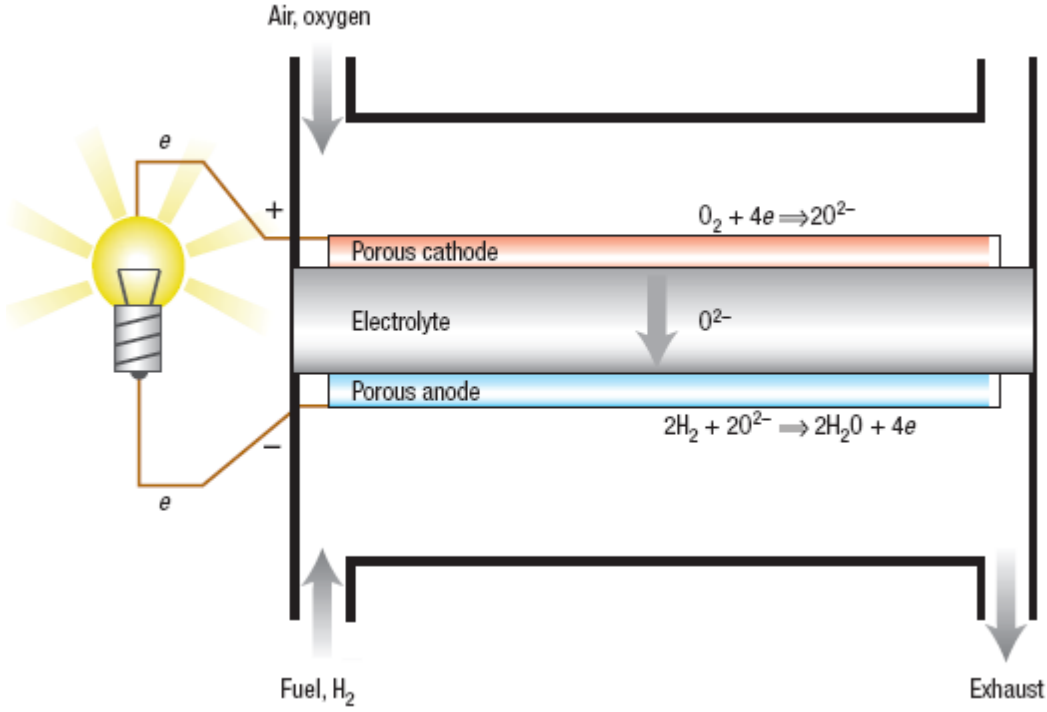

Figure 1.3 The schematic diagram of operation of a solid-oxide fuel cell (SOFC)

Fuel cells are characterized by their charge transfer mechanism; the SOFC has a solid oxide electrode-electrolyte assembly. Advantages of this class of fuel cells include high efficiency, long-term stability, fuel flexibility, low emissions, and relatively lower catalyst cost. The largest challenge is preserving oxide integrity and fuel cell lifetime due to mechanical and chemical compatibility issues. Also, the high operating temperature can increase startup times but also provides benefits of internal reforming and waste heat which can be utilized downstream [15].

"Yttria-stabilized-Zirconia" has been used as an electrolyte in SOFCs due to its ability of high amount of oxygen-ion conductivity and stability in both oxidizing and reducing atmospheres [17-20].

However, the operating temperature of YSZ is very high at around 1000 ^{o}C. Due to the high operating temperature, the cost of interconnect materials and the components needed for insulation is being so high and degradation of system occurs [21-22]. This problem can be overcome by reducing the operating temperature. This reducement improves the reliability, the life length of cell, reduces the cost, and gives a variety of choice of materials to be used [23].

CeO_2 is a rare-earth oxide with fluorite-type structure and well-known for having oxygen vacancies. Its oxygen vacancies can be modified by doping it with dopant ions so it can be used in variety of applications [24-27]. At this point, Gadolinia-doped-Ceria is one of the most promising materials for SOFC applications as oxygen-ion conducting electrolytes or electrodes at intermediate temperatures between 873-1073 K [28-29]. The crystal structure of Gadolinia Doped Ceria possesses the same fluorite structure as the stabilized zirconia but can be operated at lower temperatures for high oxygen-ion conductivity [30].

1.3. SOLID STATE & SOL-GEL COMBUSTION TECHNIQUES

1.3.1 Solid State Technique

Solid-state reaction technique is the most simple and common method used for the synthesis of ceramics in comparison with the other routes. In this synthesis route, oxide forms of metals are mixed and grinded together, and then heated to form the desired product. Although this method confronts some disadvantages, very high temperature (at around 500-2000 ^{o}C) is required and sometimes it may result in unwanted phases or compounds [31].

1.3.2 Sol-Gel Combustion Technique

In the Sol-Gel Combustion method, the precursor is prepared by dissolving salts of the metals as nitrates in small amount of distilled water and adding complexing agent. After that the solution is heated to evaporate the excess solvent. In sol-gel combustion synthesis, the exothermicity of the redox (reduction-oxidation or electron transfer) chemical reaction is used as driving force for material production. In a typical sol-gel combustion reaction, the precursor mixture of water, metal nitrates, and fuel dehydrates, decomposes and ruptures into a flame producing a voluminous, foamy powder. Then the powder is grinded, sintered, and then calcined to obtain the desired product [32]. Such powders are generally more homogeneous, having less impurities and higher surface areas than powders prepared by conventional solid-state methods. Due to these advantageous features and simplicity of preparation and equipments used, sol-gel combustion synthesis technique is an attractive method for manufacturing of these kinds of materials at lower costs compared to the other processes [33].

1.4. GDC and GDC COMPOSITES, CODOPINGS

1.4.1 GDC

Ceria based solid solutions have been used in a variety of applications such as oxygen sensors [34], exhaust catalysts [35] and electronics [36]. They also have been studied as possible electrolyte materials for usage in Intermediate-Temperature SOFCs (between 500 - 800 ^{o}C) extensively [37-40]. GDC, especially, have been particularly in interest as an alternative material for YSZ for its high ionic conductivity at low operating temperatures (at around 600 ^{o}C) [41].

For GDC, the composition for the optimum conductivity in reports is usually inconsistent, especially for 10% [30, 42], 15% [43-46], and 20% [47-51] Gd concentrations. Those differences on the results probably resulted from the differences in preparation methods and sintering temperatures. Moreover, impure composites indicate remarkable grain boundary resistivity, so purity of the product is also important.

The optimum ratio of Gd/Ce in GDC electrolyte is stated as 10% for IT-SOFC as shown in table below [30]. It is also reported that 10GDC shows better stability with respect to 20GDC at temperatures below 700 ^{o}C [52].

Table 1.1 Ionic Conductivity for selected electrolyte compositions

Composition	σ, 500^{o}C (S cm^{-1})	σ, 600^{o}C (S cm^{-1})	σ, 700^{o}C (S cm^{-1})
$Ce_{0.9}Gd_{0.1}O_{2-\delta}$	*0.0095*	*0.0253*	*0.0544*
$Ce_{0.9}Sm_{0.1}O_{2-\delta}$	*0.0030*	*0.0090*	*0.0200*
$Ce_{0.9}Y_{0.1}O_{2-\delta}$	*0.0087*	*0.0344*	*0.1015*
$Ce_{0.8}Gd_{0.2}O_{2-\delta}$	*0.0053*	*0.0180*	*0.0470*

Various synthesis methods for the preparation of doped ceria have been reported so far. $Ce_{1-x}Gd_xO_{2-x/2}$ (GDC) (x=0, 0.05, 0.10, 0.15, 0.20 and 0.25) have

been prepared by the oxalate co-precipitation route using cerium nitrate and gadolinium nitrate as starting materials [43]. The appropriate quantities of starting materials dissolved separately in water, mixed and co-precipitated with dilute oxalic acid solution, with adjusted pH to neutral (6.6 - 6.9) by using ammonia solution during the reaction. The resulting precipitate was vacuum-filtered, washed five times with water and ethanol, respectively, and dried at 50 °C in an oven. After calcination at 750 °C, the oxide powders were confirmed by X-ray diffraction analysis to be single phase and of fluorite structure. But this method had a disadvantage of pH adjustment in the production. Moreover, co-precipitation technique also has been used by using different co-precipitation agents as NaOH, NH_3, polyethylene glycol (PEG), ammonium carbonate or doping material as yttrium. [53-58]

Solid solutions of $Ce_{1-x}Gd_xO_{2-\delta}$ (x=0–0.30) have been synthesized by the hydrothermal method as the appropriate quantities of cerium (III) nitrate hexahydrate and gadolinium (III) nitrate hexahydrate were dissolved separately in water, mixed and co-precipitated with ammonium hydroxide at pH=10 [59,60]. The precipitated gels were sealed into teflon-lined steel autoclaves and hydrothermally treated at 260 °C for 10 h. The autoclaves were quenched at 260 °C to room temperature and the crystallized powder of $Ce_{1-x}Gd_xO_{2-\delta}$ (x=0–0.30) solid solutions were repeatedly washed with deionized water and dried in air at room temperature. Likely as in experiment of Shaowu Zha et al., precise controlling pH was necessary. The average crystallite size was found ranging between 68 – 41 nm.

10GDC and 20GDC nanopowders have been synthesized in a study by four different routes as oxalic acid co-precipitation, acryl amide sol-gel, solid-state reaction (70% wt oxides/30% acryl amide nano powders) and complex assisted co-

precipitation [61]. Shortly, oxalic acid co-precipitation was carried out as cationic nitrate solution had been added dropwise to an oxalic acid solution with constant pH, followed by washing the precipitate with water at the same pH, and then the treatment of powder at 700 ^{o}C for 4 hours. Acryl amide polymerization sol-gel route includes the chelating of Ce and Gd separately by adding EDTA powder and NH_4OH to adjust the pH, additions of acryl amide, bis-acrylamide and AIBN (initiator) into the solution in selected proportions, stirring vigorously, heating up to monomer dissolution and gel formation, and finally calcining at 600 ^{o}C for 2 hours. Complex assisted co-precipitation involves steps of formation of a complex between Ce–Gd ions and an organic compound in aqueous solution, its decomposition giving a precipitate formation, filtration of the precipitate, drying and crystallization at 500 °C in air. In solid state reaction, the oxide forms of Ce and Gd were mixed, milled in a ball and heat-treated at 1000 ^{o}C. Then the oxide mixture was mixed with acryl amide sol–gel CGO powders treated at 600 °C. It is reported as the oxalic acid co-precipitation and the acryl amide sol–gel processes may represent suitable synthetic routes for scaling up to industrial production. Moreover, the acryl amide sol–gel process was characterized as by small volumes of reactants and large powder production with low cost.

Nano-crystalline $Ce_{0.9}Gd_{0.1}O_{1.95}$ electrolyte has been synthesized by sol–gel thermolysis route [62]. Stoichiometric amounts of nitrates of Ce and Gd were mixed with urea as the combustion fuel and poly vinyl acetate (PVA) as the dispersing agent and secondary fuel, the solution was heated to obtain sol, and gel afterwards, and the obtained gel was calcined at 400 and 600 ^{o}C. It was stated that the product heated at 600 ^{o}C showed more agglomeration than the one heated at 400 ^{o}C, and the

one heated at 400 ^{o}C had better ionic conductivity. Same technique has also been used with different material uses, like using glycine ($C_2H_5NO_2$) as fuel [63-66].

In one study, GDC has been synthesized by the Pechini Method [67], the only difference from sol-gel thermolysis route is instead of using urea and PVA, citric acid and ethylene glycol were used. Also a similar technique, glycine-nitrate, has been studied in which glycine was used as fuel [68-70].

1.4.2. GDC Composites and Co-dopings

GDC composites synthesized so far are mostly focused on anode and cathode materials of solid oxide fuel cells.

NiO/GDC composite has been synthesized via ceramic route and the effect of Ni addition to GDC on phase stability, reduction behavior and electrical properties investigated [71]. It was found out that NiO/GDC composite had high conductivity making it useful for anode applications in SOFC. It is also reported that very high NiO content may lead to problems due to thermal expansion mismatch between anode and electrolyte.

NiO/GDC anode material has also been synthesized by preparing NiO and GDC separately via glycine-nitrate route, and anode materials prepared by dip-coating method [72]. It was reported that NiO/GDC anode showed very high performance.

Ni-Co-GDC cermet anode sample has been prepared as an alternative to NiO/GDC by aiming to prevent Ni coarsening leading to electrical degradation of the cell [73]. It was reported as alloying conventional NiO with Co_3O_4 at the weight fraction of 25 % prior to mixing with GDC ($Ni_{0.75}Co_{0.25}$-GDC) resulted in

improvement of the cell performance of the Ni-GDC anode due to an increase in electrical contacts between anode-anode and anode-electrolyte.

In another study, Fe_2O_3 was added to Ni/GDC anode composite to prevent carbon deposition on anode material [74]. They prepared NiO–Fe_2O_3/GDC anode tube by mixing NiO, Fe_2O_3, GDC powder with poly methyl methacrylate and binder. It was concluded as there was almost no carbon fiber deposited on the anode.

Complex composite of $Sr_2MgMoO_{6-\delta}$/$Gd_{0.1}Ce_{0.9}O_{1.95}$ (SMM/GDC) anode material has been synthesized to reduce tolerance to coking and sulfur impurities on anode part [75]. SMM powder was synthesized with solid state reactions of $SrCO_3$, MgO, and MoO_3 whereas GDC was synthesized by co-precipitation–calcination method. Then both SMM and GDC obtained were tape casted.

A composite of $La_{0.6}Sr_{0.4}Co_{0.2}Fe_{0.8}O_{3-\delta}$ and Gd-doped ceria (LSCF–GDC) has been synthesized to be a candidate for cathode material in SOFC, by impregnating the porous GDC scaffold with a nitrate solution containing La, Sr, Co and Fe in desired composition [76]. After testing for a very long time like 500 hours, coarsening of LSCF nanoparticles was observed. MgO and $LaNi_{0.6}Fe_{0.4}O_3$ (LNF) phases were also introduced into LSCF–GDC cathodes to prevent this coarsening and enhanced performance stability was observed.

$(La_{0.8}Sr_{0.2})MnO_3$ (LSM)/GDC - Yttria-stabilized zirconia (YSZ) dual composite cathode has been prepared via a two-step polymerizable complex (PC) method by dissolving nitrate metal salts of La, Sr, and Mn with citric acid, in de-ionized water after which ethylene glycol and YSZ core particles were added to the solution [77]. To obtain LSM/GDC – YSZ dual composite powder, same route has been repeated with LSM–YSZ single composite powders as core particles and nitrate

salts of Gd and Ce. It was reported as having results with high performance and durability of the synthesized material.

Ca Doped GDC Electrolyte Thin Film has been synthesized by electron beam deposition technique [78]. Ca Doped GDC was prepared via solid synthesis route, then GDC thin film was deposited on Ni-GDC anode substrate with e-beam gun. It was stated as the sample conductivity was higher than that of GDC and Ca Doped GDC and made it suitable for use as electrolyte material in SOFC after optimizing the film composition and e-beam operating conditions.

Another composite candidate that could be used as electrolyte material in SOFC as $Ce_{0.9}Gd_{0.1}O_{1.9}$ - $La_{0.9}Sr_{0.1}Ga_{0.8}Mg_{0.2}O_{2.85}$ (GDC - LSGM) has been reported [79]. Both GDC and LSGM were synthesized separately by glycine-nitrate processes, then GDC and LSGM powders were mixed in GDC:LSGM ratios as 95:5, 90:10 and 85:15. It was reported as product with 95:5 ratio had the highest ionic conductivity in the temperature range between 300-800 ^{o}C. Moreover, the open circuit voltage was higher in the cell with composite electrolyte than in the cell with single GDC as electrolyte at the working temperature.

Synthesis of YSZ/GDC vertically aligned nano composite electrolyte has been done by a technique called Pulsed Laser Deposition and its ionic conductivity with that of GDC, YSZ, and GDC-YSZ composite has been compared [80]. It was stated as the ionic conductivity of YSZ/GDC VAN electrolyte appears to be at least 2 times higher than that of single crystal like YSZ thin film and 50% higher than that of single crystal like GDC thin film. Moreover, as the deposition frequency of the YSZ/GDC VAN electrolyte increases, the interface density increases and the ionic conductivity of YSZ/GDC VAN electrolyte improves.

1.4.3. GDC with additional CeO_2 doping, Y_2O_3 and Yb_2O_3 co-doping

Up to now, no scientific work related to GDC/Y_2O_3 and GDC/Yb_2O_3 composite/co-doping synthesis found in literature. Works on GDC composites have been focused so far on metal composites with GDC for anode, and complex composites for cathode and electrolyte materials as described in literature review.

Because the optimum ratio of Gd/Ce for optimum ionic conductivity was inconsistent in literature, additional amounts of CeO2 was doped to 10GDC to see any possible effect it may have had.

1.5. AIM OF THE WORK

The importance and the aim of this thesis is to synthesize 10GDC and its composites with CeO_2, Y_2O_3 and Yb_2O_3 and investigate their physical and chemical properties for possible future applications in SOFC. It should be noted that no scientific work related to GDC/Y_2O_3 or GDC/ Yb_2O_3 composite or co-doping is found up-to-date in literature. In this work, 10% Gadolinia Doped Ceria (10GDC), 10GDC/CeO_2, 10GDC/Y_2O_3 and 10GDC/Yb_2O_3 composites with CeO_2 and Y_2O_3 % molar dopings as 1%, 5%, 10%, 15%, 20%, and Yb_2O_3 molar doping as 0.6%, 2.5%, 6.0%, 9.2%, and 12.5% will be synthesized with both sol-gel combustion and solid state reaction techniques. All samples will be heated up to 800 ^oC and analyzed with IR, EDX/SEM and XRD analysis techniques.

CHAPTER II

EXPERIMENTAL TECHNIQUES

2.1. CHEMICALS

The following chemicals were used in the synthesis of the products:

$Gd(NO_3)_3.6H_2O$: Sigma Aldrich 99.9%

$(NH_4)_2Ce(NO_3)_6$: Sigma Aldrich 99.9%

Gd_2O_3: Merck 99.9%

CeO_2: Merck 99.9%

$Y(NO_3)_3.6H_2O$:Sigma Aldrich 99.9%

Y_2O_3: Merck 99.9%

$Yb(NO_3)_3.5H_2O$:Sigma Aldrich 99.9%

Yb_2O_3: Merck 99.9%

$C_2H_6O_2$: Merck

2.2. INSTRUMENTATION

i.) X-Ray Powder Diffractometer

X-ray powder diffraction measurements were done on Rigaku Miniflex II with CuKα radiation and the comparison of the obtained data was done with the reference data obtained from the Pearson's Crystal Data database software.

ii.) Infrared Spectrophotometer

Perkin Elmer Frontier Fourier Transform Infrared (FTIR) Spectrophotometer with ATR attachment was used to obtain the IR spectra of the samples in the region of 3500-400 cm^{-1}.

iii.) Scanning Electron Microscope (SEM) – Energy Dispersive X-Ray (EDX)

Ultra High Resolution SEM images of samples were taken by Hitachi SU70 Ultra-high Resolution Analytical Scanning Electron Microscope. EDX measurements were done on Hitachi TM3000 Tabletop Microscope.

2.3. EXPERIMENTAL PROCEDURE

2.3.1. Synthesis of 10GDC and 10GDC/CeO_2 products

10GDC and 10GDC/CeO_2 products were synthesized by two routes as Sol-Gel Combustion Synthesis and Solid State Reaction Synthesis. The ratio of pure GDC is determined as 10% Gadolinium doped ceria having optimum oxygen ion conductivity at lower operating temperatures [30].

2.3.1.1. Solid State Reaction Route

In this technique, stoichiometric amounts of Gd_2O_3 and CeO_2 were mixed and grinded after adding a little amount of acetone to favor the boundary reaction between gadolinium and cerium. After grinding, the mixtures were heated at 300 ^oC for 2 hours at 1 ^oC/min rate in furnace. Afterwards, they were grinded again and heated at 800 ^oC for 2 hours at 2 ^oC/min rate in furnace. They were grinded for one more time at the end of heating.

Samples of products in oxide mixtures state, after heating at 300 ^oC, and after heating 800 ^oC were taken to be analyzed. To all of the samples taken IR, EDX, SEM and XRD techniques were applied to characterize them.

2.3.1.2. Sol-Gel Combustion Route

For each composite, stoichiometric amounts of gadolinium nitrate and cerium nitrate were dissolved in a small amount of distilled water and ethylene glycol was added as complexing agent. Each solution was stirred and heated at 50 ^oC for 2 hours with its top closed to prevent much evaporation and to obtain the complexation. After that, each solution was heated and dried at 80 ^oC until excess solvents were evaporated and the gel-like state was reached. And then each solution was self-burned at approximately 140 ^oC. After self-burning, foam-like powders were obtained. They were grinded finely in alumina mortar. After grinding, the powders were heated at 300 ^oC for 2 hours at 1 ^oC/min rate in furnace. Afterwards, they were grinded again and heated at 800 ^oC for 2 hours at 2 ^oC/min rate in furnace. They were grinded for one more time at the end of final heating.

Small amounts of materials were taken as samples in gel state, after self-burning, after heating at 300 ^{o}C, and after heating 800 ^{o}C. Gel samples were subjected to IR analysis. The rest of the samples taken after self-burning, heating at 300^{o}C and 800 ^{o}C were subjected to IR, EDX, SEM and XRD analyses to characterize the products.

2.3.2. Synthesis of 10GDC/Y_2O_3 composites

2.3.2.1. Solid State Reaction Route

Stoichiometric amounts of Gd_2O_3, CeO_2 and Y_2O_3 were mixed and grinded by adding a little amount of acetone to favor the boundary reaction between Gadolinium and Cerium. After grinding, the mixtures were heated at 300 ^{o}C for 2 hours at 1 ^{o}C/min rate in furnace, grinded again, heated at 800 ^{o}C for 2 hours at 2 ^{o}C/min rate in furnace and then grinded again. IR, EDX, SEM and XRD analysis techniques were used to characterize the products.

2.3.2.2. Sol-Gel Combustion Route

Gadolinium nitrate and cerium nitrate and yttrium nitrate were taken in stoichiometric amounts and dissolved in small amounts of distilled water. Next, ethylene glycol was added as complexing agent. Each solution was stirred and heated on hot plates at 50 ^{o}C for 2 hours with its top closed to prevent much evaporation and obtain the complexation. Afterwards, solutions were dried at 80 ^{o}C until excess solvents were evaporated and the gel-like state was reached. And then each solution was self-burned at approximately 140 ^{o}C. After self-burning, foam-like powders were obtained. They were grinded finely in mortar. After grinding, the samples were heated at 300 ^{o}C for 2 hours at 1 ^{o}C/min rate in furnace. Afterwards, they were

grinded again and heated at 800 ^{o}C for 2 hours at 2 ^{o}C/min rate in furnace. They were grinded for one more time at the end of heating.

Small amounts of samples were taken from materials in gel state, after self-burning, after heating at 300 ^{o}C, and after heating 800 ^{o}C. All of the samples taken were subjected to IR, EDX, SEM and XRD techniques for characterization.

2.3.3. Synthesis of 10GDC/Yb_2O_3 composites

2.3.3.1. Solid State Reaction Route

The same solid state synthesis procedure for 10GDC/Y_2O_3 composites was followed for 10GDC/Yb_2O_3 composites with the difference of mol% of Yb in 10GDC.

Again, small amounts of samples were taken from materials in oxide mixtures state, after heating at 300 ^{o}C, and after heating 800 ^{o}C for analyses. To all of the samples taken EDX, SEM and XRD techniques were applied to characterize them.

2.3.3.2. Sol-Gel Combustion Route

Like in the for 10GDC/Y_2O_3 composite synthesis, stoichiometric amounts of gadolinium nitrate and cerium nitrate and ytterbium nitrate were dissolved in a small amount of distilled water and ethylene glycol was added as complexing agent. Each solution was stirred and heated at 50 ^{o}C for 2 hours with its top closed to prevent much evaporation and to obtain the complexation. After that, each solution was heated and dried at 80 ^{o}C until excess solvents were evaporated the gel-like state was reached. And then each solution was self-burned at approximately 140 ^{o}C. After self-burning, foam-like powders were obtained. They were grinded finely in mortar. After

grinding, the samples were heated at 300 ^{o}C for 2 hours at 1 ^{o}C/min rate in furnace. Afterwards, they were grinded again and heated at 800 ^{o}C for 2 hours at 2 ^{o}C/min rate in furnace. They were grinded for one more time at the end of heating.

Small amounts of samples were taken from materials in gel state, after self-burning, after heating at 300 ^{o}C, and after heating 800 ^{o}C. IR, EDX, SEM and XRD techniques were used for characterization.

CHAPTER III

RESULTS AND DISCUSSION

3.1. SOLID STATE SYNTHESIS RESULTS

3.1.1. Synthesis of 10%Gadolinium Doped Ceria, 10GDC

3.1.1.1. X-Ray Powder Diffraction (XRD) Studies

Figure 3.1 shows X-ray powder diffraction patterns of gadolinium doped ceria synthesized by solid state synthesis technique with 10% gadolinium doping (10GDC).

Examination of the XRD patterns showed that obtained product is not pure 10GDC by comparison with the ICDD cards 00-075-0161 for 10GDC and 00-088-2165 for Gd_2O_3.

From the XRD patterns, very small diffraction lines related to additional Gd_2O_3 phases are observed; especially at 20, and between 35-60 2theta values. So it cannot be said that single phase 10GDC crystals were synthesized by this method.

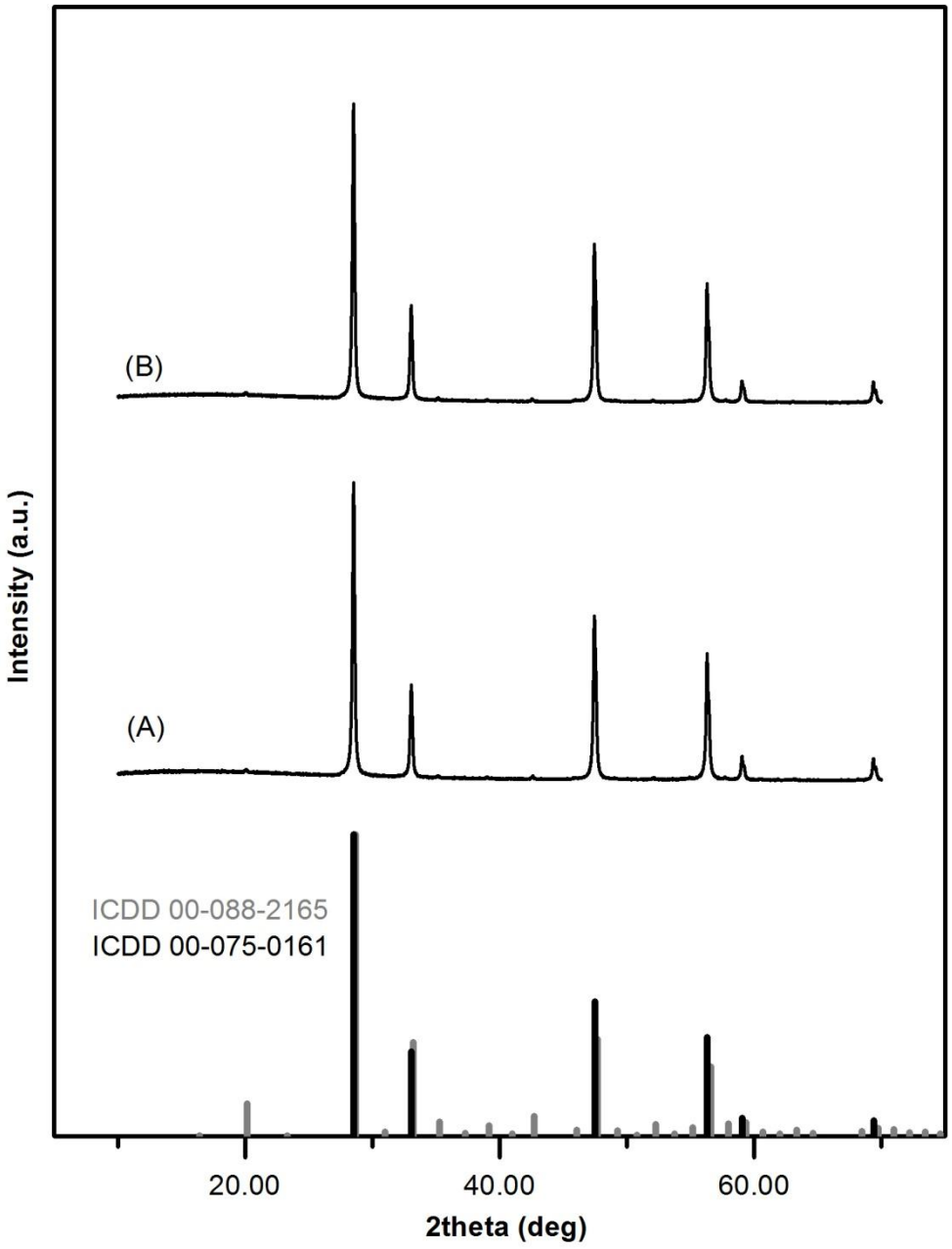

Figure 3.1 XRD Patterns for 10GDC synthesized by Solid State Synthesis Route (A) after heating at 300 ^{o}C, (B) after heating at 800 ^{o}C, ICDD 00-075-0161 and ICDD 00-088-2165

3.2.1.2. Infrared Spectroscopy Studies

The infrared spectra of 10GDC synthesized by the solid state synthesis method are given in Figure 3.2.

Because the starting materials were oxide forms, there was no organic part in the product so no bands were observed related to organic materials. The bands between 2200-1750 cm^{-1} are related to CO_2 in the air and the band at 573 cm^{-1} is predicted to be related to metal-oxide bonds [84]. It is also clear that both spectra are almost identical to each other.

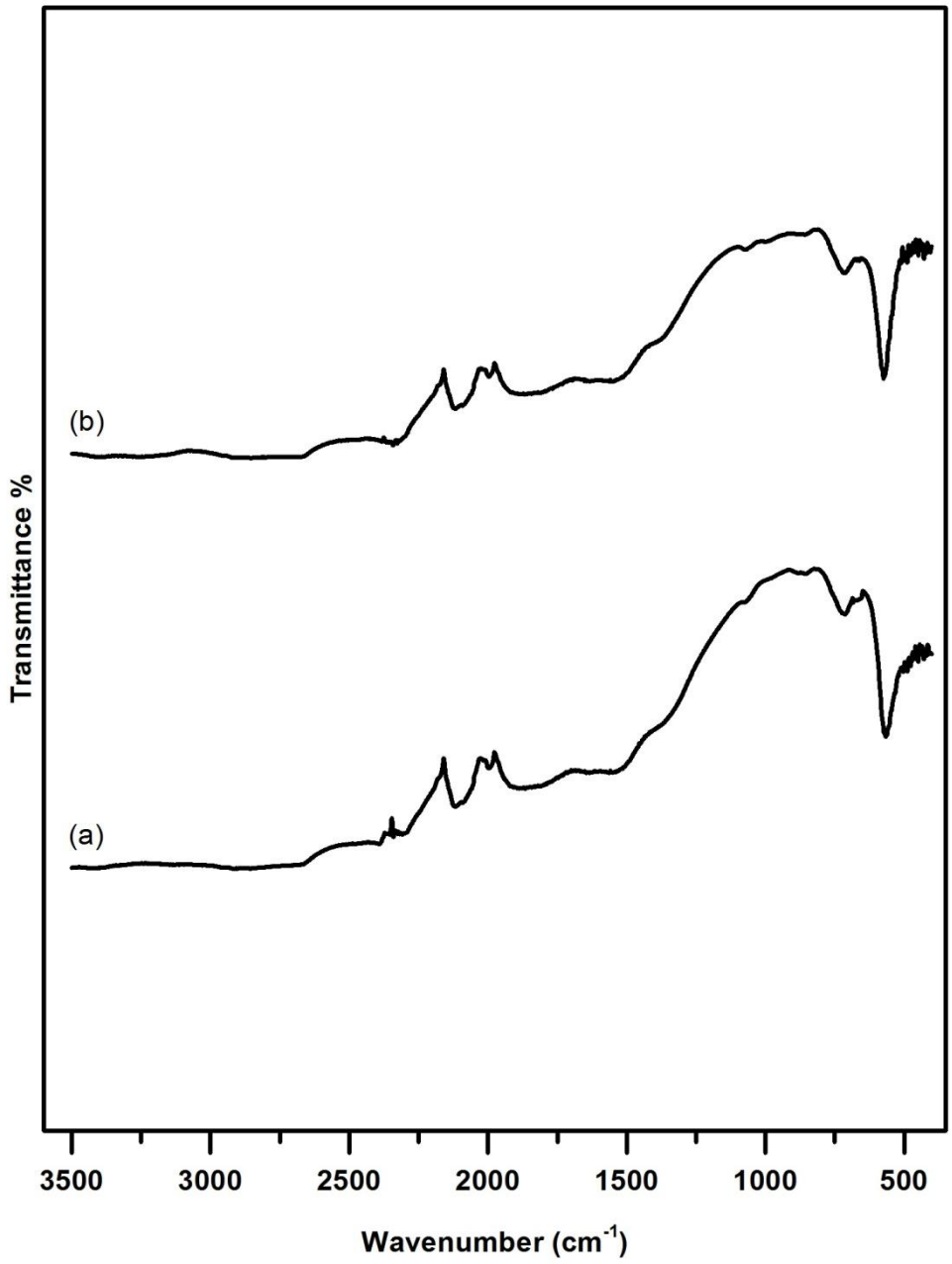

Figure 3.2 IR Spectra of 10GDC (a) after heating at 300 ^{o}C, (b) after heating at 800 ^{o}C

3.2.1.3. SEM and EDX Analysis of 10GDC

The SEM images of 10GDC synthesized by solid state synthesis technique after heating at 800 ^{o}C are given in Figure 3.3. The images give information about the particle size and the morphology of the product.

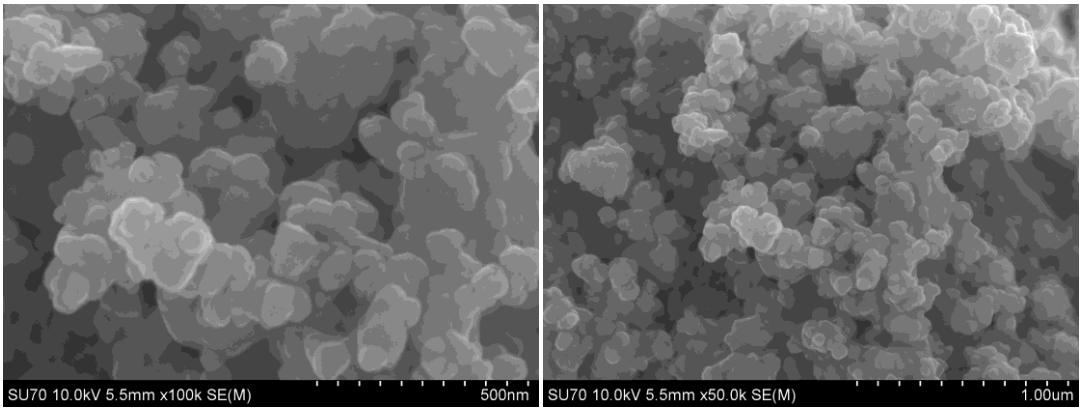

Figure 3.3 SEM images of 10GDC with 100k and 50k magnifications

EDX analysis, shown in figure 3.4, shows that there is no impurity and it is in a good agreement with nominal compositions of elements.

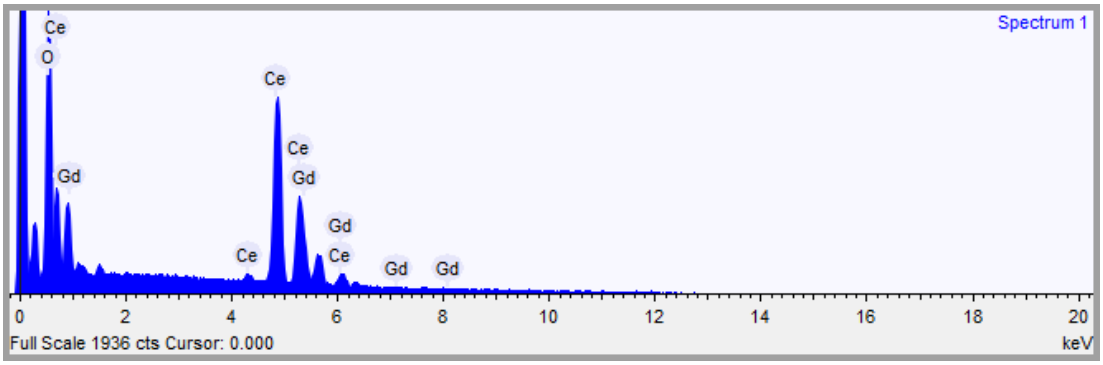

Figure 3.4 EDX spectrum of 10GDC

3.1.2. Synthesis of 10GDC with additional amounts of Cerium

To see the possible effects of ratio of Gd/Ce, 10GDC was also synthesized with additional amounts of Ce with % mol ratios of Ce/10GDC as 1/99, 5/95, 10/90, 15/85 and 20/80.

3.1.2.1. X-Ray Powder Diffraction (XRD) Studies

Figure 3.5 and 3.6 shows X-ray powder diffraction patterns of gadolinium doped ceria with additional cerium oxide, CeO_2, synthesized by solid state synthesis technique, after heating at 300 ^oC and 800 ^oC respectively.

Examination of the XRD patterns showed that obtained product is not pure 10GDC by comparison with the ICDD cards 00-075-0161 for 10GDC and 00-088-2165 for Gd_2O_3.

From the XRD pattern, very small diffraction lines related to additional Gd_2O_3 phase are observed; as it was observed in the 10GDC product synthesized by solid state route.

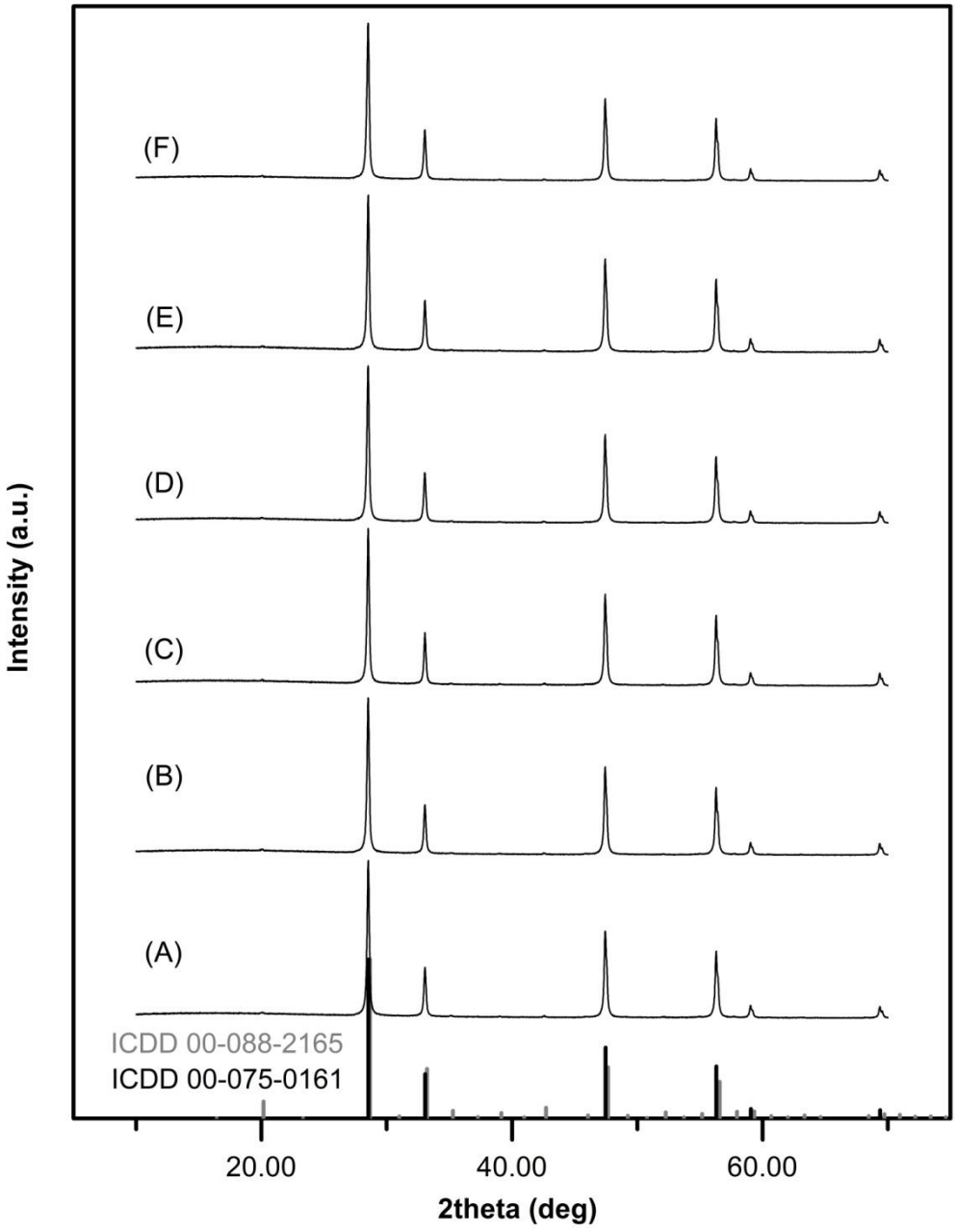

Figure 3.5 XRD Patterns of (A) 10GDC with additional amounts of Cerium as (B) 1%, (C) 5%, (D) 10%, (E) 15%, (F) 20%, after heating at 300 ^{o}C, synthesized by Solid State Synthesis Route, ICDD 00-075-0161 and ICDD 00-088-2165

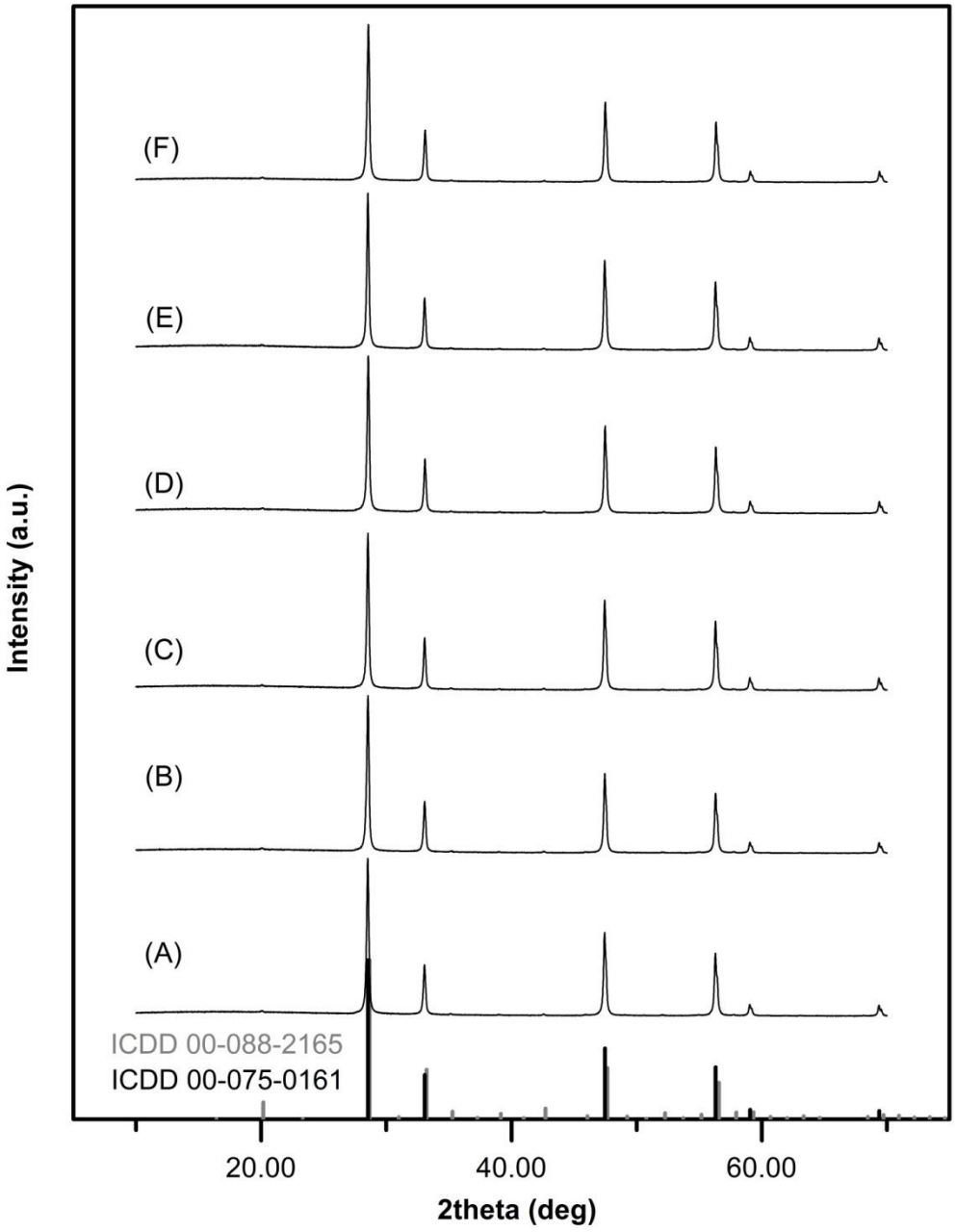

Figure 3.6 XRD Patterns of (A) 10GDC with additional amounts of Cerium as (B) 1%, (C) 5%, (D) 10%, (E) 15%, (F) 20%, after heating at 800 ^{o}C, synthesized by Solid State Synthesis Route, ICDD 00-075-0161 and ICDD 00-088-2165

3.1.2.2. Infrared Spectroscopy Studies

The infrared spectra of 10GDC with additional amounts of cerium oxide, CeO_2, after heating at 300 ^oC and 800 ^oC, synthesized by the solid state method are given in Figure 3.7 and 3.8 respectively.

These spectra follow the same trend with the spectra of 10GDC of solid state route. Vibrational bands of CO_2 are seen between 2200-1750 cm^{-1} and band of metal-oxide bonds is seen at 573 cm^{-1} [84].

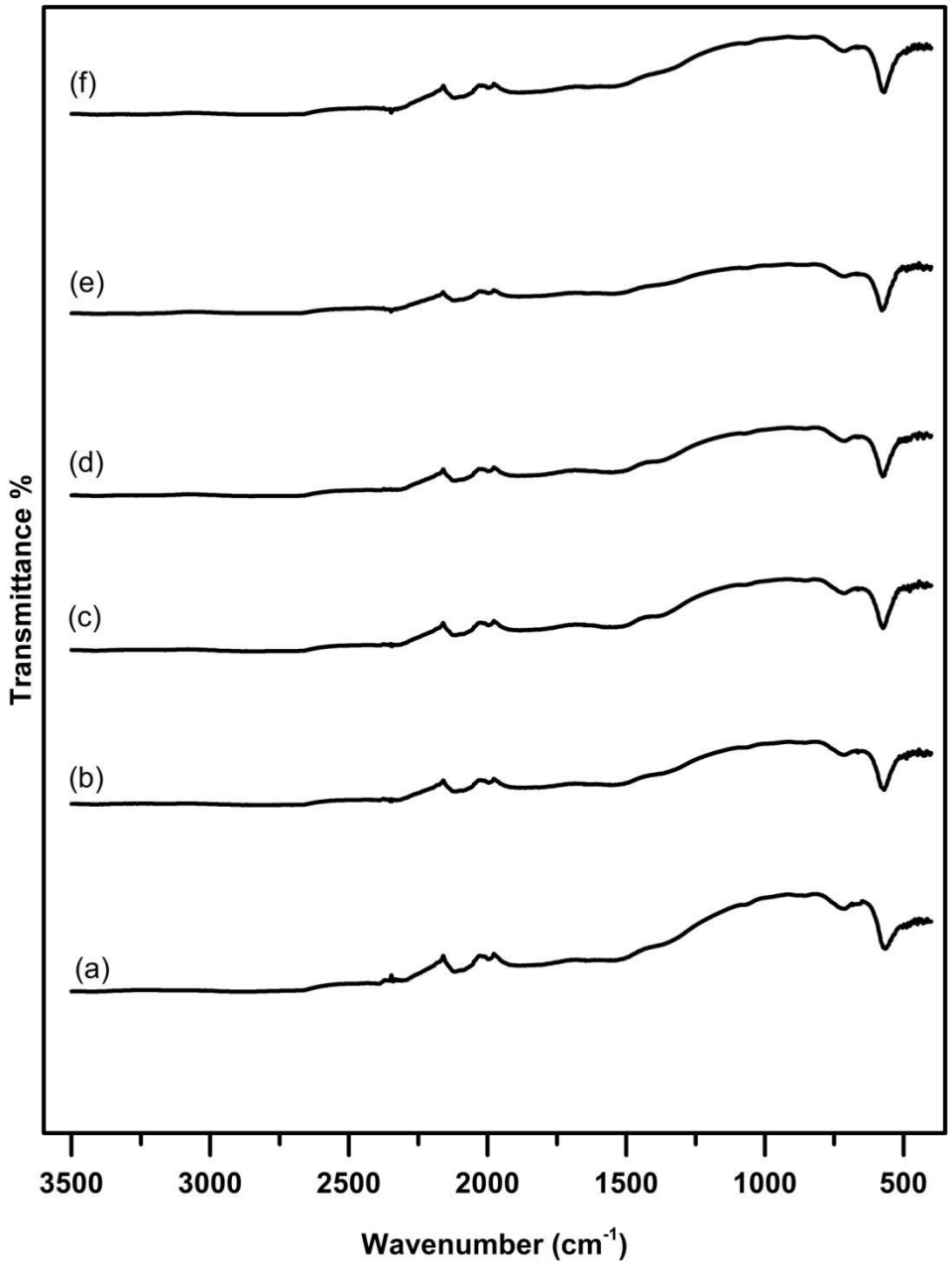

Figure 3.7 IR Spectra of (a) 10GDC with additional amounts of Cerium as (b) 1%, (c) 5%, (d) 10%, (e) 15%, (f) 20% after heating at 300 ^{o}C synthesized by Solid State Synthesis Method

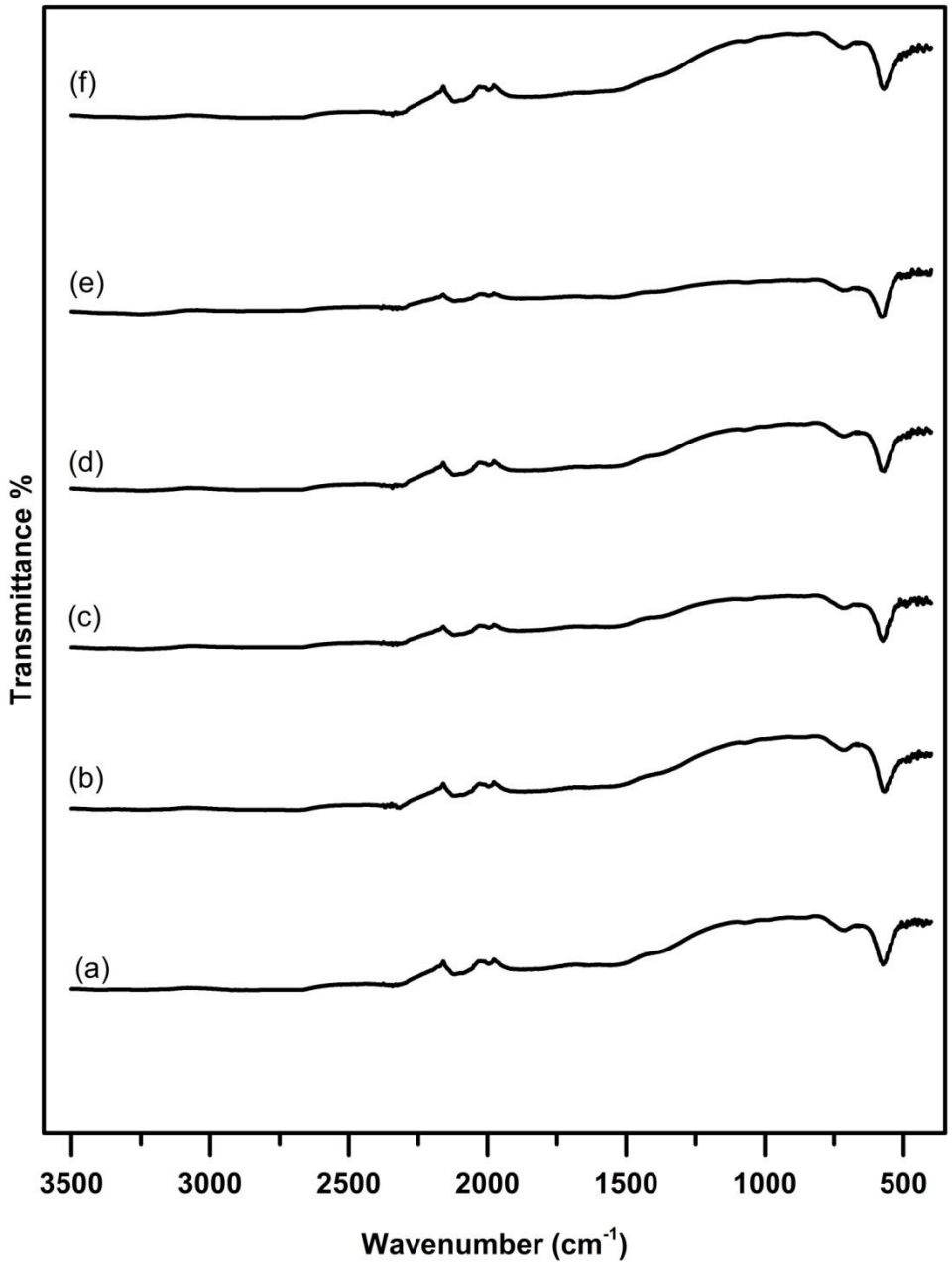

Figure 3.8 IR Spectra of (a) 10GDC with additional amounts of Cerium as (b) 1%, (c) 5%, (d) 10%, (e) 15%, (f) 20% after heating at 800 ^{o}C synthesized by Solid State Synthesis Method

3.1.2.3. SEM and EDX Analysis of 10GDC with additional amounts of Cerium

The SEM images of (a) 10GDC + 15%CeO_2 and (b) 10GDC after heating at 800 ^oC, synthesized by solid state synthesis technique, is given in Figure 3.9. With the comparison of the images, we can say the morphology of the products are same, so it does not depend on the amount of doping.

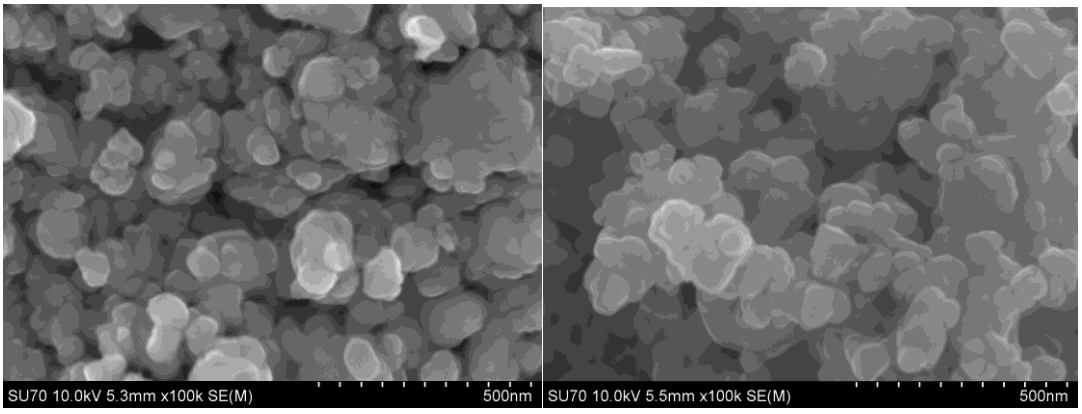

Figure 3.9 SEM images of (a) 10GDC + 15% CeO2 and (b) 10GDC with 100k magnifications after heating at 800 ^oC

EDX analysis, shown in Figure 3.10, 3.11, and 3.12 shows that there is no impurity and it is in a good agreement with nominal compositions of elements.

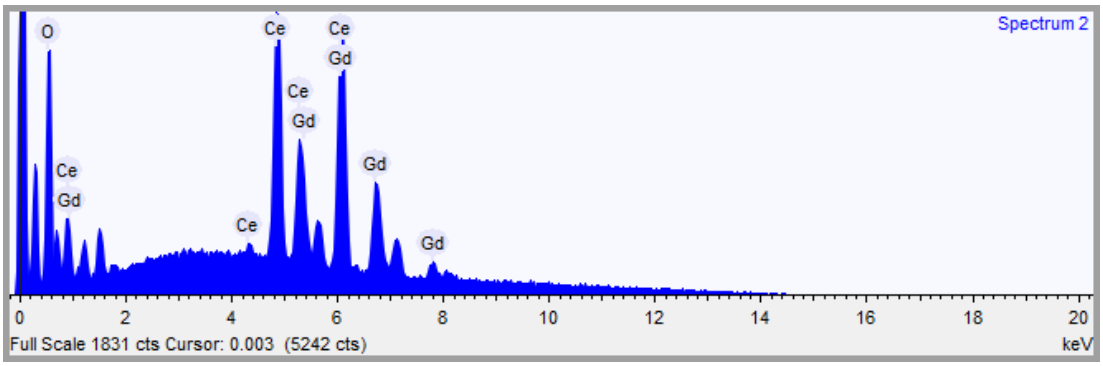

Figure 3.10 EDX spectrum of 10GDC + 10% CeO2

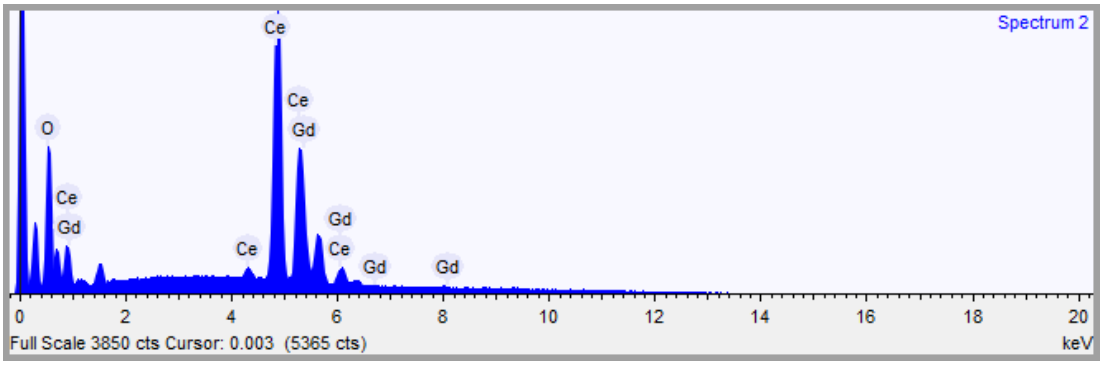

Figure 3.11 EDX spectrum of 10GDC + 15% CeO2

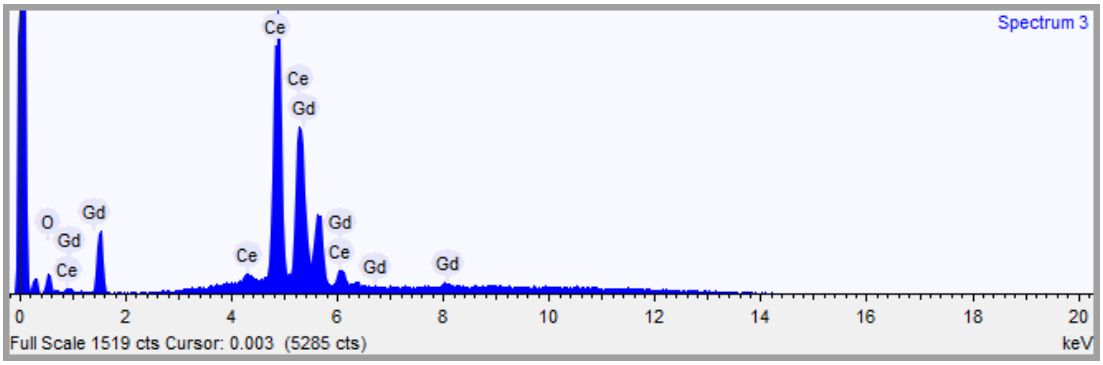

Figure 3.12 EDX spectrum of 10GDC + 20% CeO2

3.1.3. Synthesis of 10GDC/Y_2O_3 composites

To see the effects of addition of yttrium in 10GDC, yttrium was added into 10GDC mixture in mol % ratios of Y/10GDC as 1/99, 5/95, 10/90, 15/85 and 20/80.

3.1.3.1. X-Ray Powder Diffraction (XRD) Studies

Figure 3.13 shows X-ray powder diffraction patterns of gadolinium doped ceria with addition of yttrium oxide, Y_2O_3, synthesized by solid state synthesis technique, in the oxide mixture state. Figure 3.14 and 3.15 show X-ray powder diffraction patterns of products after heating at 300 ^oC, and 800 ^oC, respectively.

Examination of the XRD patterns showed that single phase crystal samples of GDC/Y_2O_3 could not be synthesized by comparison with the ICDD cards 00-075-0161 for 10GDC and 00-086-1326 for Y_2O_3.

On the XRD patterns, diffraction lines related to additional phase of Y_2O_3 are observed in the 2theta range between 20 and 60 degrees. As the amount of Y_2O_3 increase, additional phase lines get intense and can be seen easier.

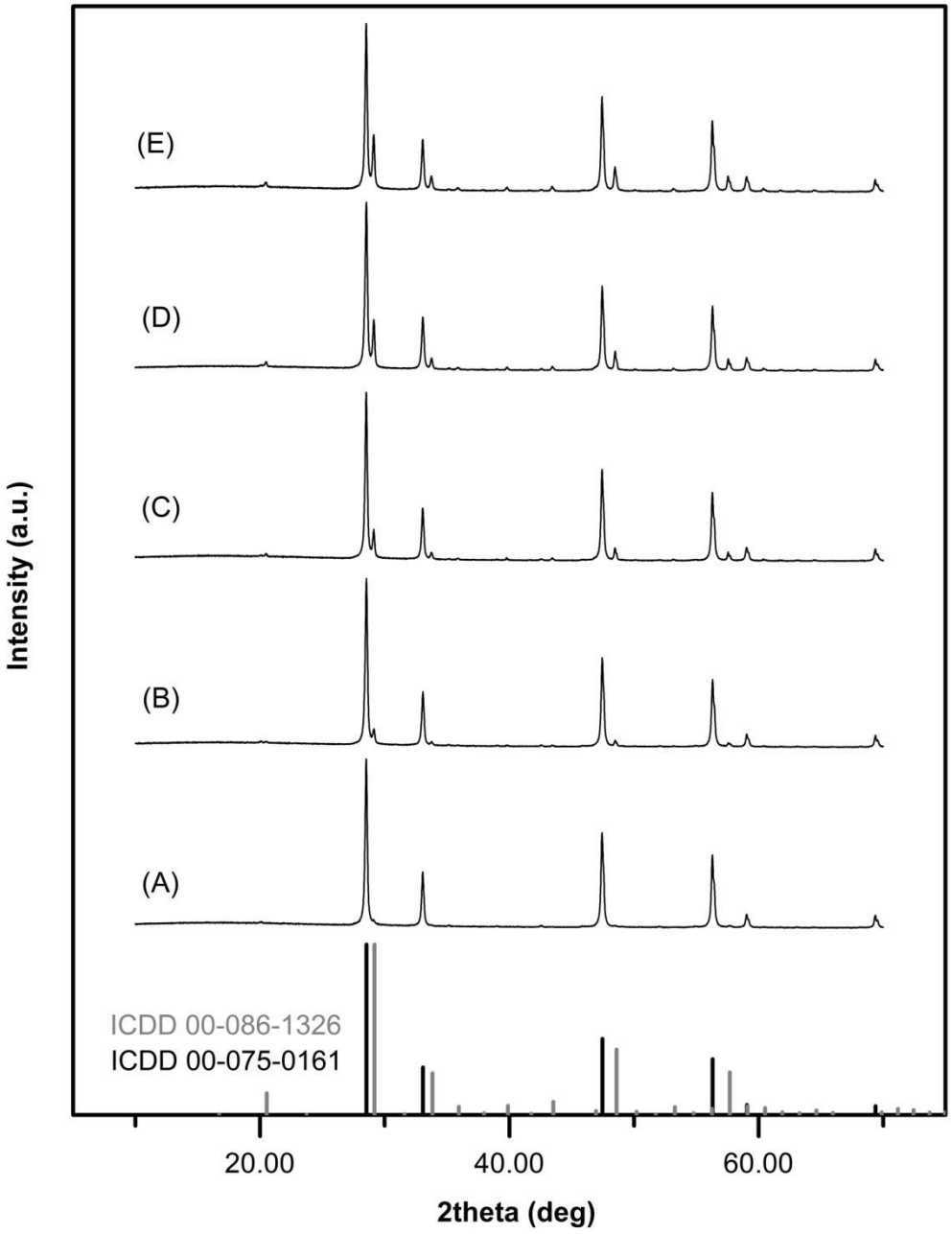

Figure 3.13 XRD Patterns of 10GDC/Y_2O_3 composites with mol% amounts of Yttrium as (A) 1%, (B) 5%, (C) 10%, (D) 15%, (E) 20% in oxide mixture state synthesized by Solid State Synthesis Route, ICDD 00-075-0161 and ICDD 00-086-1326

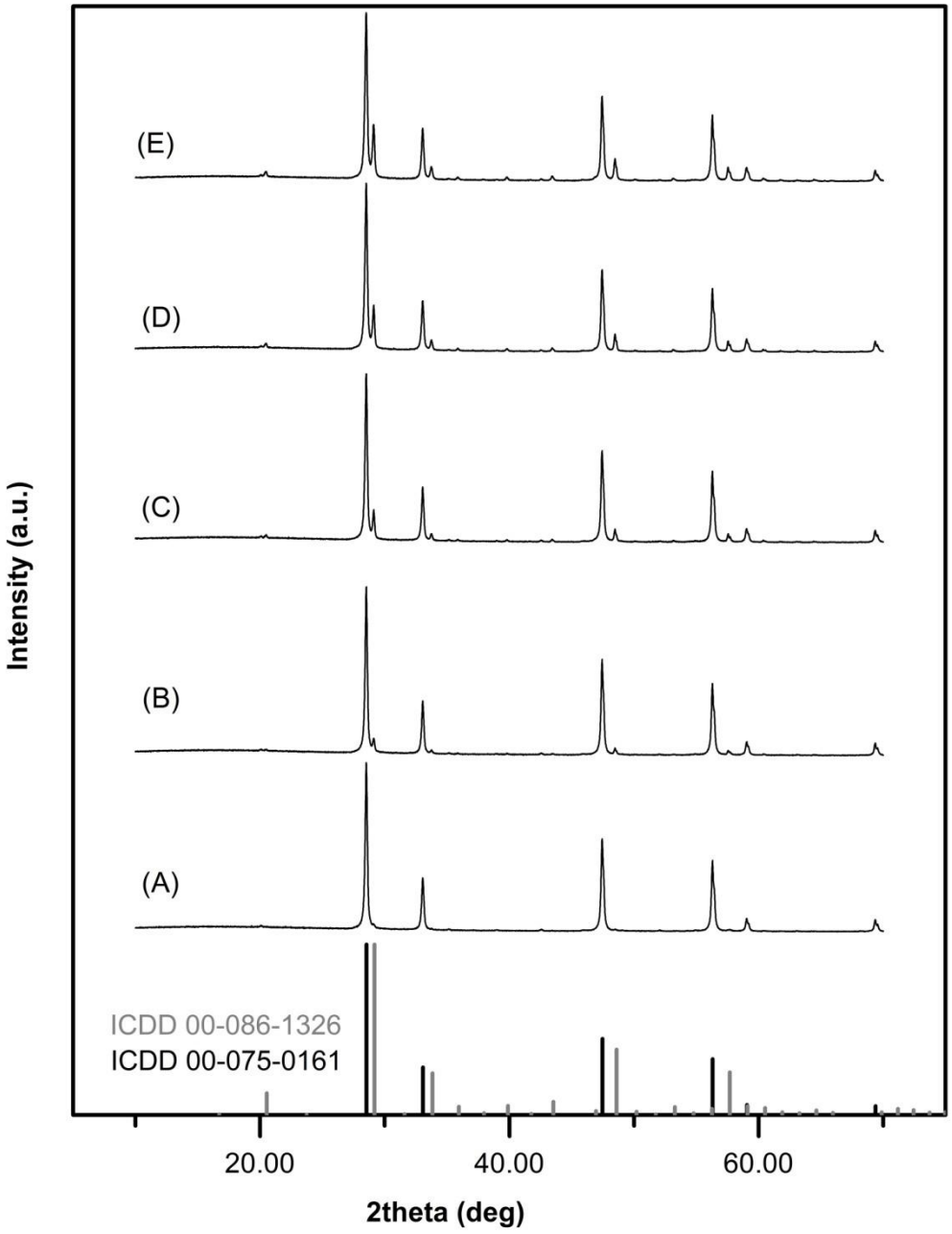

Figure 3.14 XRD Patterns of 10GDC/Y_2O_3 composites with mol% amounts of Yttrium as (A) 1%, (B) 5%, (C) 10%, (D) 15%, (E) 20% after heating at 300 ^{o}C synthesized by Solid State Synthesis Route, ICDD 00-075-0161 and ICDD 00-086-1326

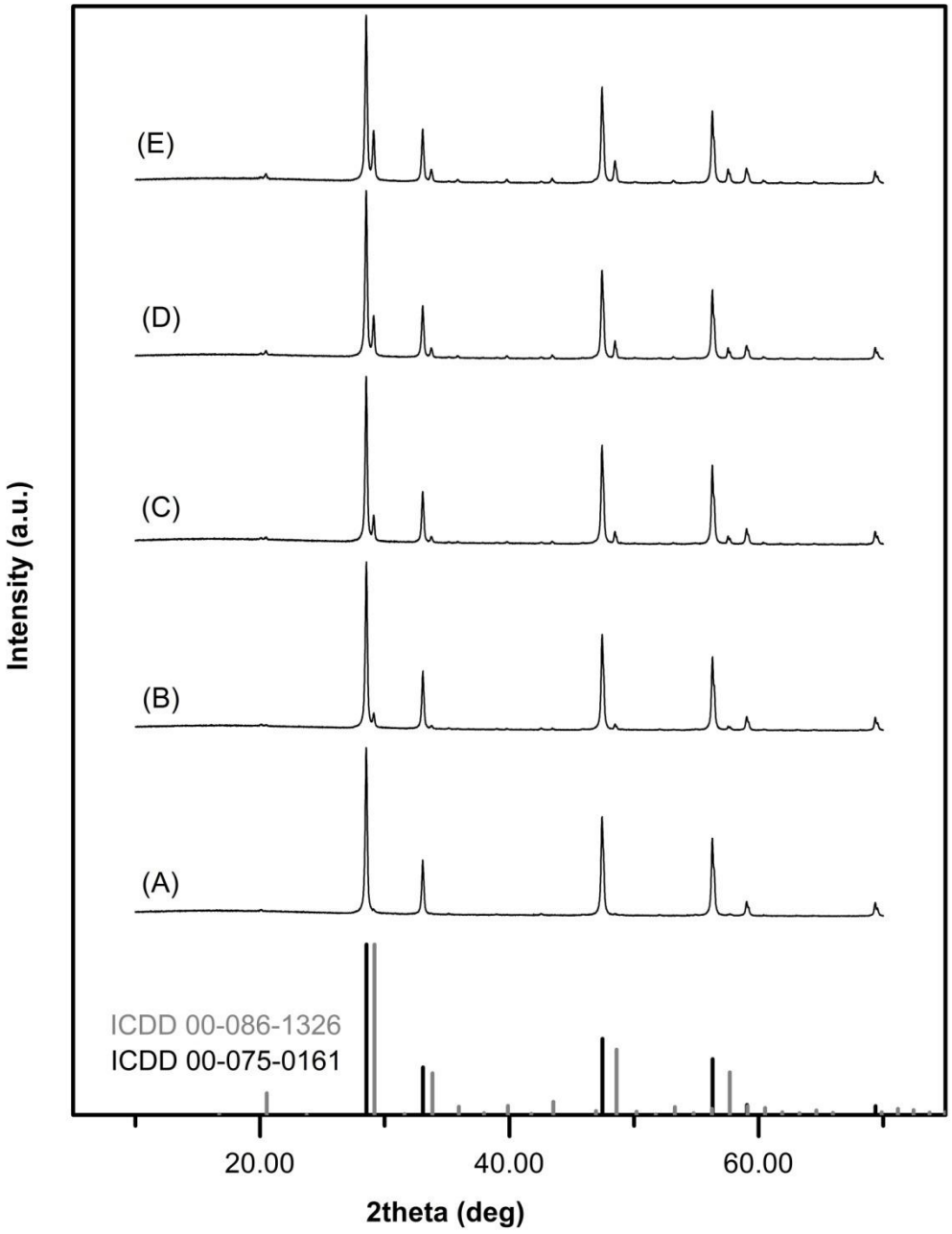

Figure 3.15 XRD Patterns of 10GDC/Y_2O_3 composites with mol% amounts of Yttrium as (A) 1%, (B) 5%, (C) 10%, (D) 15%, (E) 20% after heating at 800 ^{o}C synthesized by Solid State Synthesis Route, ICDD 00-075-0161 and ICDD 00-086-1326

3.1.3.2. Infrared Spectroscopy Studies

The infrared spectra of 10GDC with addition of yttrium oxide, Y_2O_3, synthesized by the solid state synthesis method are given in Figure 3.16. Figure 3.17 and Figure 3.18 represents the spectra for after heating at 300 ^oC and 800 ^oC, respectively.

These spectra follow the same routine as the spectra of the solid state synthesis products. Again, vibrational bands of CO_2 are seen at between 2200-1750 cm^{-1} and band of metal-oxide bonds is seen at 573 cm^{-1} [84].

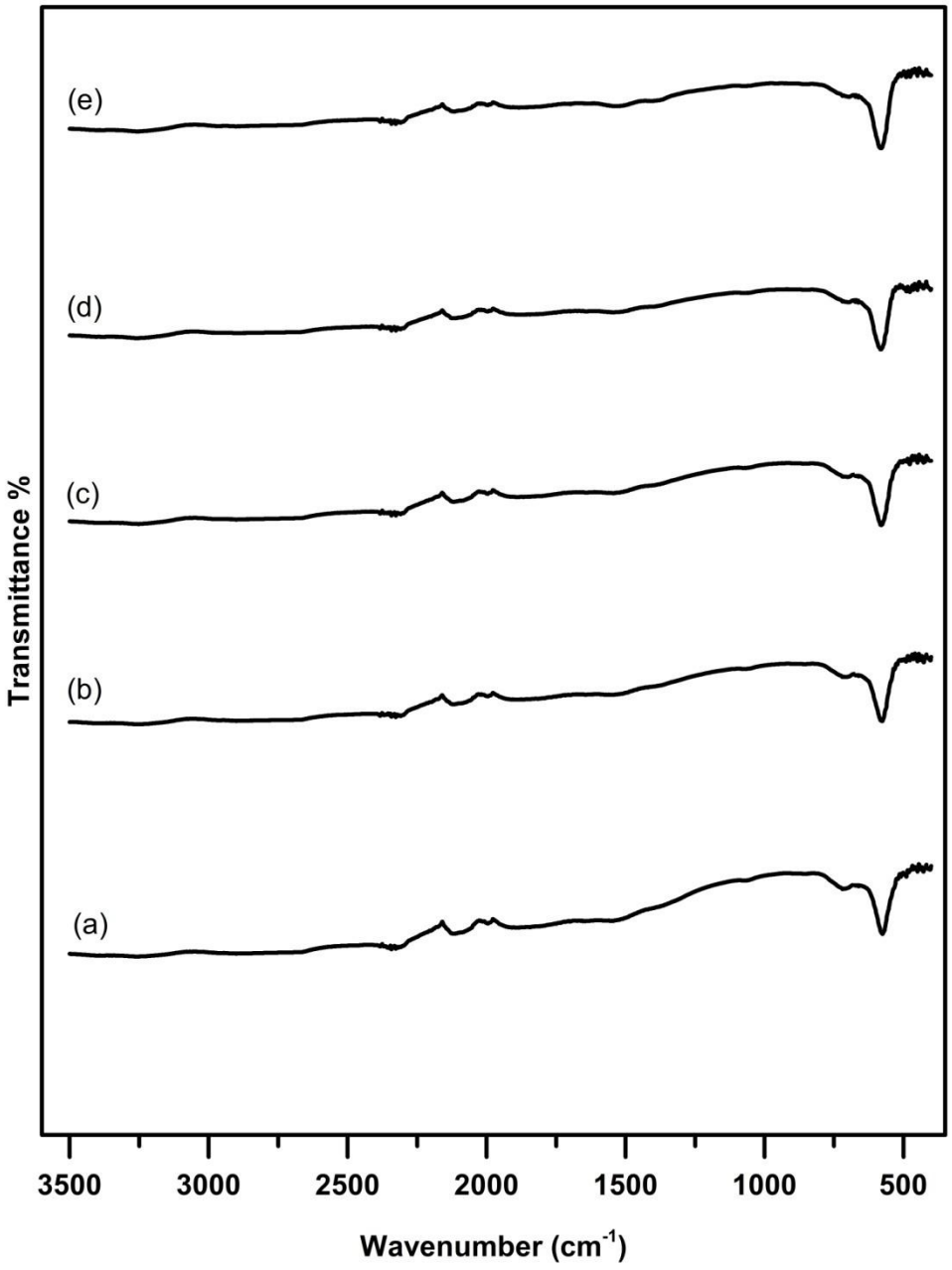

Figure 3.16 IR Spectra of (a) 10GDC and 10GDC/Y_2O_3 composites with mol% amounts of Yttrium as (b) 1%, (c) 5%, (d) 10%, (e) 15%, (f) 20% in oxide mixture state synthesized by Solid State Synthesis Route

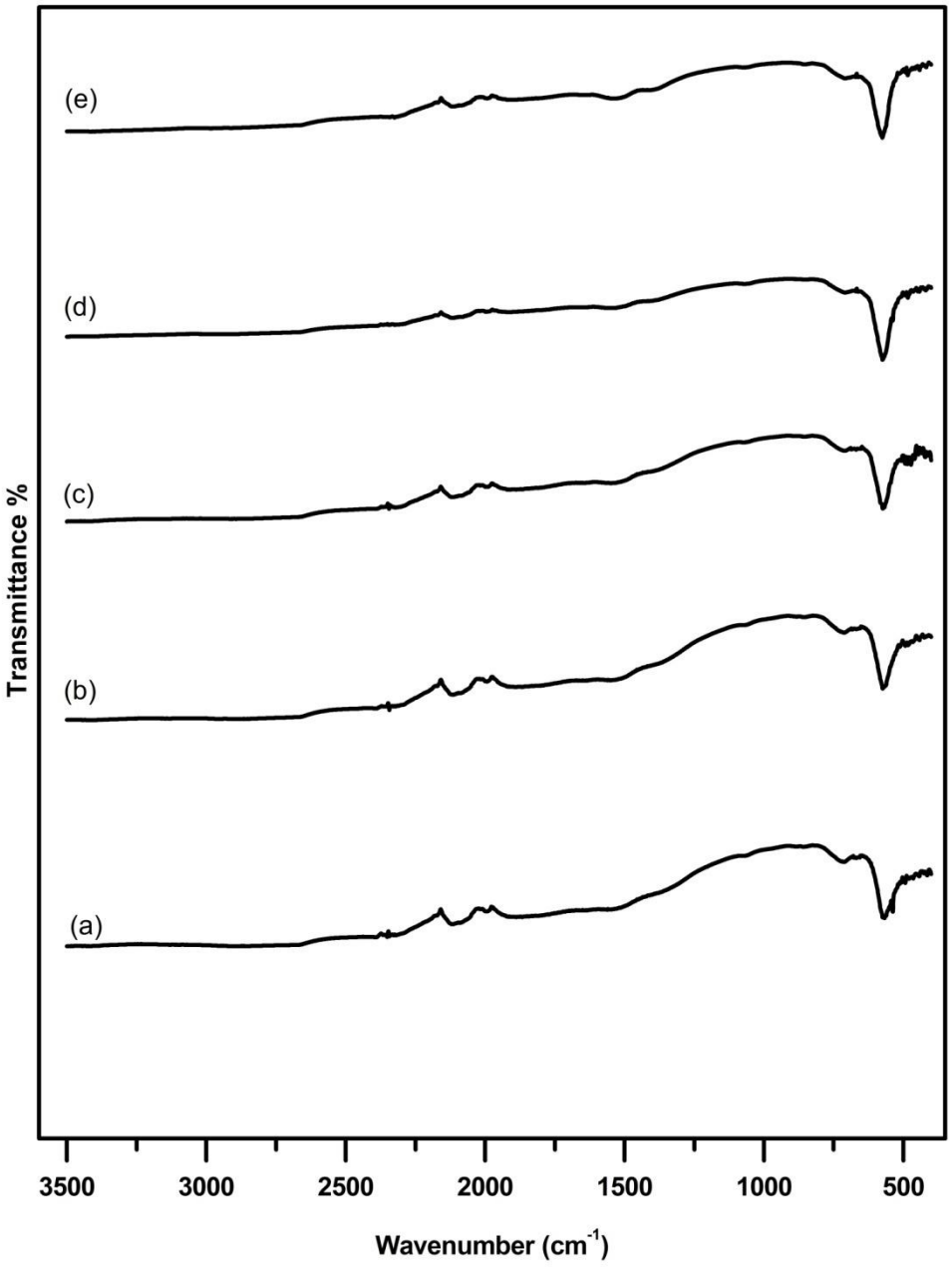

Figure 3.17 IR Spectra of (a) 10GDC and 10GDC/Y_2O_3 composites with mol% amounts of Yttrium as (b) 1%, (c) 5%, (d) 10%, (e) 15%, (f) 20% after heating at 300 ^{o}C, synthesized by Solid State Synthesis Route

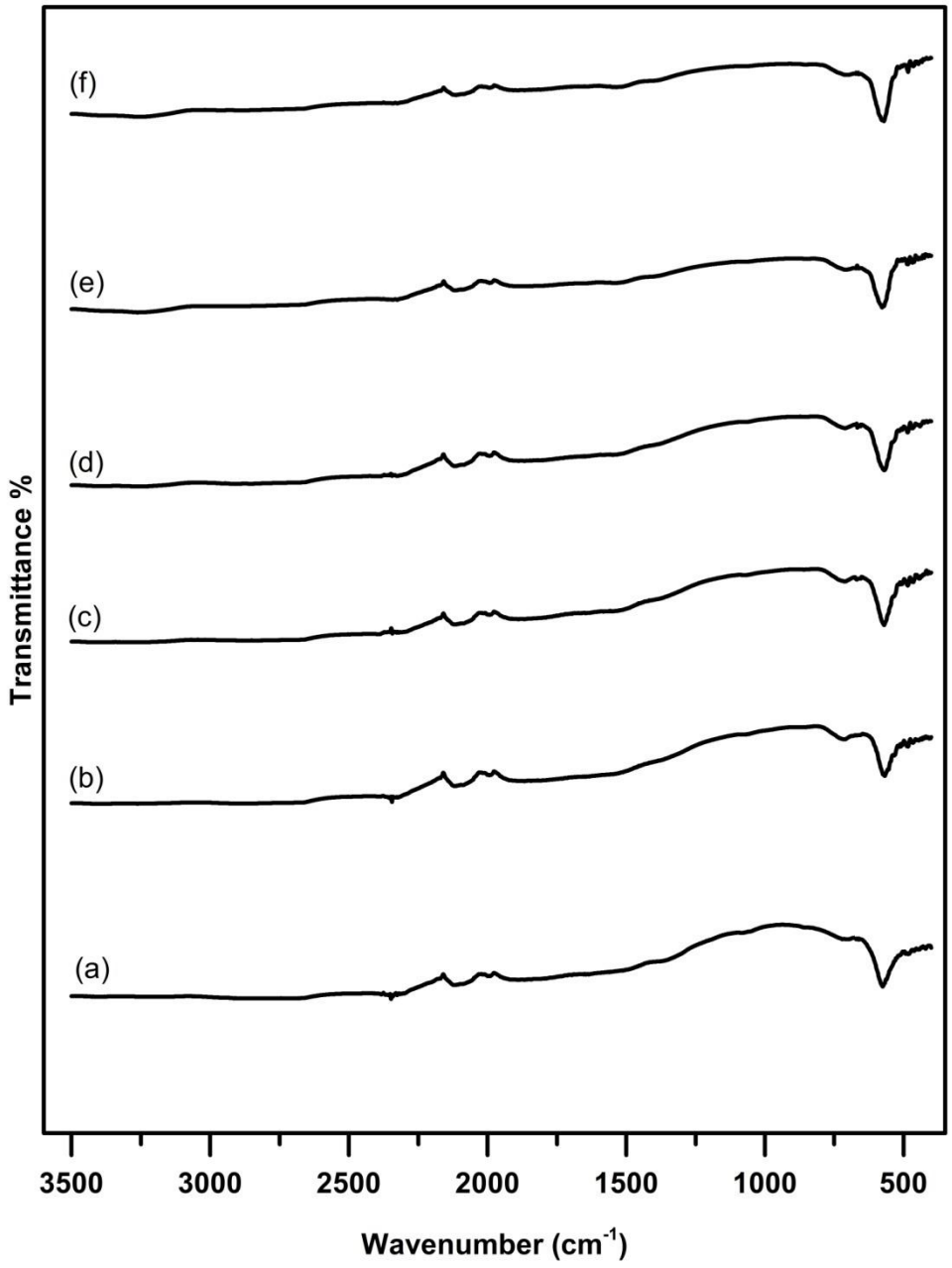

Figure 3.18 IR Spectra of (a) 10GDC and 10GDC/Y_2O_3 composites with mol% amounts of Yttrium as (b) 1%, (c) 5%, (d) 10%, (e) 15%, (f) 20% after heating at 800 ^{o}C synthesized by Solid State Synthesis Route

3.1.3.3. SEM and EDX Analysis of 10GDC/Y_2O_3 composites

The SEM images of 10GDC + 10% Y_2O_3 (a) heated at 300 ^oC and (b) heated at 800 ^oC, synthesized by solid state synthesis technique, is given in Figure 3.19. The images give information about the particle size and the morphology of the product. From the pictures it is seen that the morphology of particles does not depend on the heating temperature.

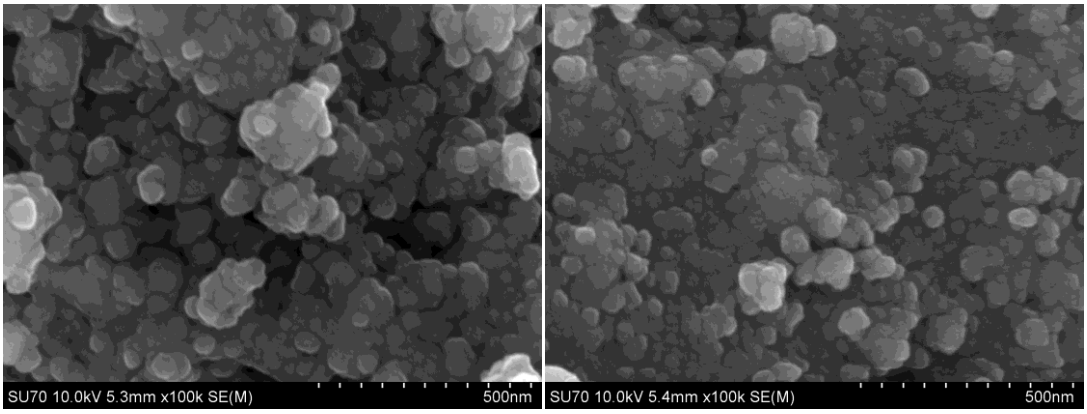

Figure 3.19 SEM images of 10GDC + 10% Y_2O_3 (a) heated at 300 ^oC and (b) heated at 800 ^oC, synthesized by Solid State Synthesis Technique with 100k magnifications

EDX analysis, shown in Figure 3.20, 3.21, and 3.22 shows that there is no impurity and it is in a good agreement with nominal compositions of elements. As the amount of Y_2O_3 doping increases, yttrium peak intensity increases.

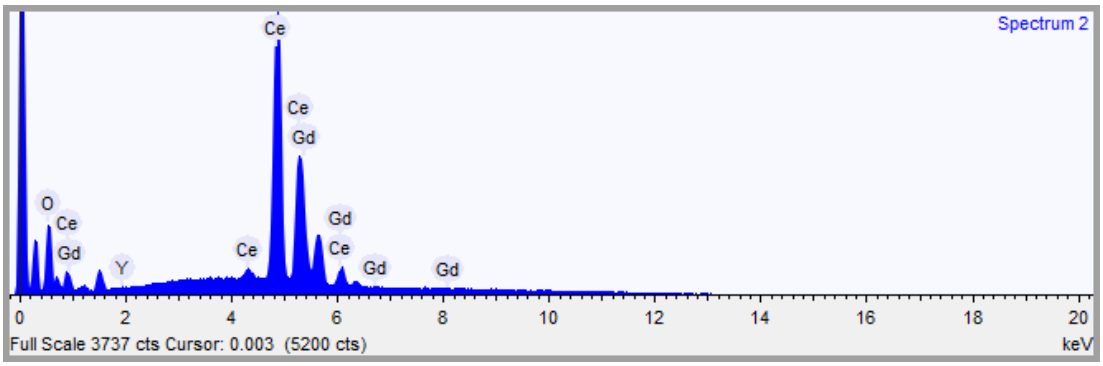

Figure 3.20 EDX spectrum of 10GDC + 1% Y_2O_3

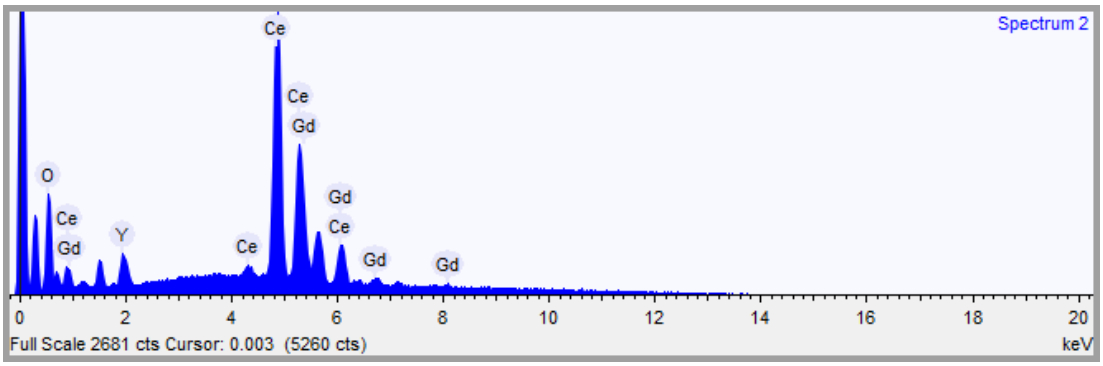

Figure 3.21 EDX spectrum of 10GDC + 5% Y_2O_3

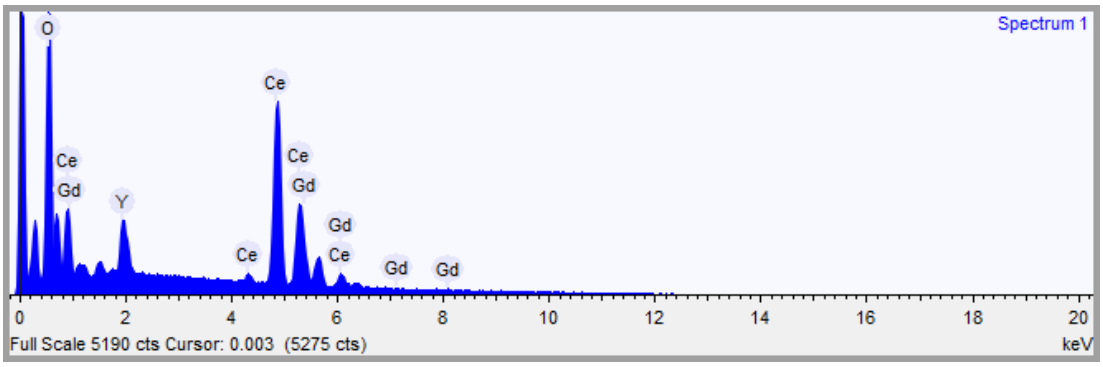

Figure 3.22 EDX spectrum of 10GDC + 10% Y_2O_3

3.1.4. Synthesis of 10GDC/Yb_2O_3 composites

To see the effects of amount and addition of ytterbium in 10GDC, ytterbium was added into 10GDC mixture with different mol % ratios of Yb/10GDC than that of cerium and yttrium as 0.6/99.4, 2.5/97.5, 6/94, 9.2/90.8 and 12.5/87.5.

3.1.4.1. X-Ray Powder Diffraction (XRD) Studies

Figure 3.23 shows X-ray powder diffraction patterns of gadolinium doped ceria with addition of ytterbium oxide, Yb_2O_3, synthesized by solid state synthesis technique, in the oxide mixture state. Figure 3.24 and 3.25 show X-ray powder diffraction patterns of products after heating at 300 ^oC, and 800 ^oC, respectively.

Examination of the XRD patterns showed that single phase crystal samples of GDC/Yb_2O_3 could not be synthesized by comparison with the ICDD cards 00-075-0161 for 10GDC and 04-012-8055 for Yb_2O_3.

On the XRD patterns, diffraction lines related to additional phase of Yb_2O_3 are observed in the 2theta range between 20 and 60 degrees. As the amount of Yb_2O_3 increase, additional phase lines get intense and can be seen clearly.

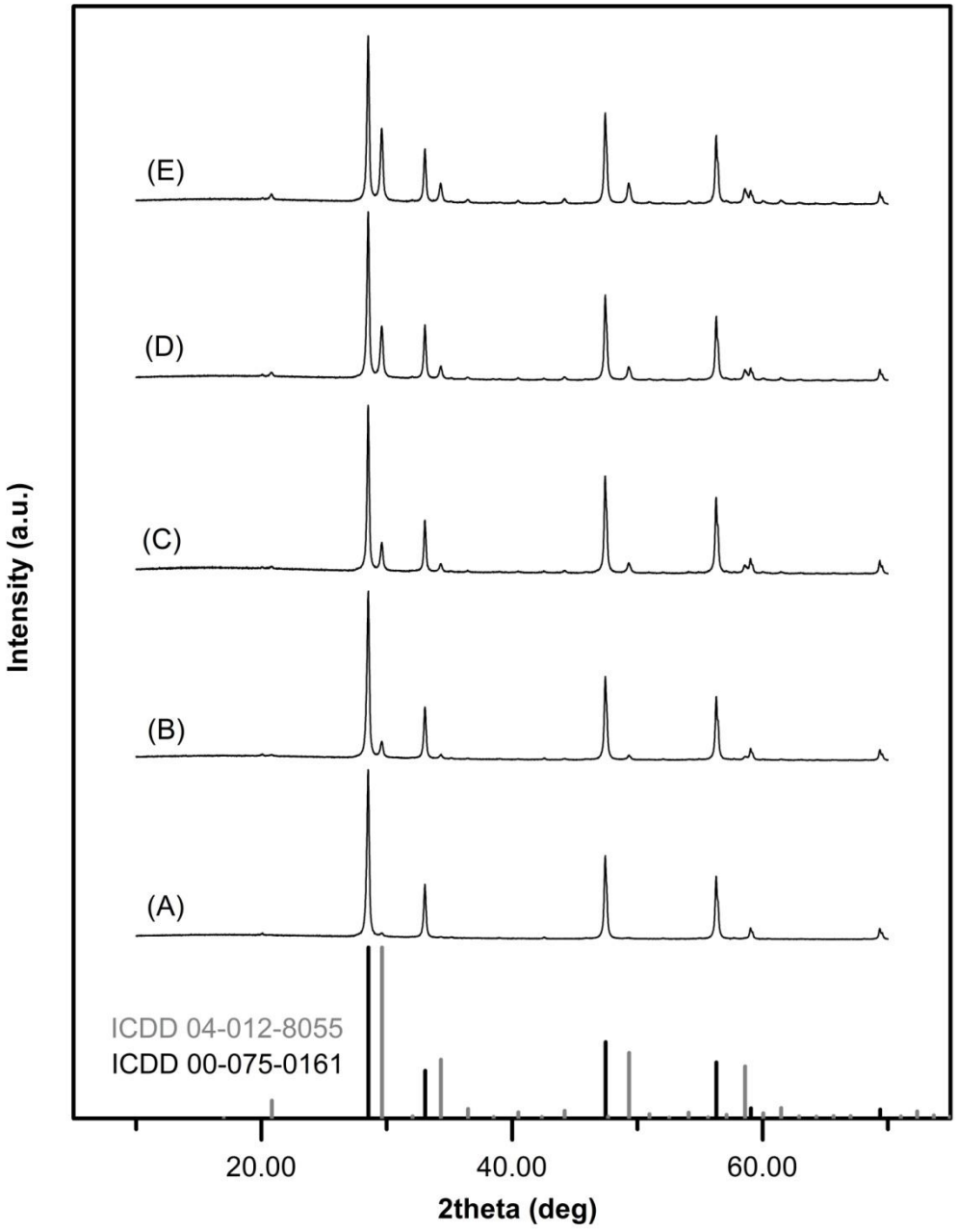

Figure 3.23 XRD Patterns of 10GDC/Yb_2O_3 composites with mol% amounts of Ytterbium as (A) 0.6%, (B) 2.5%, (C) 6.0%, (D) 9.2%, (E) 12.5% in oxide mixture state synthesized by Solid State Synthesis Route, ICDD 00-075-0161 and ICDD 04-012-8055

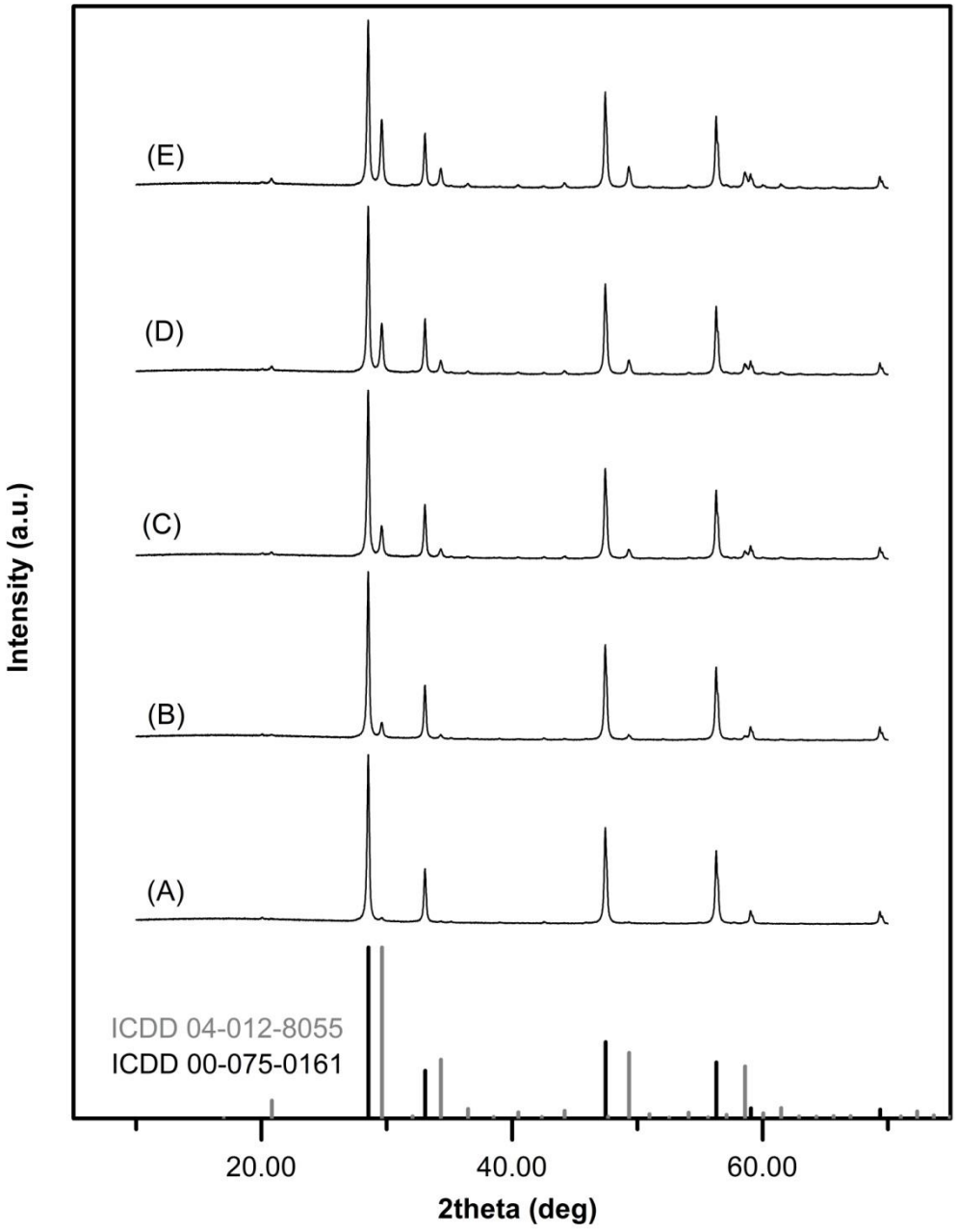

Figure 3.24 XRD Patterns of 10GDC/Yb_2O_3 composites with mol% amounts of Ytterbium as (A) 0.6%, (B) 2.5%, (C) 6.0%, (D) 9.2%, (E) 12.5% after heating at 300 ^{o}C synthesized by Solid State Synthesis Route, ICDD 00-075-0161 and ICDD 04-012-8055

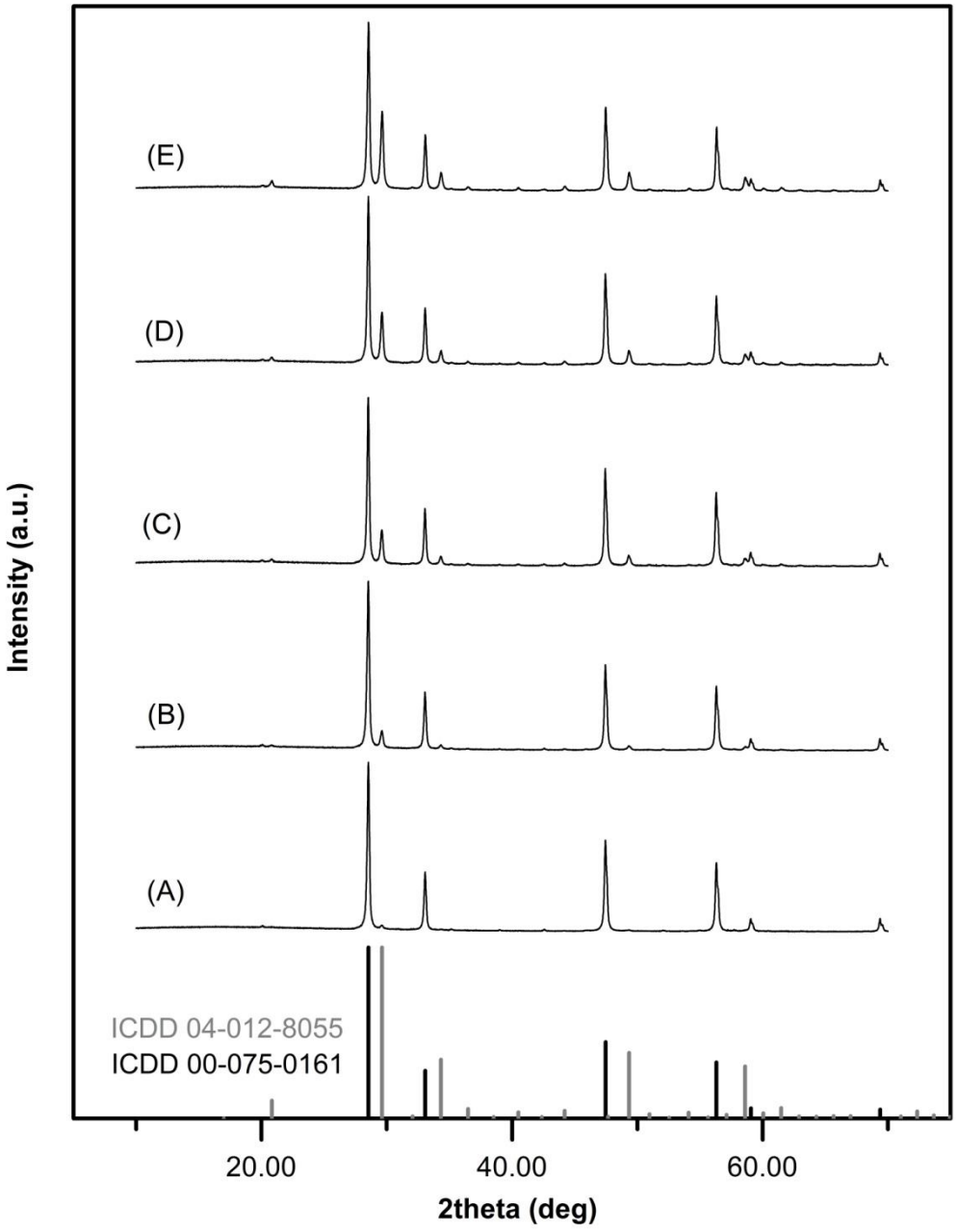

Figure 3.25 XRD Patterns of 10GDC/Yb_2O_3 composites with mol% amounts of Ytterbium as (A) 0.6%, (B) 2.5%, (C) 6.0%, (D) 9.2%, (E) 12.5% after heating at 800 ^{o}C synthesized by Solid State Synthesis Route, ICDD 00-075-0161 and ICDD 04-012-8055

3.1.4.2. SEM and EDX Analysis of 10GDC/Yb_2O_3 composites

The SEM images of (a) 10GDC + 0.6% Yb_2O_3 and (b) 10GDC, heated at 800 ^oC, synthesized by solid state synthesis technique, are given in Figure 3.26. The images give information about the particle size and the morphology of the product. From the pictures it is seen that the morphology of particles does not change with the addition of ytterbium in comparison with 10GDC.

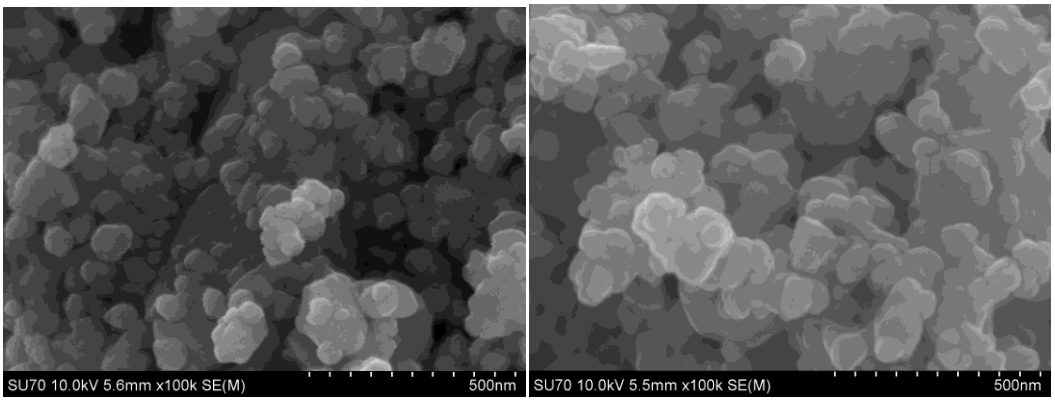

Figure 3.26 SEM images of (a) 10GDC + 0.6% Yb_2O_3 and (b) 10GDC, heated at 800 ^oC with x100k magnifications

EDX analysis, shown in Figure 3.27, 3.28, and 3.29 shows that there is no impurity and it is in a good agreement with nominal compositions of elements. As the amount of Yb_2O_3 doping increases, ytterbium peak intensity increases.

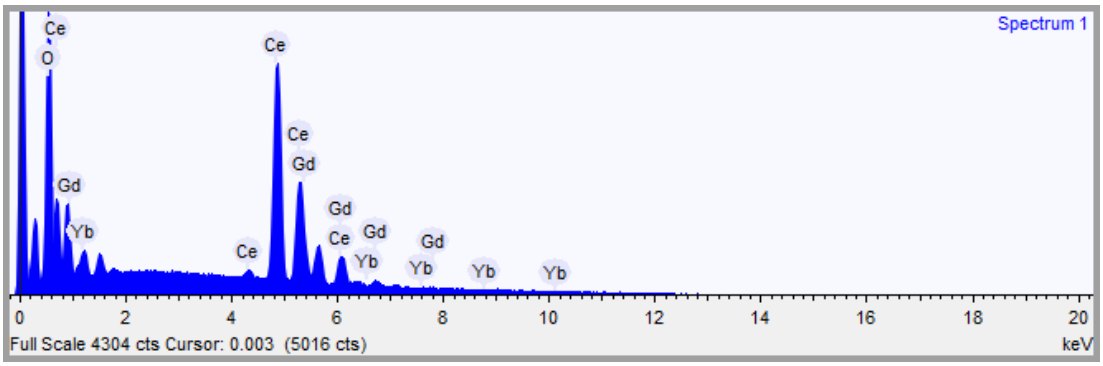

Figure 3.27 EDX spectrum of 10GDC + 0.6% Yb_2O_3

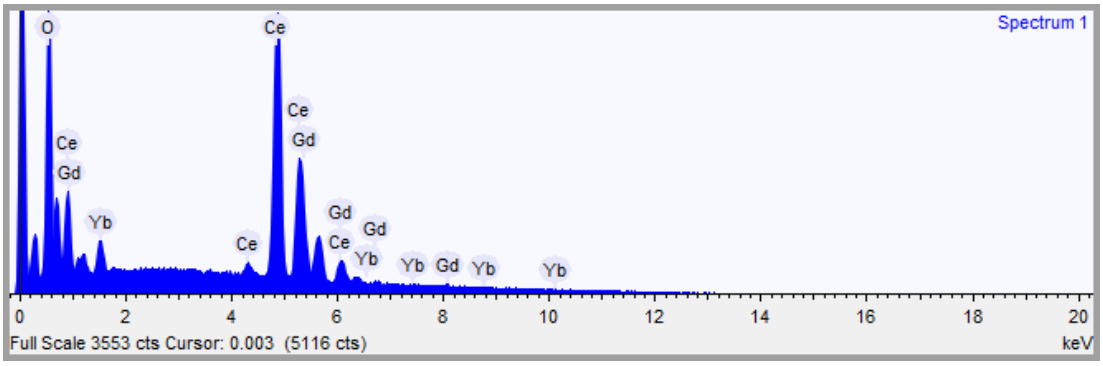

Figure 3.28 EDX spectrum of 10GDC + 2.9% Yb_2O_3

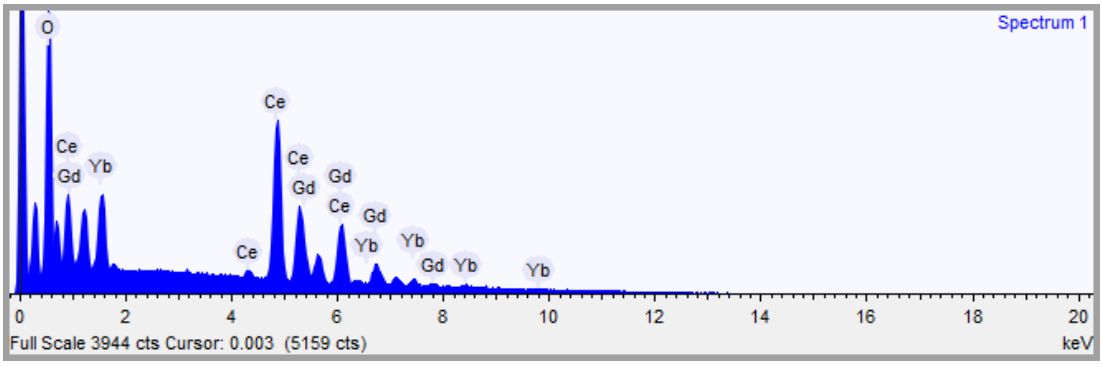

Figure 3.29 EDX spectrum of 10GDC + 6.0% Yb_2O_3

3.2. SOL GEL COMBUSTION RESULTS

3.2.1. Synthesis of 10%Gadolinium Doped Ceria, 10GDC

3.2.1.1. X-Ray Powder Diffraction (XRD) Studies

Figure 3.30 shows X-ray powder diffraction patterns of gadolinium doped ceria synthesized by sol gel combustion technique with 10% Gadolinium doping (10GDC).

Examination of the XRD patterns showed that the obtained product is pure 10GDC by comparison with the ICDD cards 00-075-0161 for 10GDC and 00-088-2165 for Gd_2O_3.

From the XRD patterns it is seen that diffraction lines are broad and wider at lower temperatures. But as the temperature raise, the formation of crystals increase and the size of the crystals increase. As a result, diffraction lines become sharper and narrower. Also no impurity lines belonging to Gd_2O_3 is observed in the XRD result.

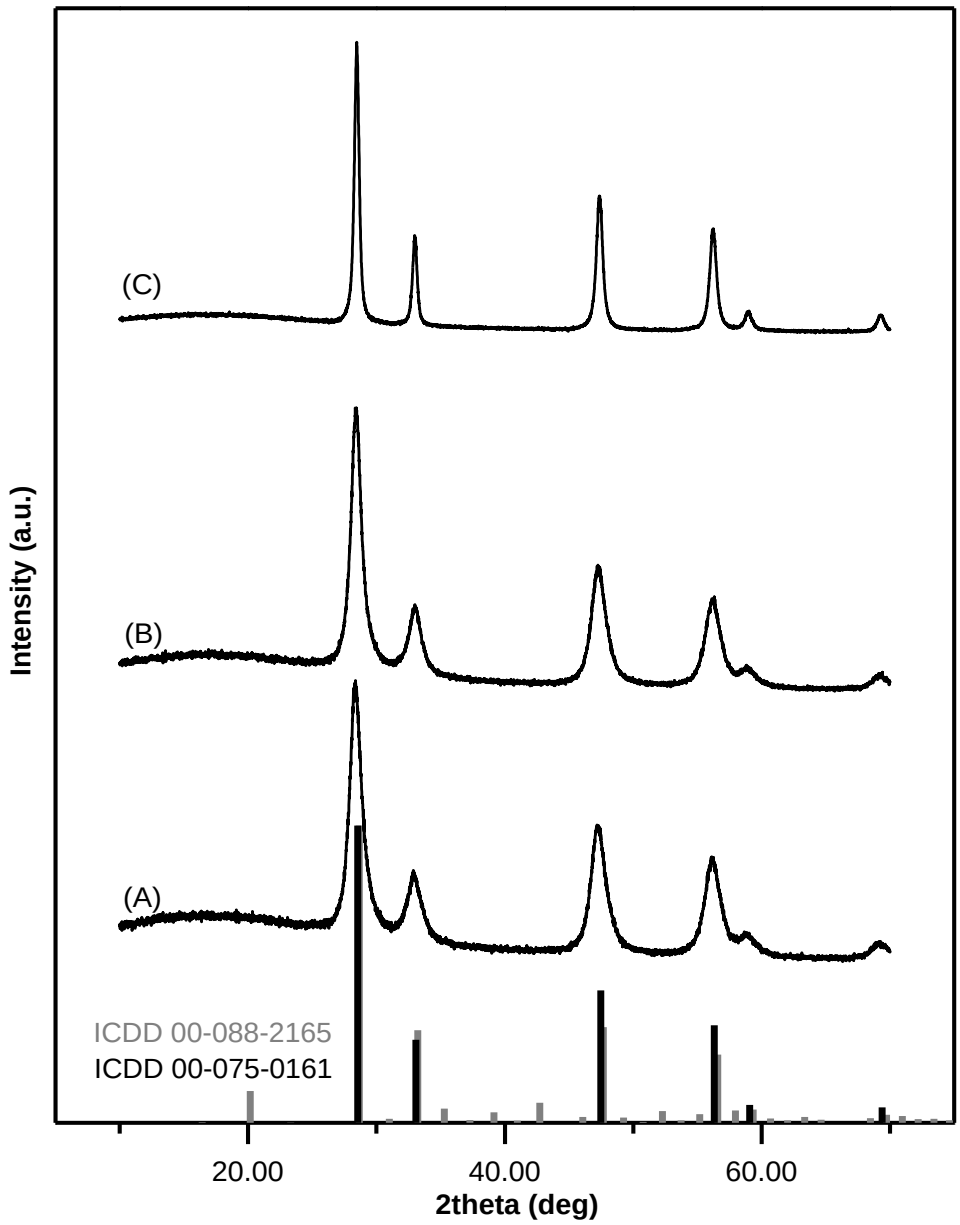

Figure 3.30 XRD Patterns for 10GDC synthesized by Sol Gel Combustion Route for (A) after self burning, (B) after heating at 300 ^{o}C, (C) after heating at 800 ^{o}C, ICDD 00-075-0161 and ICDD 00-088-2165

3.2.1.2. Infrared Spectroscopy Studies

The infrared spectra of 10GDC synthesized by the sol gel combustion method are given in Figure 3.31.

In the gel state of the 10GDC, a wide broad band at around 3250 cm^{-1} is seen related to OH^- ions of water molecules [81]. Also organic parts of complexing agent, ethylene glycol, and NO_3^- group of metal nitrates, give vibrational bands at around 1650, 1450, 1350 and 1040 and 820 cm^{-1} [82, 83].

All the bands mentioned above are disappearing as the temperature is raised up to 800 ^oC. The bands between 2200-1750 cm^{-1} are related to CO_2 in the air and the band at 573 cm^{-1} is predicted to be related to metal-oxide bonds [84].

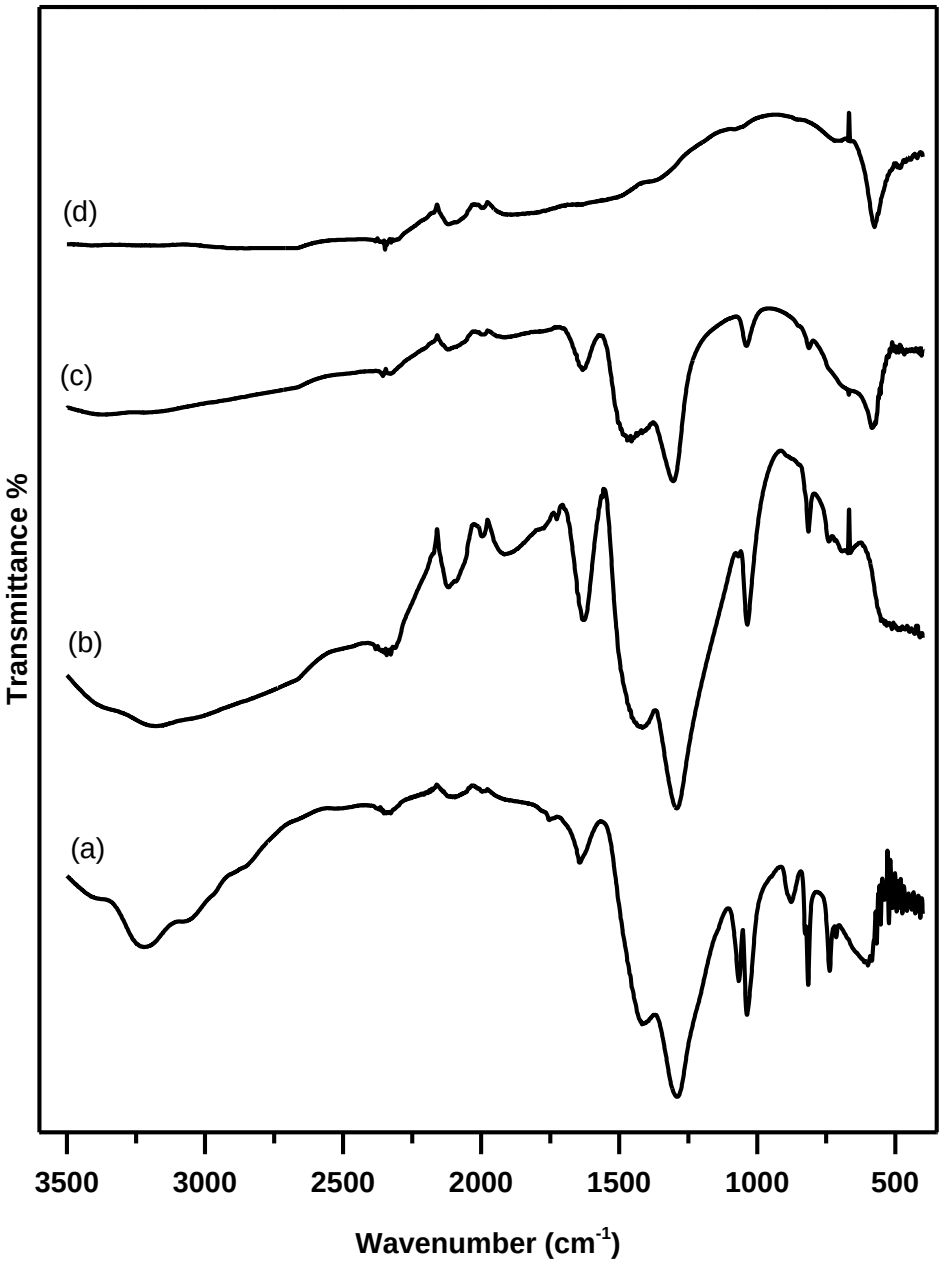

Figure 3.31 IR Spectra of 10GDC in (a) gel state, (b) after self-burning state, (c) after heating at 300 ^{o}C, (d) after heating at 800 ^{o}C

3.2.1.3. SEM and EDX Analysis of 10GDC

The SEM images of 10GDC synthesized by sol gel combustion technique after heating at 800 ^{o}C are given in Figure 3.32. The images give information about the particle size and the morphology of the product. As seen from the pictures, particles are formed as spherical grains.

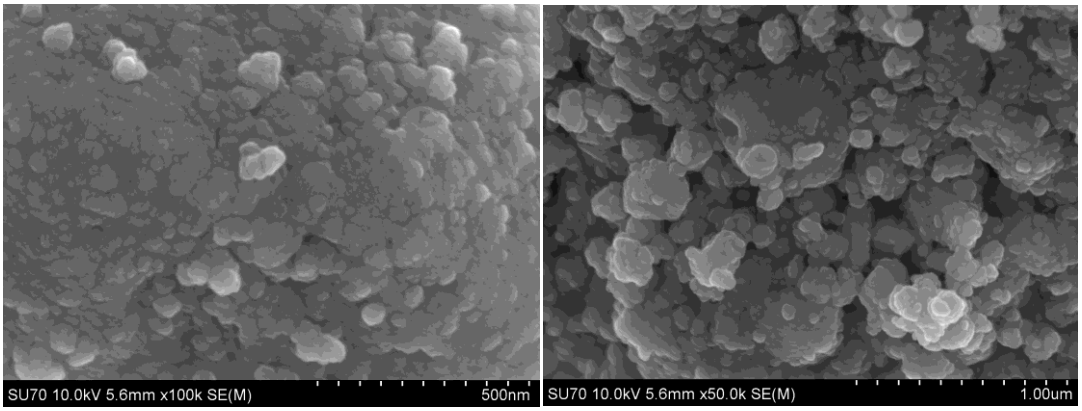

Figure 3.32 SEM images of 10GDC with 100k and 50k magnifications

EDX analysis, shown in figure 3.33, shows that there is no impurity in the product.

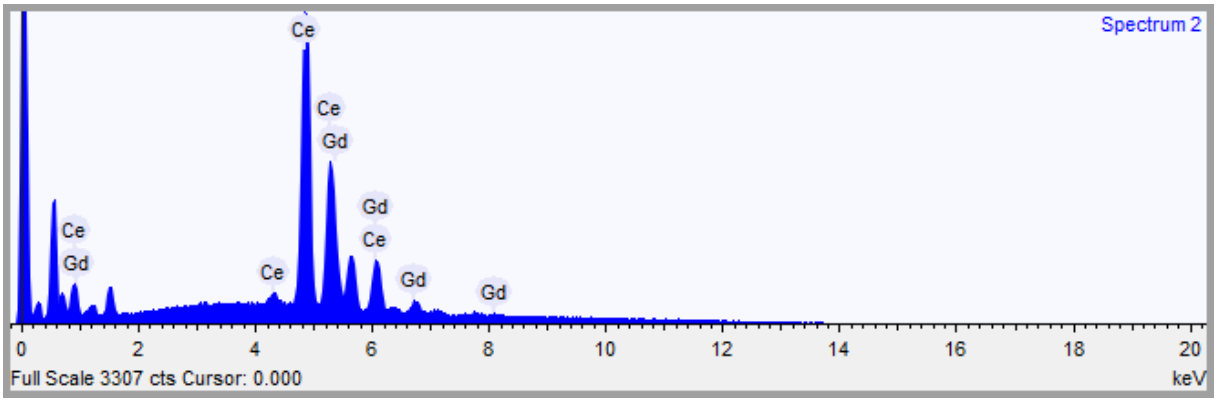

Figure 3.33 EDX spectrum of 10GDC

3.2.2. Synthesis of 10GDC with additional amounts of Cerium

3.2.2.1. X-Ray Powder Diffraction (XRD) Studies

Figure 3.34 shows x-ray powder diffraction patterns of gadolinium doped ceria with additional cerium oxide, CeO_2, synthesized by sol gel combustion technique, after the self-burning state. Figure 3.35 and 3.36 show X-ray powder diffraction patterns of products after heating at 300 ^oC, and 800 ^oC, respectively.

From the XRD patterns it is seen that the single phase product is obtained by comparison with the ICDD cards 00-075-0161 for 10GDC and 00-088-2165 for Gd_2O_3.

The diffraction lines in the patterns are broad and wide at lower temperatures. As the temperature rise, the diffraction lines become narrower and sharper, leading to the result of increase in the formation and size of the crystals. No impurity lines or additional phase lines belonging to Gd_2O_3 is observed in the XRD patterns.

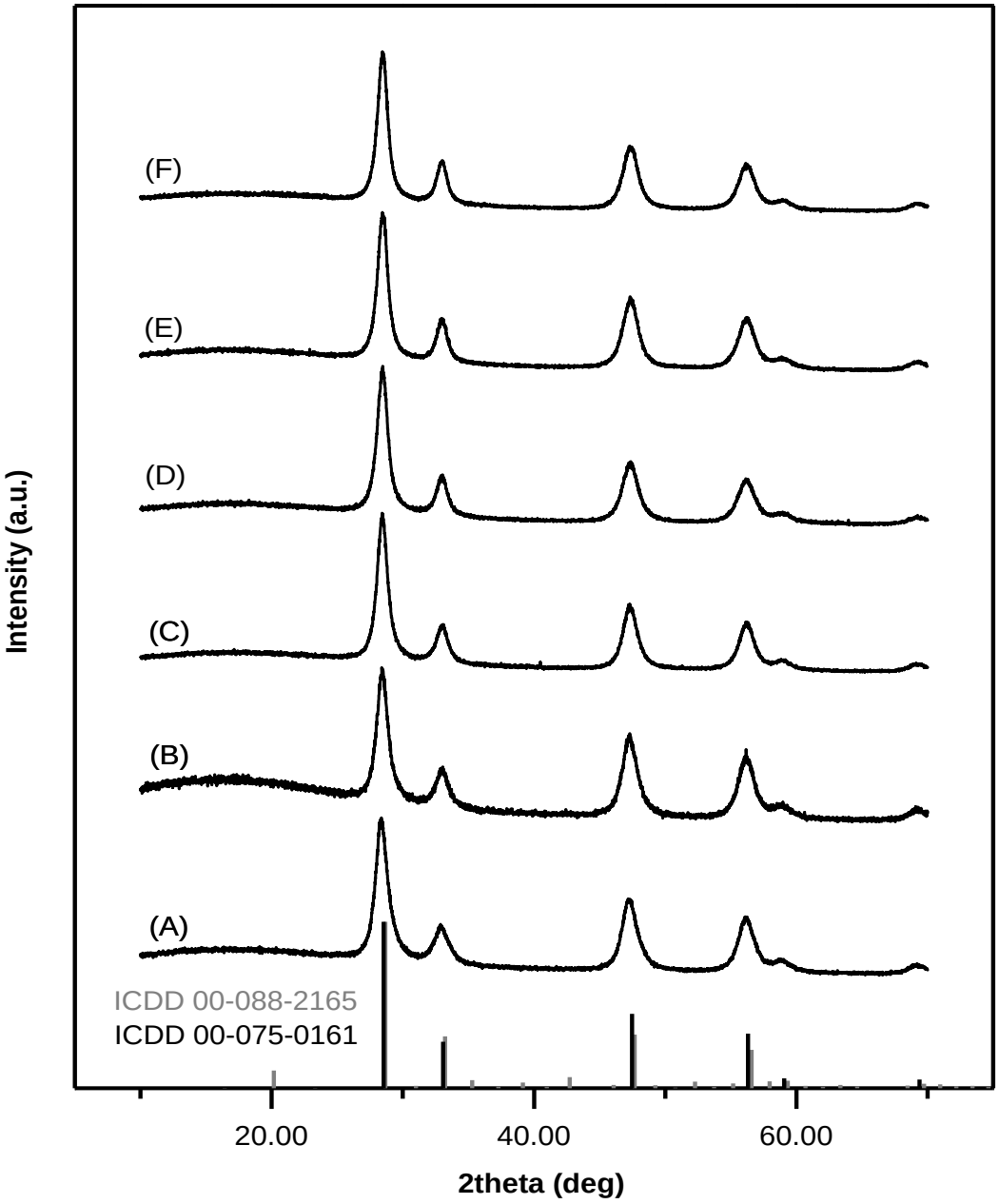

Figure 3.34 XRD Patterns of (A) 10GDC with additional amounts of Cerium as (B) 1%, (C) 5%, (D) 10%, (E) 15%, (F) 20% after self-burning, synthesized by Sol Gel Combustion Route, ICDD 00-075-0161 and ICDD 00-088-2165

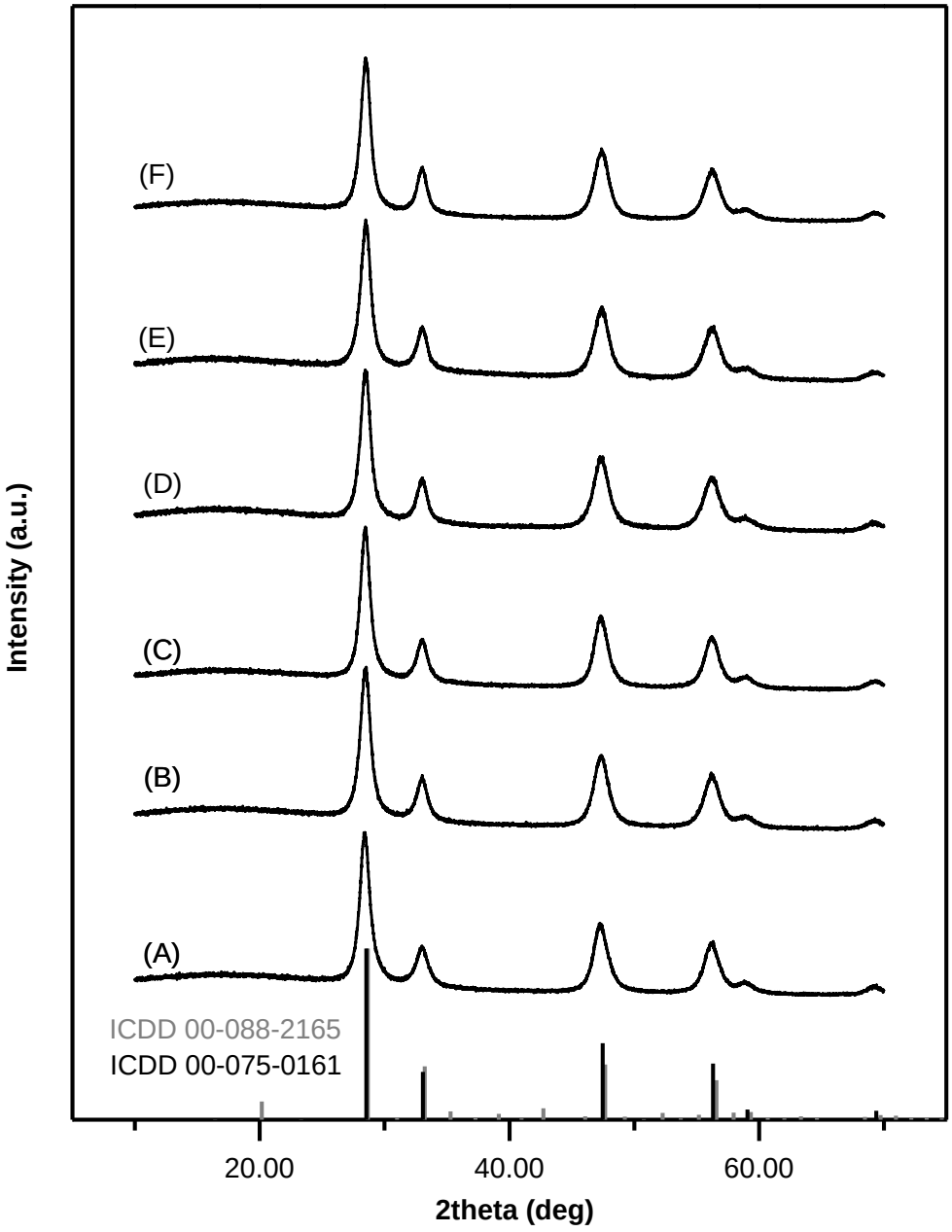

Figure 3.35 XRD Patterns of (A) 10GDC with additional amounts of Cerium as (B) 1%, (C) 5%, (D) 10%, (E) 15%, (F) 20% after heating at 300 ^{o}C, synthesized by Sol Gel Combustion Route, ICDD 00-075-0161 and ICDD 00-088-2165

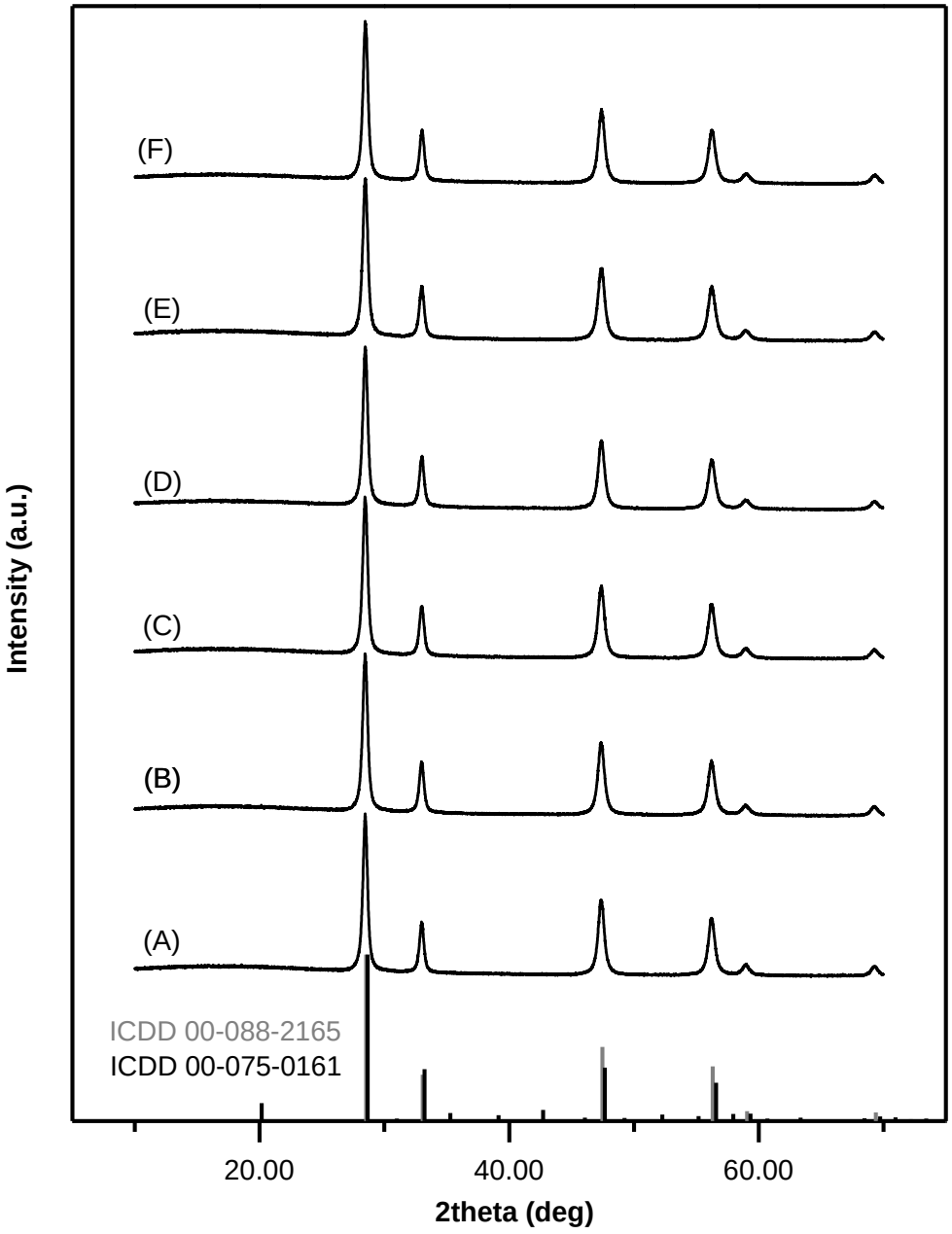

Figure 3.36 XRD Patterns of (A) 10GDC with additional amounts of Cerium as (B) 1%, (C) 5%, (D) 10%, (E) 15%, (F) 20% after heating at 800 ^{o}C, synthesized by Sol Gel Combustion Route, ICDD 00-075-0161 and ICDD 00-088-2165

3.2.2.2. Infrared Spectroscopy Studies

The infrared spectra of 10GDC with additional amounts of cerium oxide, CeO_2, in gel state, synthesized by the sol gel combustion method are given in Figure 3.37. Figure 3.38, Figure 3.39 and Figure 3.40 represent spectra for after self burning state, after heating at 300 ^oC and 800 ^oC, respectively.

Similar to that of 10GDC, in the gel state, a wide broad band at around 3250 cm^{-1} is seen related to OH^- ions of water molecules [81]. Also organic parts of complexing agent, ethylene glycol, give vibrational bands at around 1650, 1450, 1350 and 1040 cm^{-1} [82]. The band at 820 cm^{-1} can be related to NO_3^- group [83].

All the bands mentioned above are disappearing as the temperature is raised up to 800 ^oC. The bands between 2200-1750 cm^{-1} are related to CO_2 in the air and the band at 573 cm^{-1} is predicted to be related to metal-oxide bonds [84].

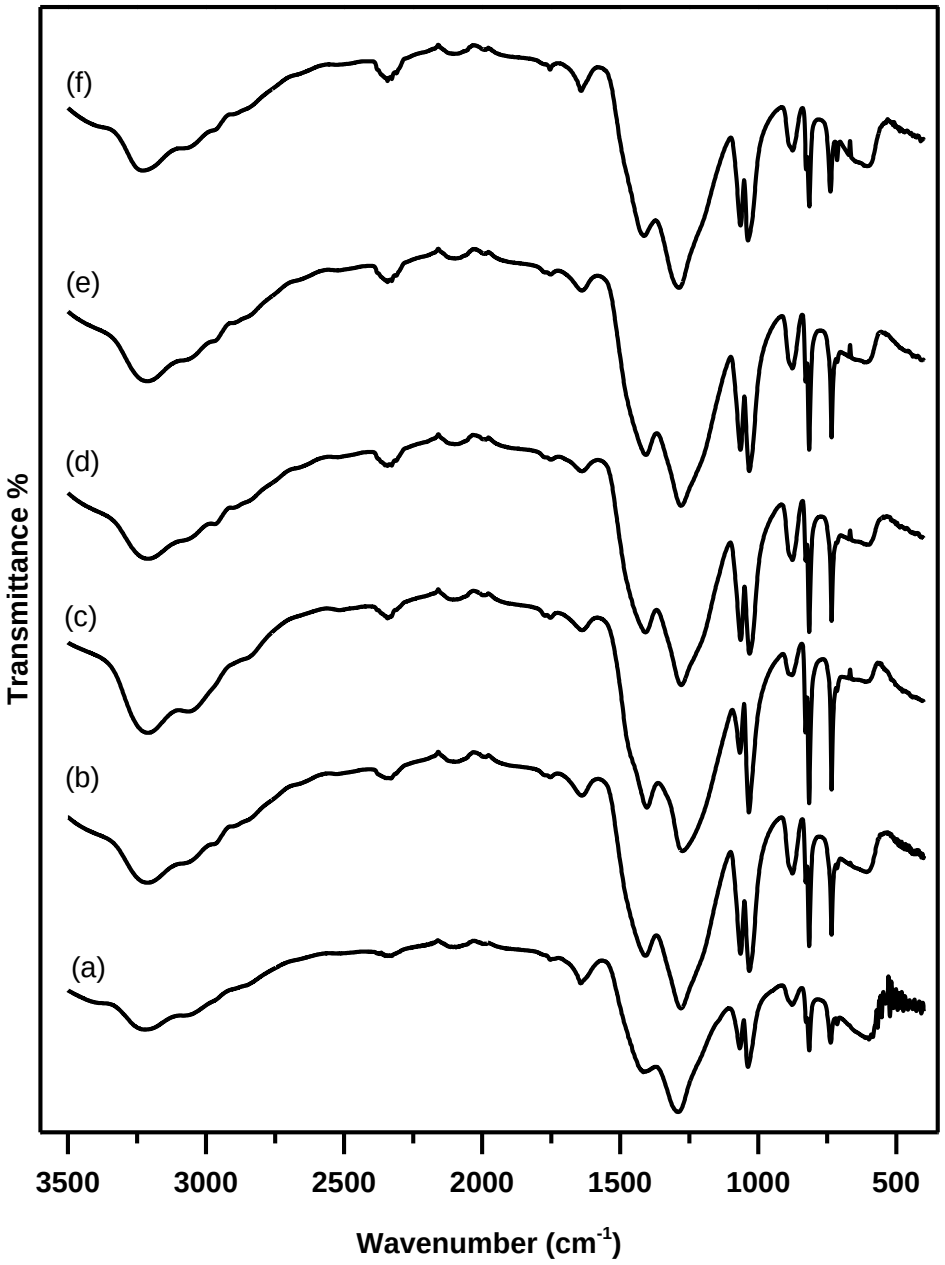

Figure 3.37 IR Spectra of (a) 10GDC with additional amounts of Cerium as (b) 1%, (c) 5%, (d) 10%, (e) 15%, (f) 20% in gel state synthesized by Sol Gel Combustion Route

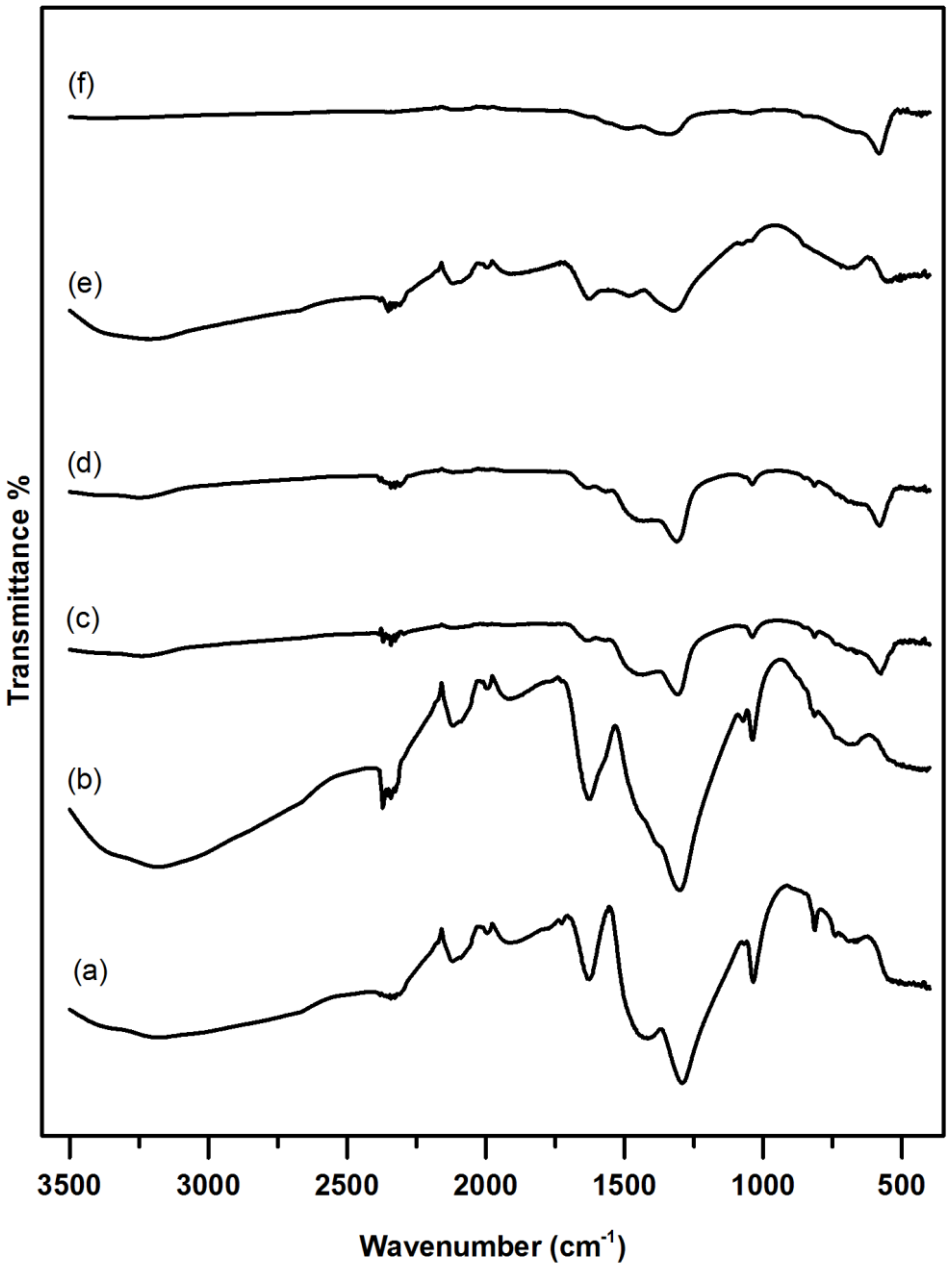

Figure 3.38 IR Spectra of (a) 10GDC with additional amounts of Cerium as (b) 1%, (c) 5%, (d) 10%, (e) 15%, (f) 20% after self burning, synthesized by Sol Gel Combustion Route

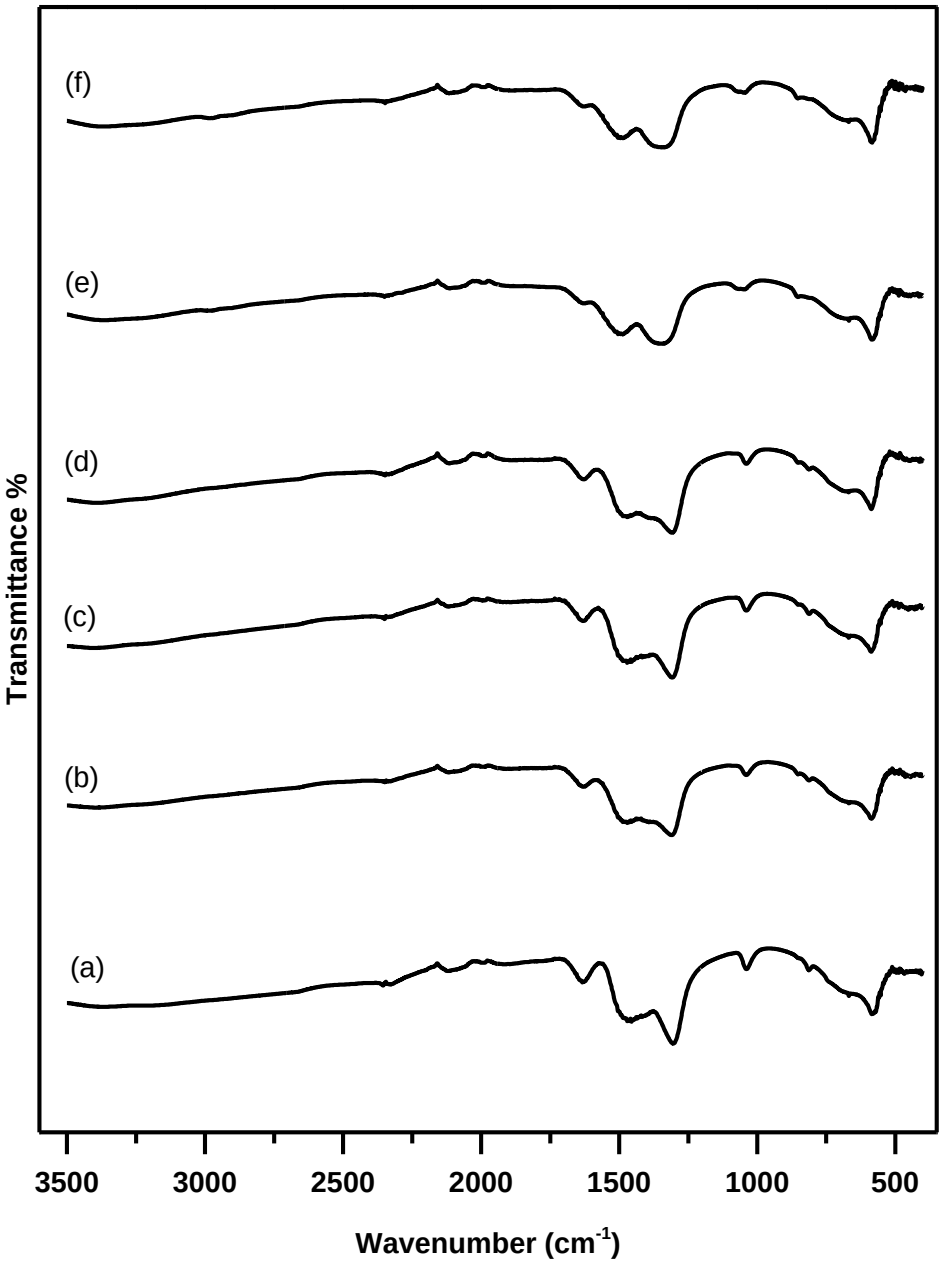

Figure 3.39 IR Spectra of (a) 10GDC with additional amounts of Cerium as (b) 1%, (c) 5%, (d) 10%, (e) 15%, (f) 20% after heating at 300 ^{o}C synthesized by Sol Gel Combustion Route

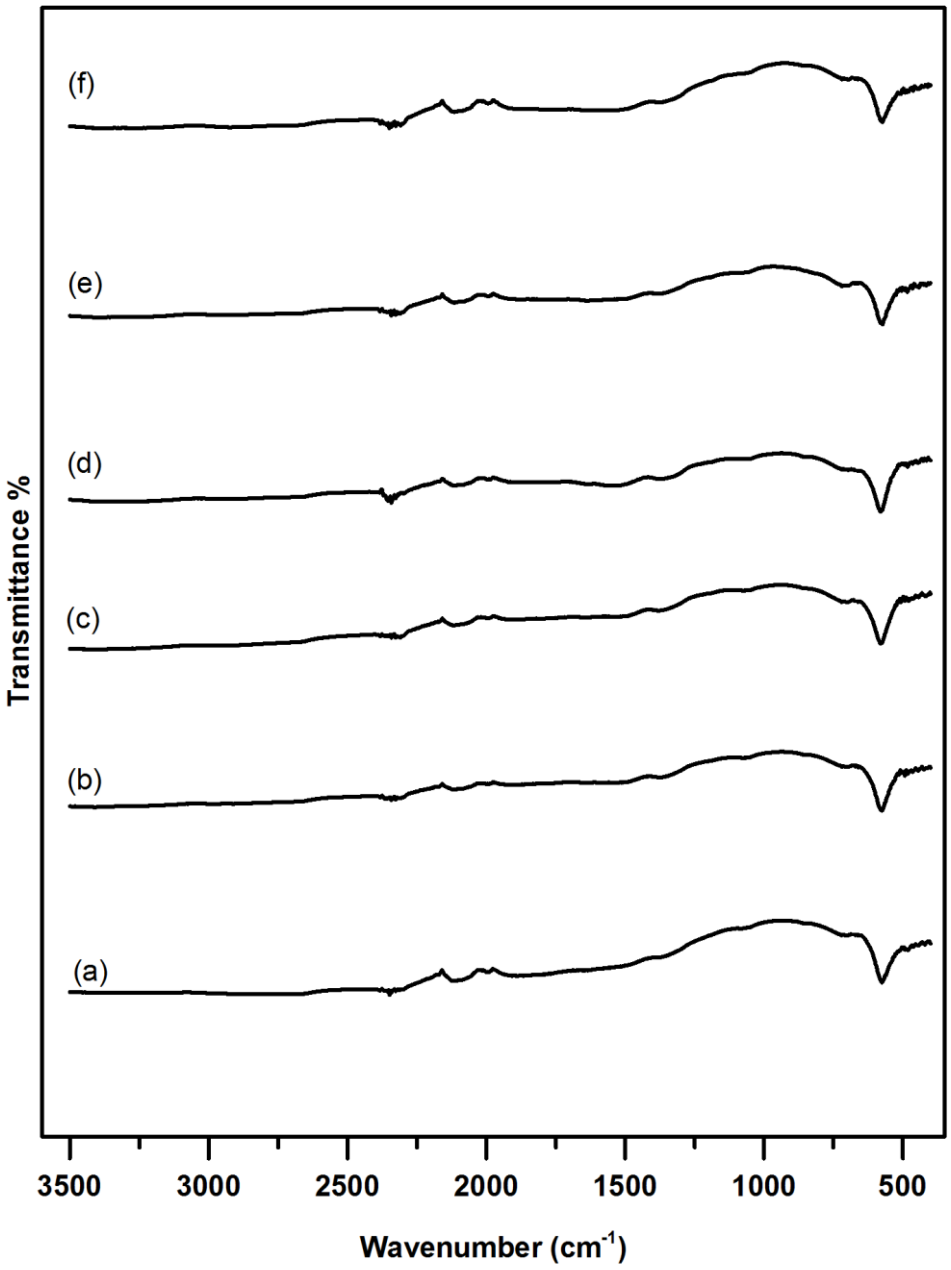

Figure 3.40 IR Spectra of (a) 10GDC with additional amounts of Cerium as (b) 1%, (c) 5%, (d) 10%, (e) 15%, (f) 20% after heating at 800 ^{o}C synthesized by Sol Gel Combustion Route

3.2.2.3. SEM and EDX Analysis of 10GDC with additional amounts of Cerium

The SEM images of 10GDC + 15%CeO_2 (a) after self burning state and (b) after heating at 800 ^oC, synthesized by sol gel combustion technique, is given in Figure 3.41. The images give information about the particle size and the morphology of the product. In the second picture, it is seen that more crystals with better shapes are formed.

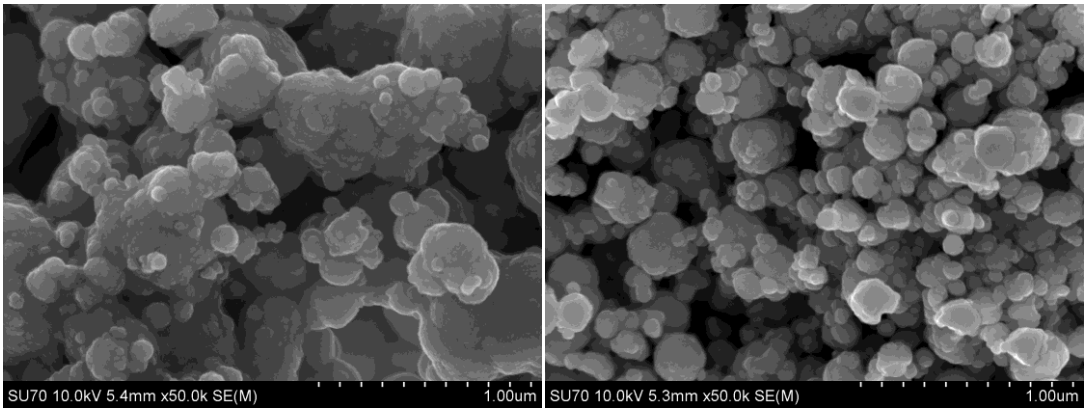

Figure 3.41 SEM images of 10GDC + 15% CeO_2 with 50k magnifications (a) after self burning state and (b) after heating at 800 ^oC

EDX analysis, shown in Figure 3.42, 3.43, and 3.44 shows that there is no impurity and it is in a good agreement with nominal compositions of elements. As the Ce amount in total increase, there is a decrease in the intensity of Gd lines.

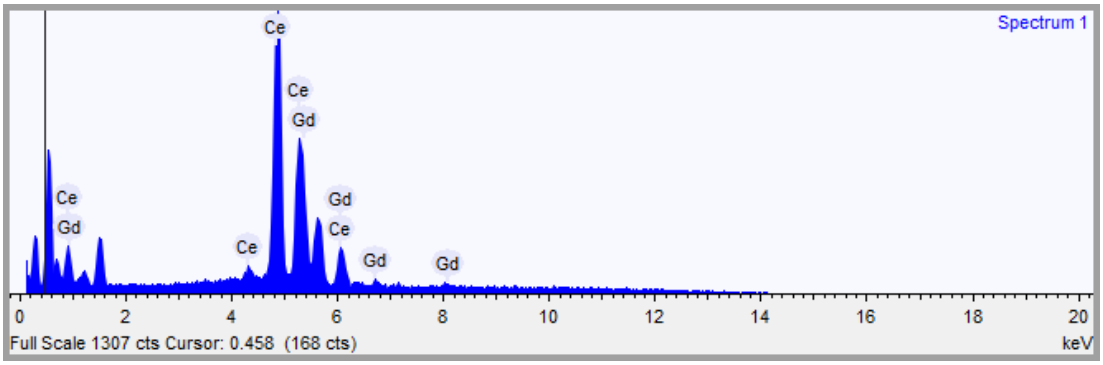

Figure 3.42 EDX spectrum of 10GDC + 10% CeO_2

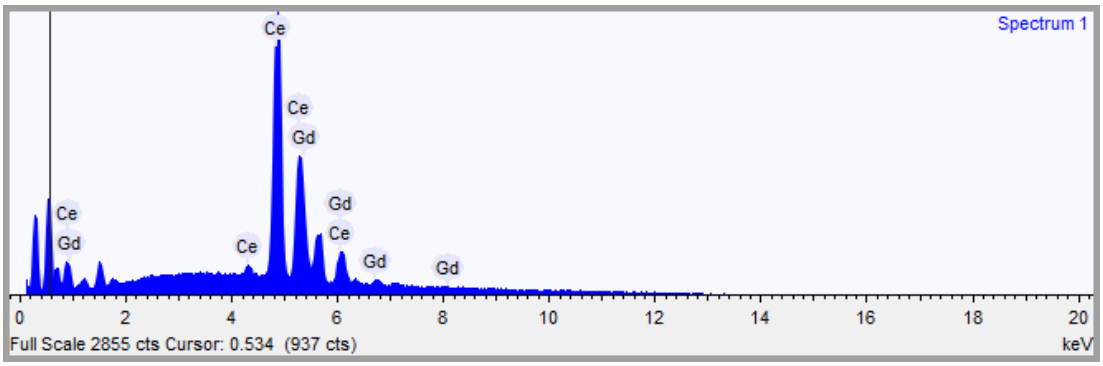

Figure 3.43 EDX spectrum of 10GDC + 15% CeO_2

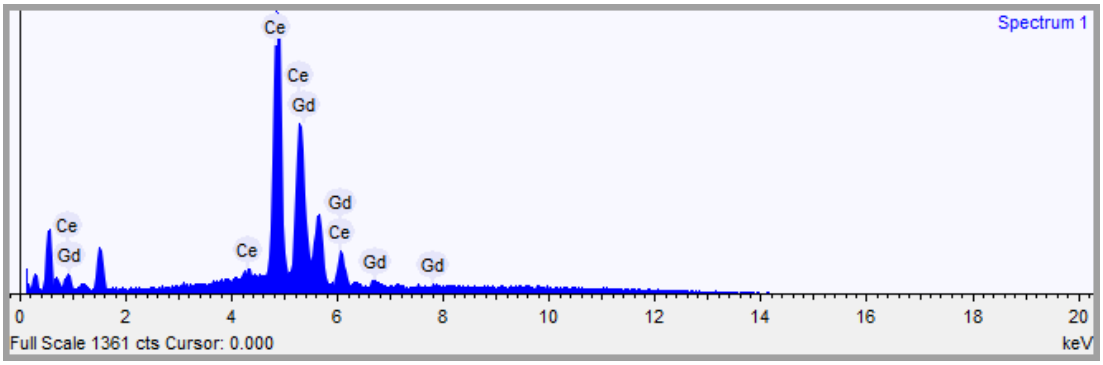

Figure 3.44 EDX spectrum of 10GDC + 20% CeO_2

3.2.3. Synthesis of 10GDC/Y_2O_3 composites

3.2.3.1. X-Ray Powder Diffraction (XRD) Studies

Figure 3.45 shows X-ray powder diffraction patterns of gadolinium doped ceria with addition of yttrium oxide, Y_2O_3, synthesized by sol gel combustion technique, after the self-burning states. X-ray powder diffraction patterns of products after heating at 300 ^oC and 800 ^oC are given in Figure 3.46 and 3.47, respectively.

Examination of the XRD patterns resulted in the successful synthesis of single phase crystal samples of GDC/Y_2O_3 compared with the ICDD cards 00-075-0161 for 10GDC and 00-086-1326 for Y_2O_3.

It is seen from the patterns as lines are broad and wider at lower temperatures. However, the formation and the size of the crystals as the temperature rise. As a result, lines become sharper and narrower. Also no impurity or additional phase lines belonging to Y_2O_3 is observed in the final XRD patterns.

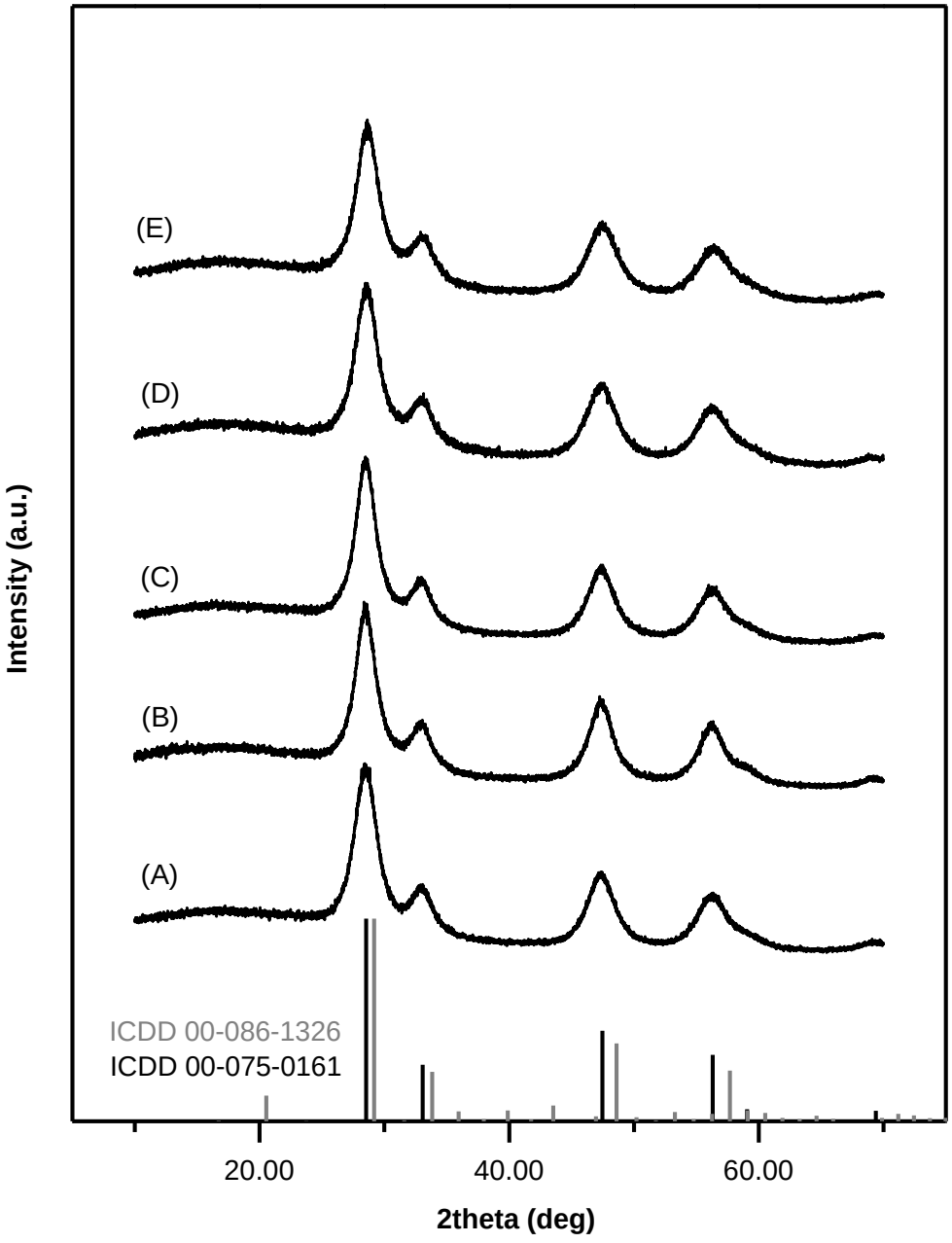

Figure 3.45 XRD Patterns of 10GDC/Y_2O_3 composites with mol% amounts of Yttrium as (A) 1%, (B) 5%, (C) 10%, (D) 15%, (E) 20% after self-burning state synthesized by Sol Gel Combustion Route, ICDD 00-075-0161 and ICDD 00-086-1326

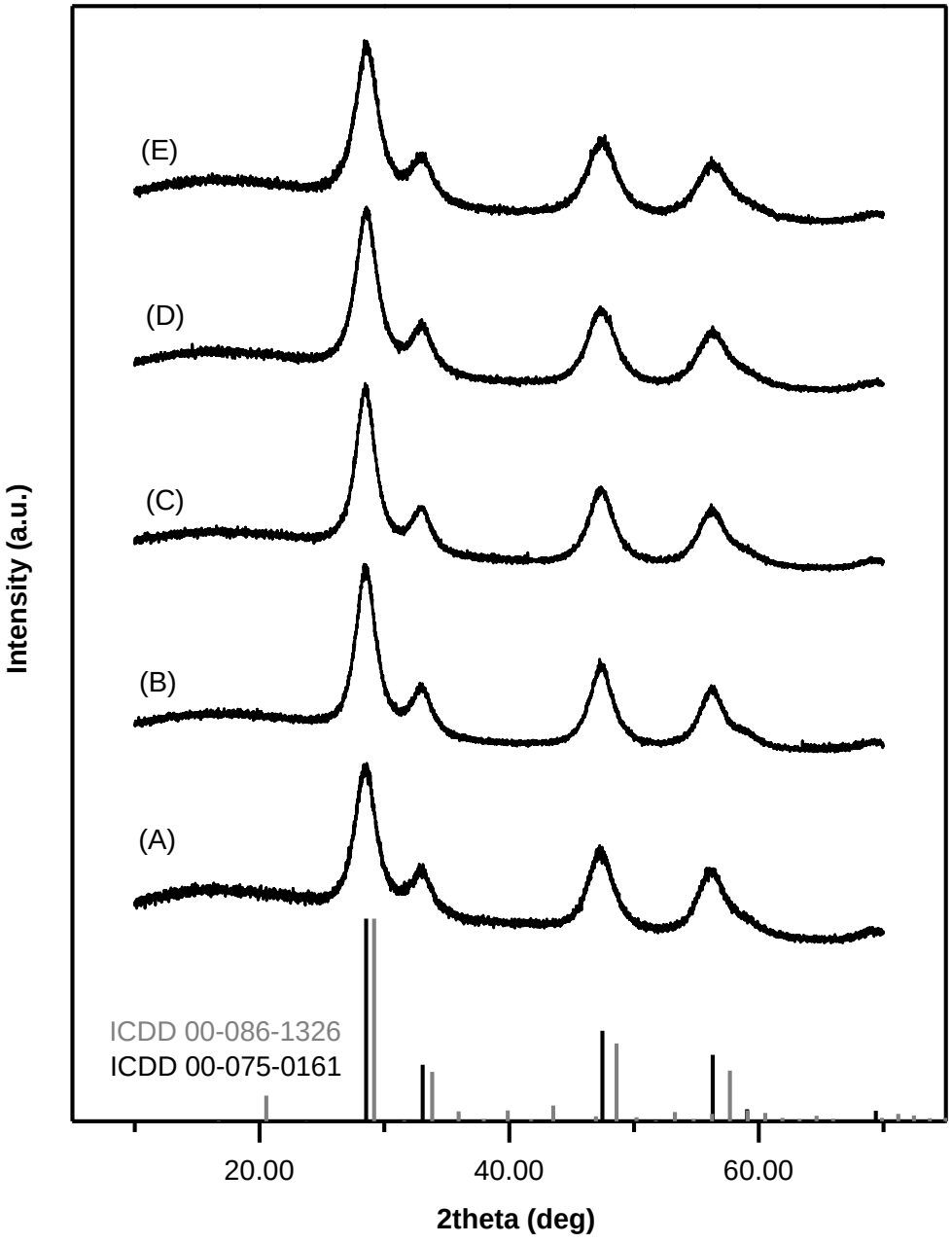

Figure 3.46 XRD Patterns of 10GDC/Y_2O_3 composites with mol% amounts of Yttrium as (A) 1%, (B) 5%, (C) 10%, (D) 15%, (E) 20% after heating at 300 ^{o}C synthesized by Sol Gel Combustion Route, ICDD 00-075-0161 and ICDD 00-086-1326

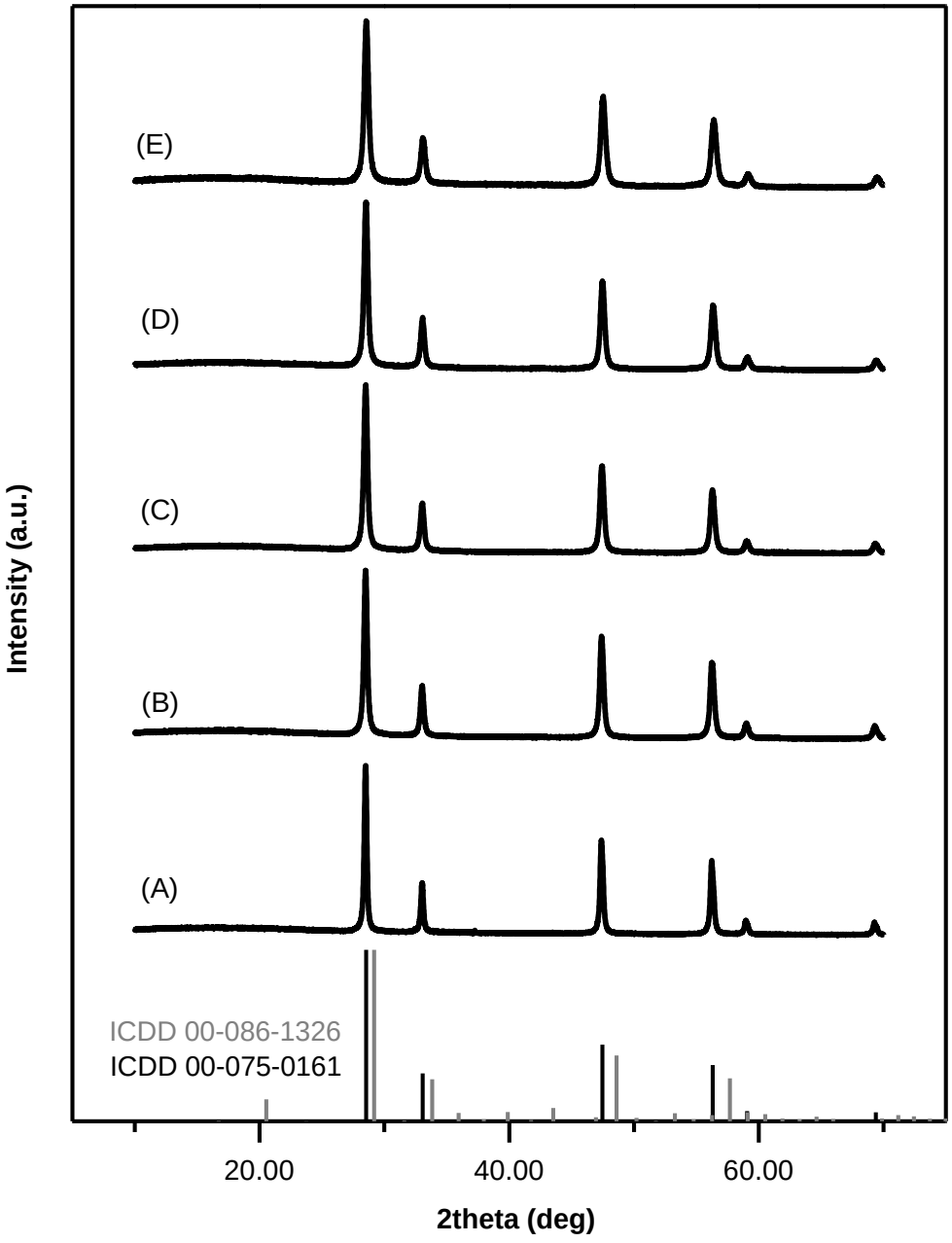

Figure 3.47 XRD Patterns of 10GDC/Y_2O_3 composites with mol% amounts of Yttrium as (A) 1%, (B) 5%, (C) 10%, (D) 15%, (E) 20% after heating at 800 ^oC synthesized by Sol Gel Combustion Route, ICDD 00-075-0161 and ICDD 00-086-1326

3.2.3.2. Infrared Spectroscopy Studies

The infrared spectra of 10GDC with addition of yttrium oxide, Y_2O_3, in gel state, synthesized by the sol gel combustion method are given in Figure 3.48. Figure 3.49, Figure 3.50 and Figure 3.51 represent spectra for after self-burning state, after heating at 300 ^oC and 800 ^oC, respectively.

The wide broad band at around 3250 cm^{-1} is related to OH^- ions of water molecules [81]. The bands at around 1650, 1450, 1350 and 1040 cm^{-1} are the vibrational bands of ethylene glycol [82]. The band at 820 cm^{-1} can be assigned to NO_3^- group [83].

As the temperature rise up to 800 ^oC, most of the bands related to organic parts disappear. The bands between 2200-1750 cm^{-1} are related to CO_2 in the air and the band at 573 cm^{-1} is predicted to be related to metal-oxide bonds [84].

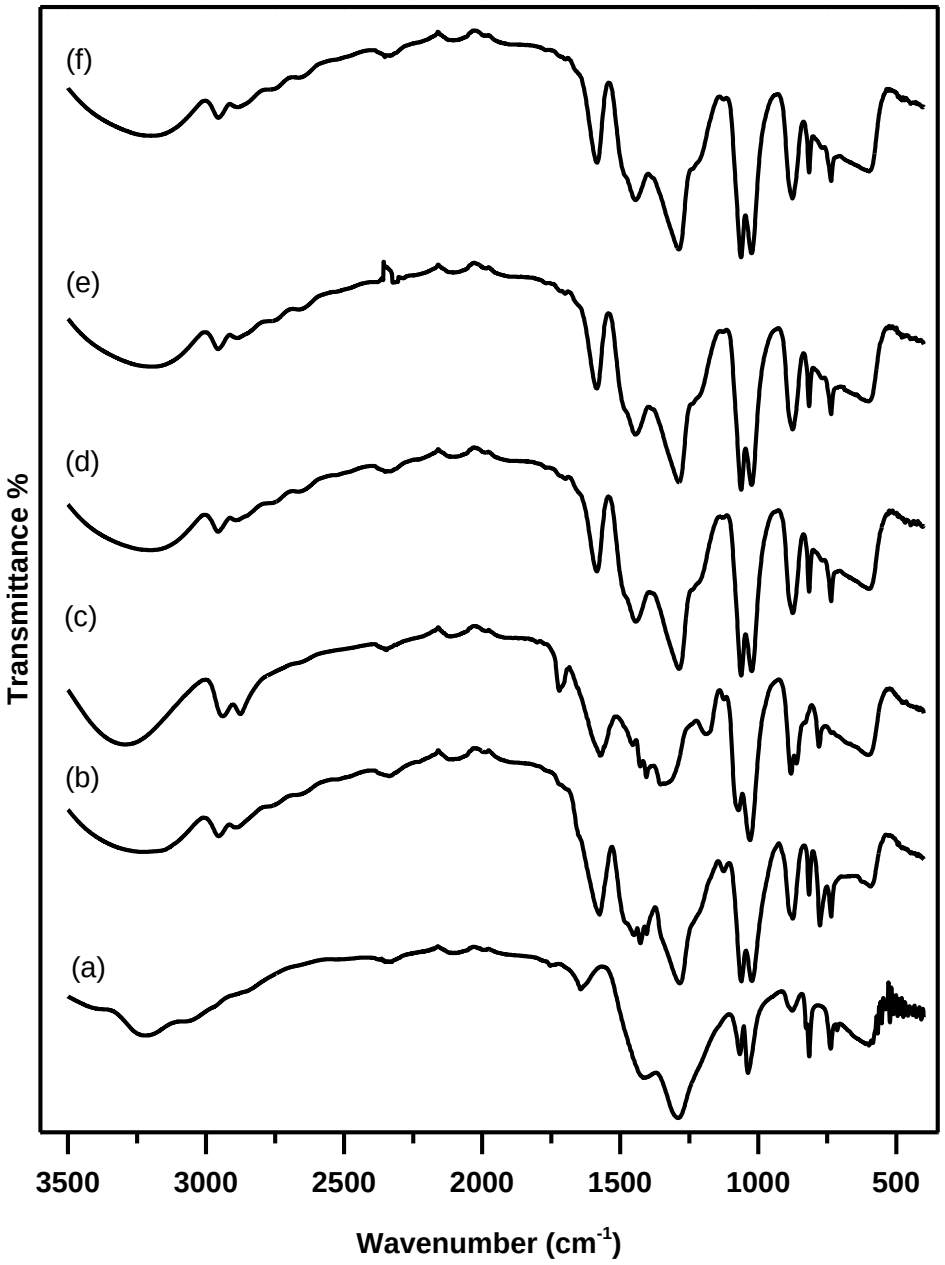

Figure 3.48 IR Spectra of (a) 10GDC and 10GDC/Y_2O_3 composites with mol% amounts of Yttrium as (b) 1%, (c) 5%, (d) 10%, (e) 15%, (f) 20% in gel state synthesized by Sol Gel Combustion Route

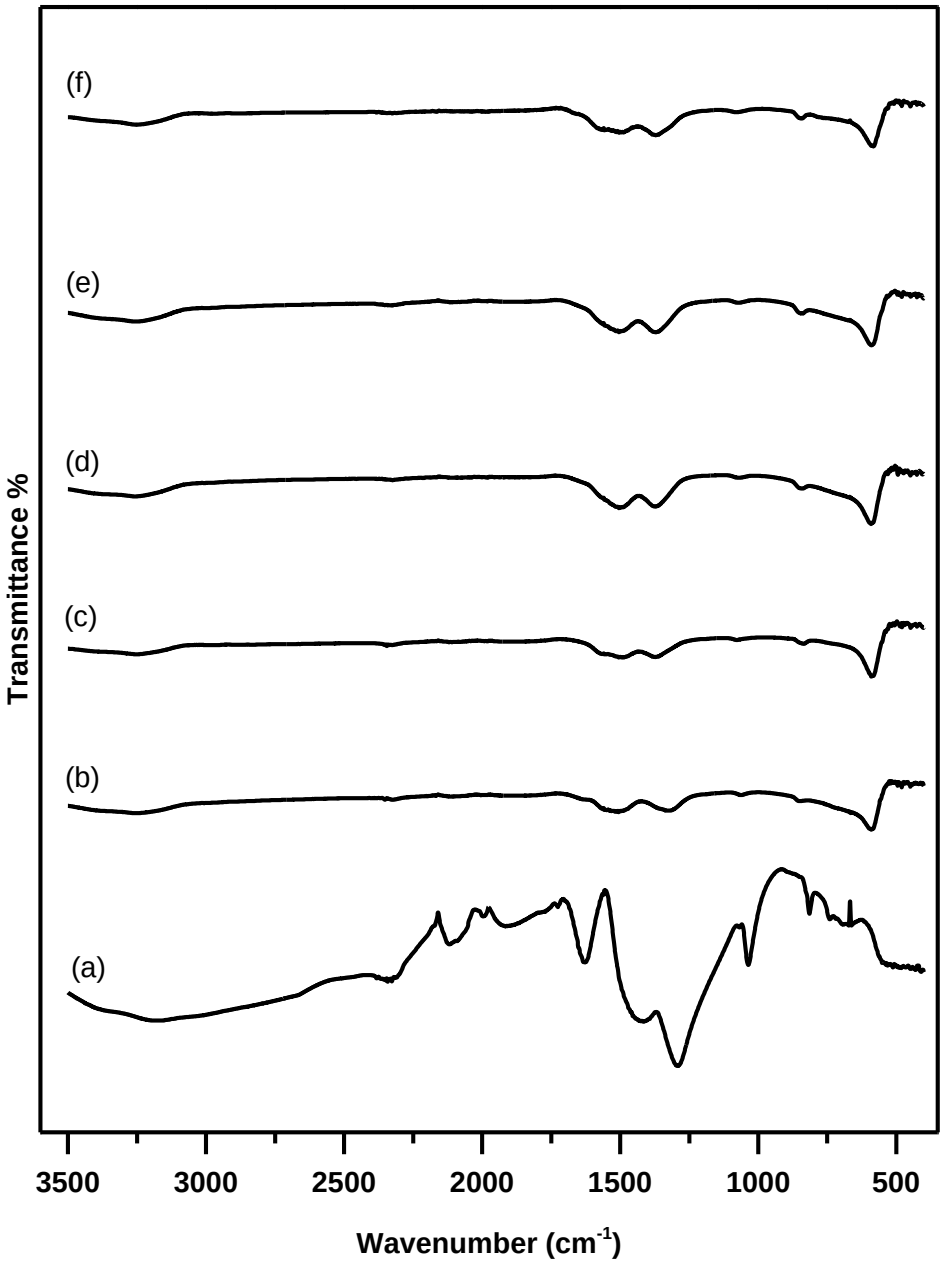

Figure 3.49 IR Spectra of (a) 10GDC and 10GDC/Y_2O_3 composites with mol% amounts of Yttrium as (b) 1%, (c) 5%, (d) 10%, (e) 15%, (f) 20% after self burning state synthesized by Sol Gel Combustion Route

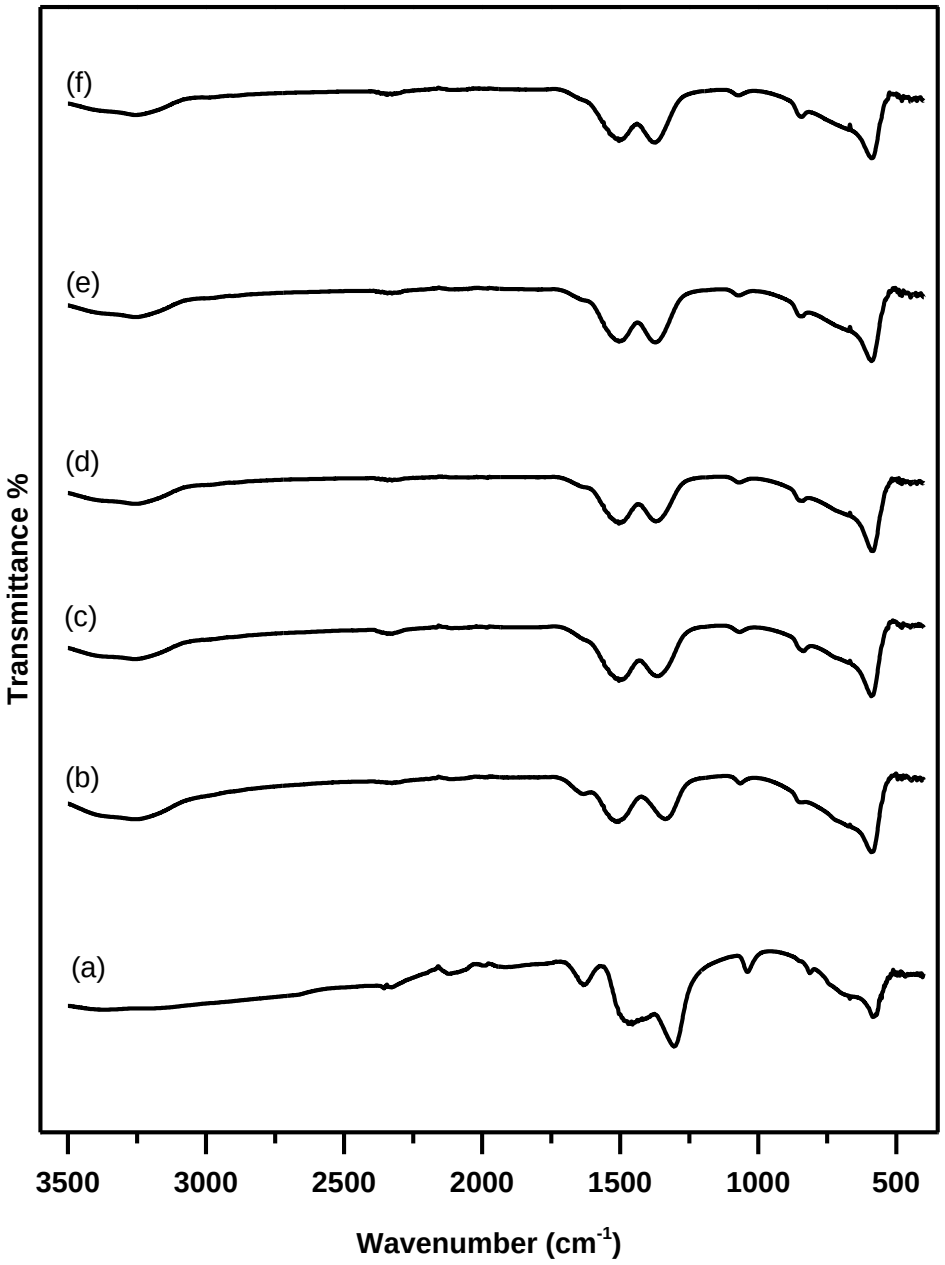

Figure 3.50 IR Spectra of (a) 10GDC and 10GDC/Y_2O_3 composites with mol% amounts of Yttrium as (b) 1%, (c) 5%, (d) 10%, (e) 15%, (f) 20% after heating at 300 ^{o}C synthesized by Sol Gel Combustion Route

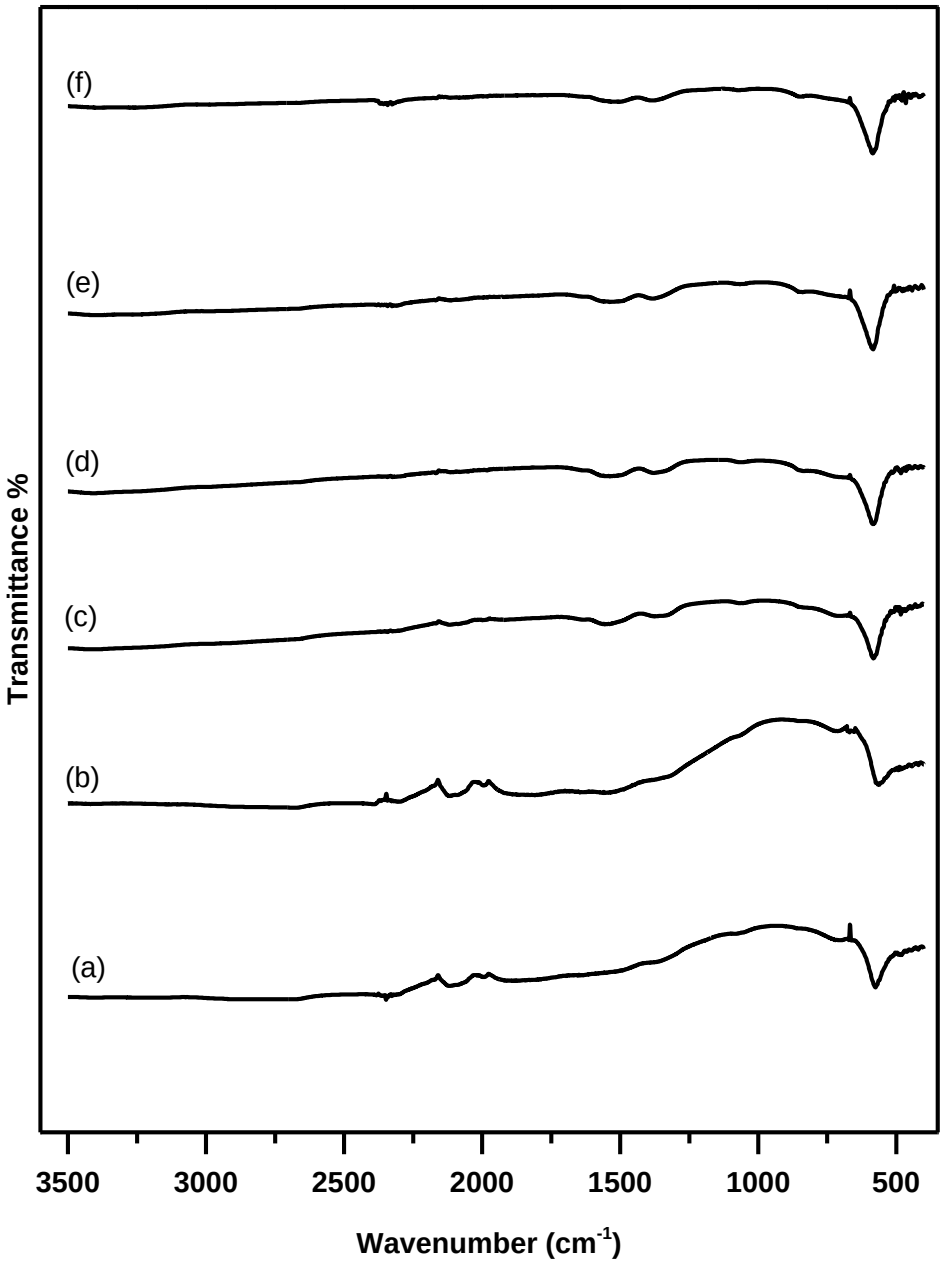

Figure 3.51 IR Spectra of (a) 10GDC and 10GDC/Y_2O_3 composites with mol% amounts of Yttrium as (b) 1%, (c) 5%, (d) 10%, (e) 15%, (f) 20% after heating at 800 ^{o}C synthesized by Sol Gel Combustion Route

3.2.3.3. SEM and EDX Analysis of 10GDC/Y_2O_3 composites

The SEM images of (a) 10GDC + 5% Y_2O_3 and (b) 10GDC + 10% Y_2O_3 both heated at 800 ^oC, synthesized by sol gel combustion technique, is given in Figure 3.52. The images give information about the particle size and the morphology of the product. From the pictures it is seen that the morphology of particles does not depend on the nature and amount of additional oxide.

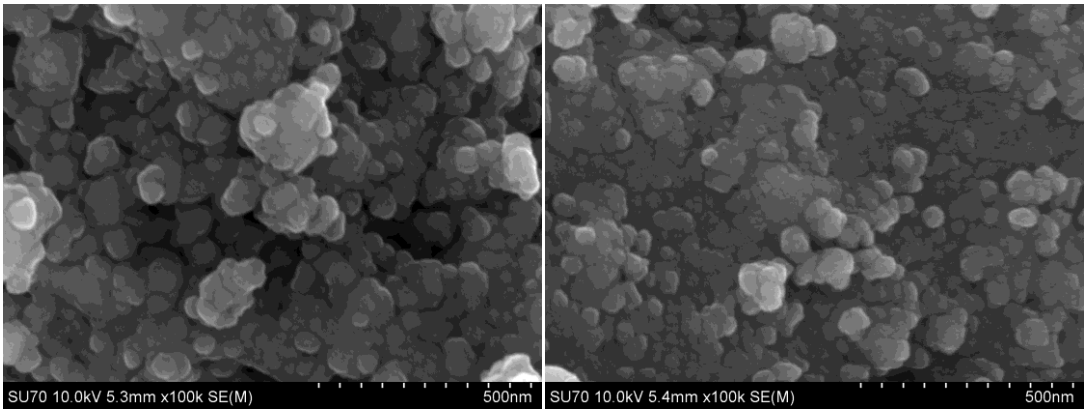

Figure 3.52 SEM images of (a) 10GDC + 5% Y_2O_3 and (b) 10GDC + 10% Y_2O_3 both heated at 800 ^oC with 100k magnifications

EDX analysis, shown in Figure 3.53, 3.54, and 3.55 shows that there is no impurity and it is in a good agreement with nominal compositions of elements. As the amount of Y_2O_3 doping increases, yttrium peak intensity increases.

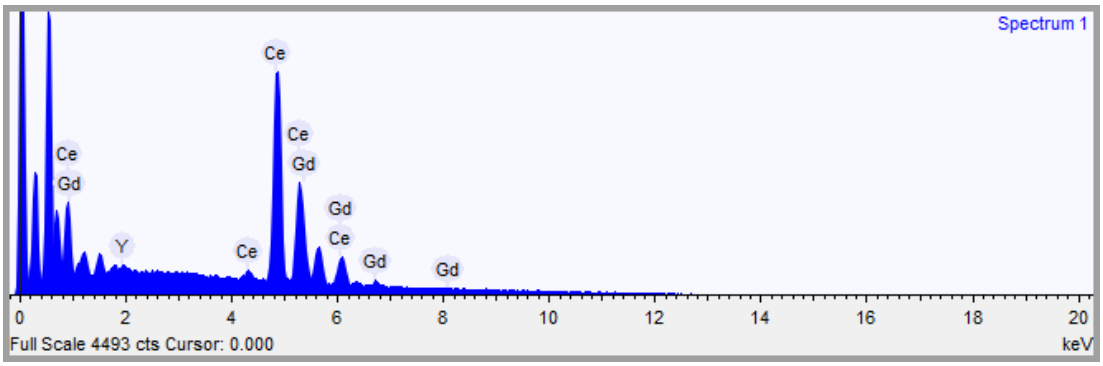

Figure 3.53 EDX spectrum of 10GDC + 1% Y_2O_3

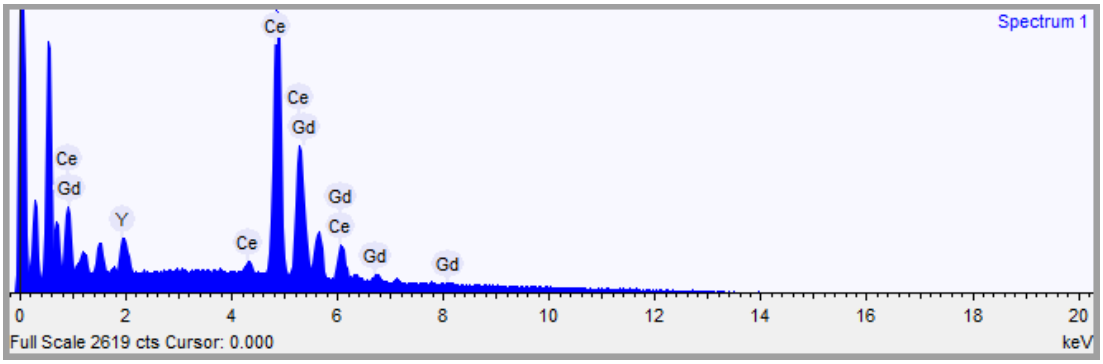

Figure 3.54 EDX spectrum of 10GDC + 5% Y_2O_3

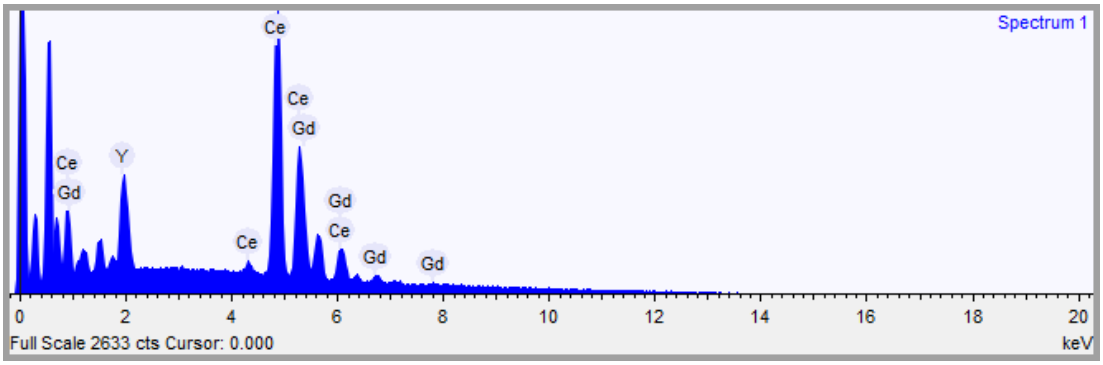

Figure 3.55 EDX spectrum of 10GDC + 10% Y_2O_3

3.2.4. Synthesis of 10GDC/Yb_2O_3 composites

3.2.4.1. X-Ray Powder Diffraction (XRD) Studies

Figure 3.56 shows X-ray powder diffraction patterns of gadolinium doped ceria with addition of ytterbium oxide, Yb_2O_3, synthesized by sol gel combustion technique, after the self-burning state. X-ray powder diffraction patterns of products after heating at 300 ^oC, and 800 ^oC, are given in Figure 3.57 and 3.58, respectively.

Examination of the XRD patterns showed that single phase crystal samples of GDC/Yb_2O_3 is synthesized by comparison with the ICDD cards 00-075-0161 for 10GDC and 04-012-8055 for Yb_2O_3.

The XRD patterns of ytterbium products follow the same trend as of 10GDC, 10GDC/CeO_2 and 10GDC/Y_2O_3 samples. Also no impurity or additional phase lines belonging to Yb_2O_3 is observed in the XRD patterns of final product.

In Figure 3.27, there are some noise-like diffraction lines between 10-45 2theta values for product with 0.6 % ratio of ytterbium. Those lines may have occurred because the product including 0.6 % mole Yb_2O_3 was very little in amount so there could have been interference of XRD ring material we used to stick our samples on.

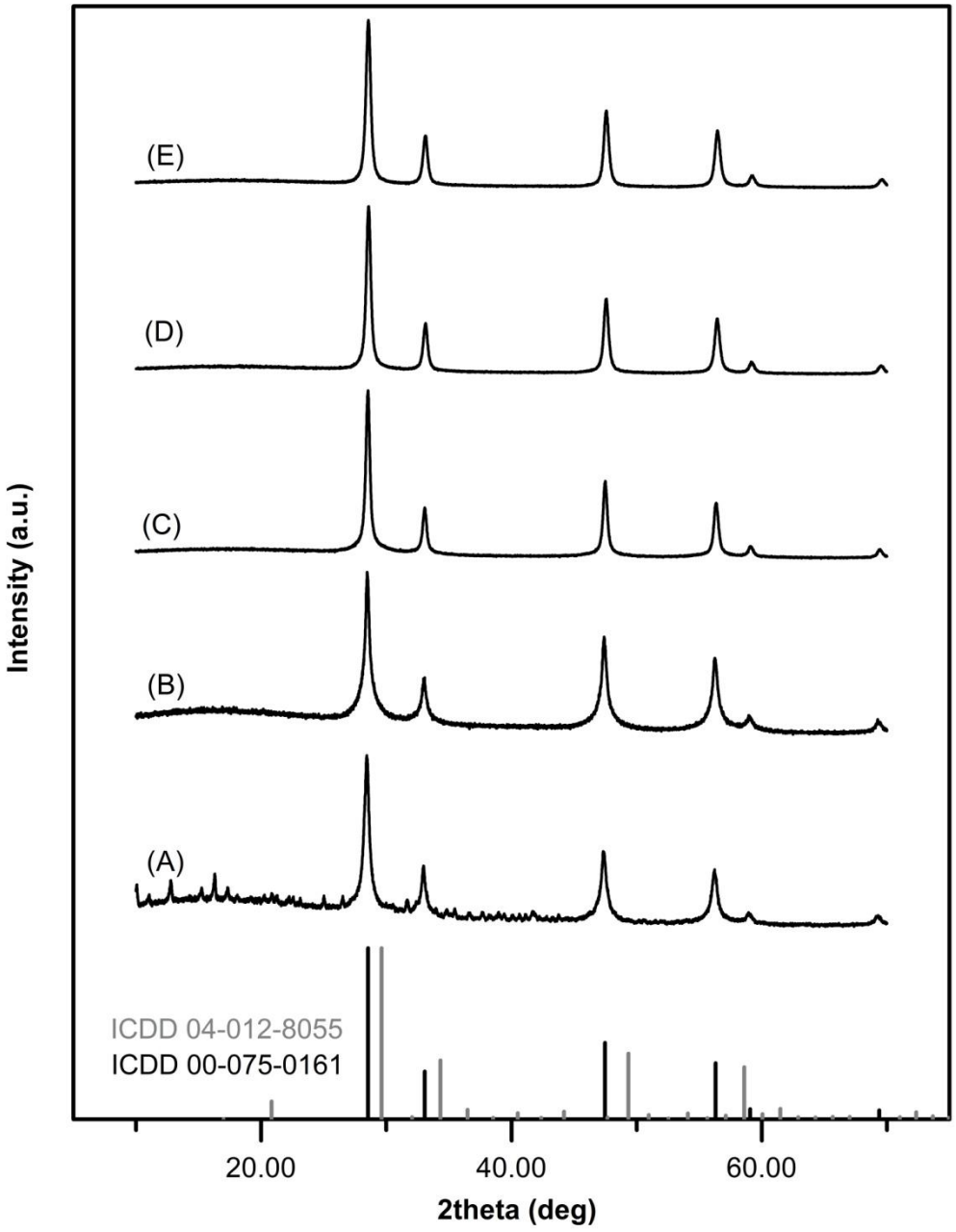

Figure 3.56 XRD Patterns of 10GDC/Yb_2O_3 composites with mol% amounts of Ytterbium as (A) 0.6%, (B) 2.5%, (C) 6.0%, (D) 9.2%, (E) 12.5% after self burning state, synthesized by Sol Gel Combustion Route, ICDD 00-075-0161 and ICDD 04-012-8055

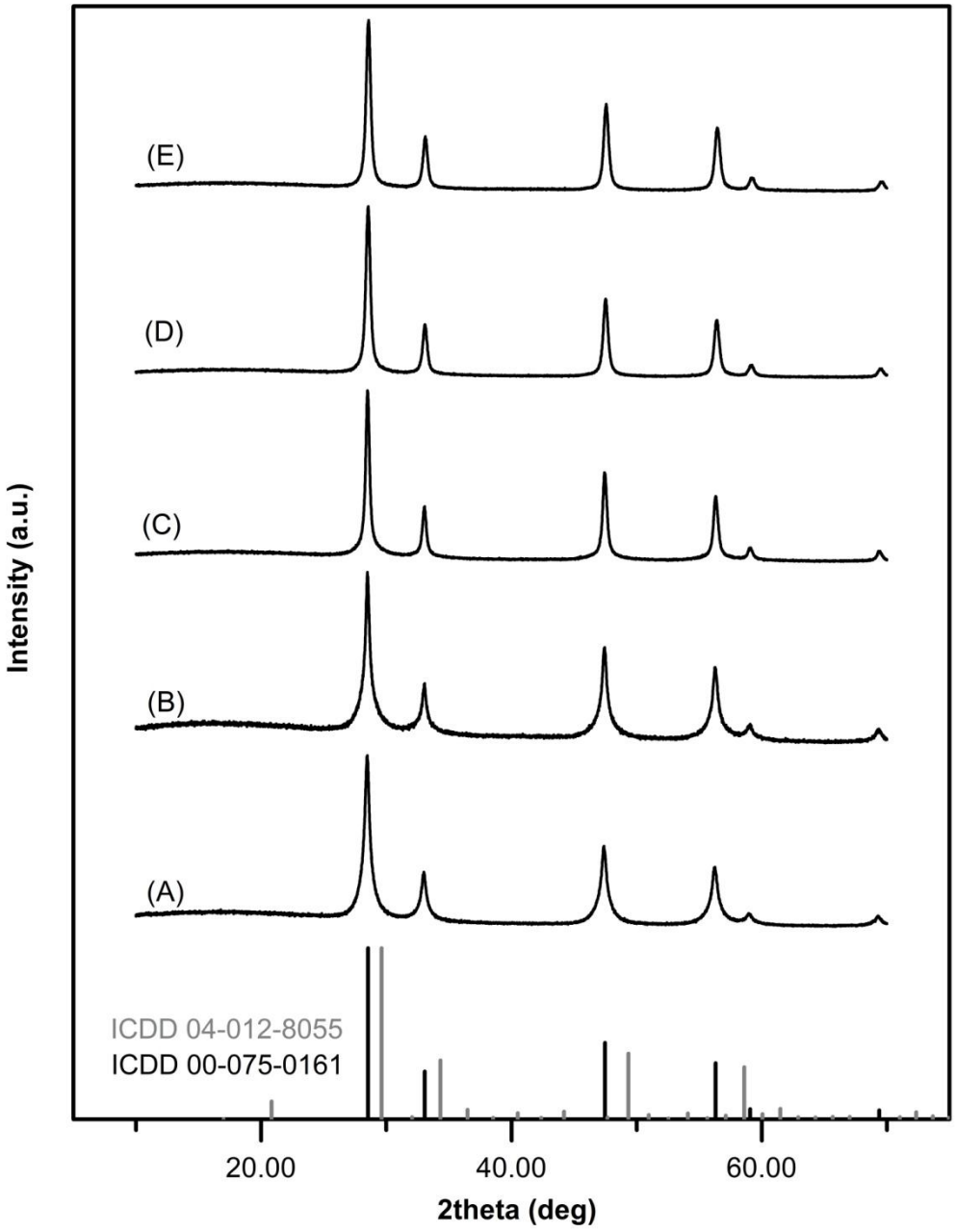

Figure 3.57 XRD Patterns of 10GDC/Yb_2O_3 composites with mol% amounts of Ytterbium as (A) 0.6%, (B) 2.5%, (C) 6.0%, (D) 9.2%, (E) 12.5% after heating at 300 ^oC, synthesized by Sol Gel Combustion Route, ICDD 00-075-0161 and ICDD 04-012-8055

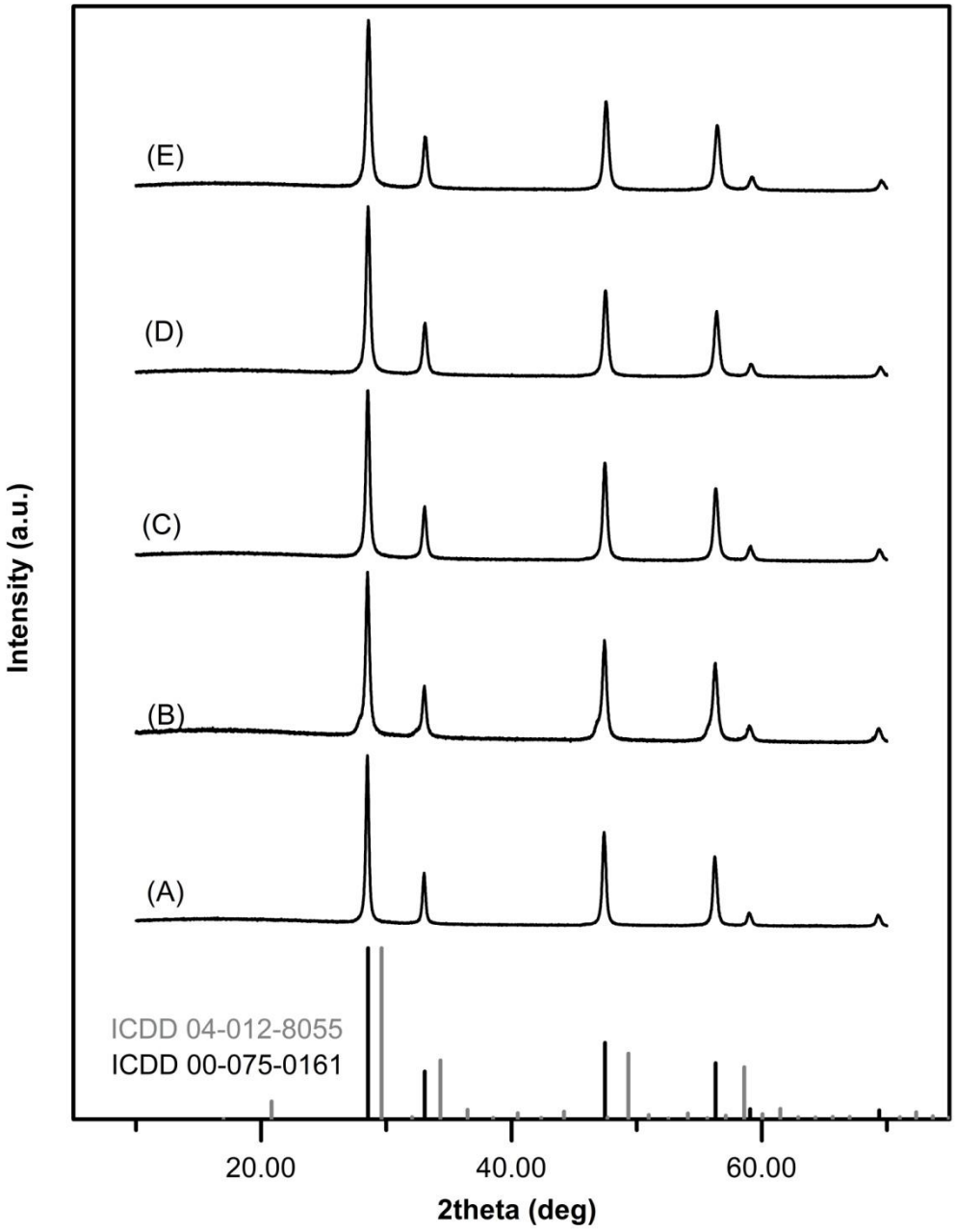

Figure 3.58 XRD Patterns of 10GDC/Yb_2O_3 composites with mol% amounts of Ytterbium as (A) 0.6%, (B) 2.5%, (C) 6.0%, (D) 9.2%, (E) 12.5% after heating at 800 ^oC, synthesized by Sol Gel Combustion Route, ICDD 00-075-0161 and ICDD 04-012-8055

3.2.4.2. SEM and EDX Analysis of 10GDC/Yb_2O_3 composites

The SEM images of 10GDC + 0.6% Yb_2O_3 at x100k and x50k magnifications heated at 800 ^oC and synthesized by sol gel combustion technique, is given in Figure 3.59. The images give information about the particle size and the morphology of the product. The pictures are very similar with the samples studied with 10GDC and 10GDC/Y_2O_3 products.

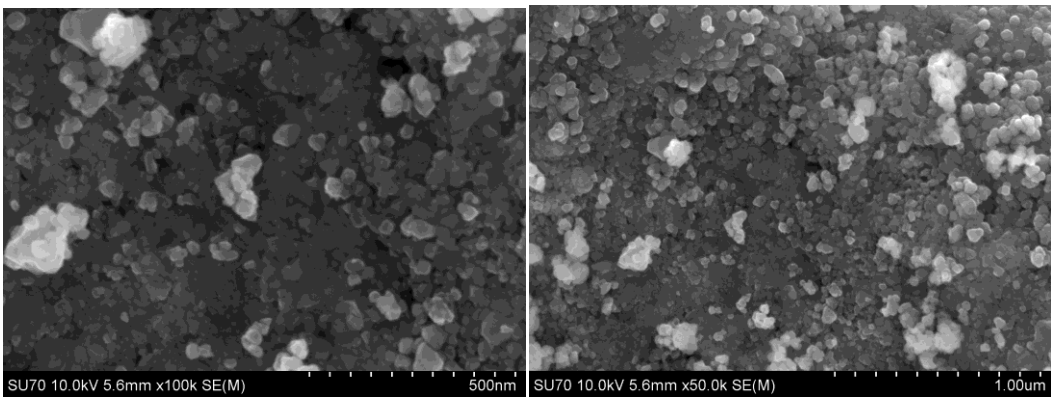

Figure 3.59 SEM images of 10GDC + 0.6% Yb_2O_3 heated at 800 ^oC with x100k and x50k magnifications

EDX analysis, shown in Figure 3.60, 3.61, and 3.62 shows that there is no impurity and it is in a good agreement with nominal compositions of elements. As the amount of Yb_2O_3 doping increases, ytterbium peak intensity increases.

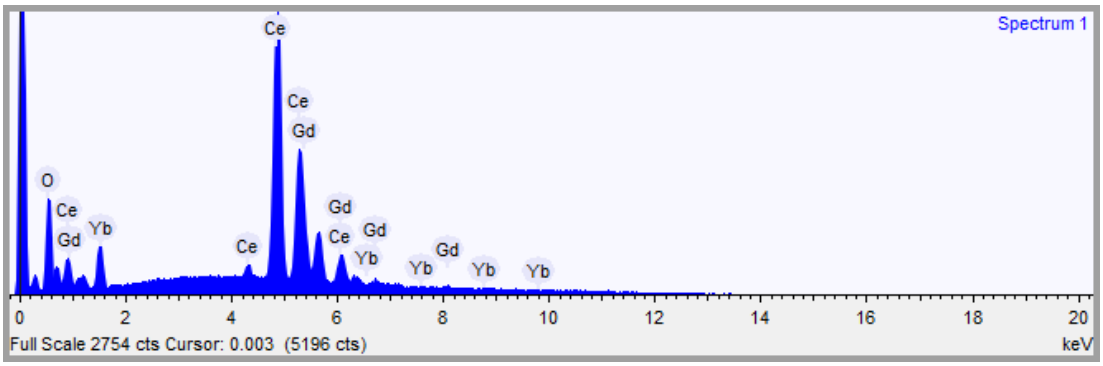

Figure 3.60 EDX spectrum of 10GDC + 0.6% Yb_2O_3

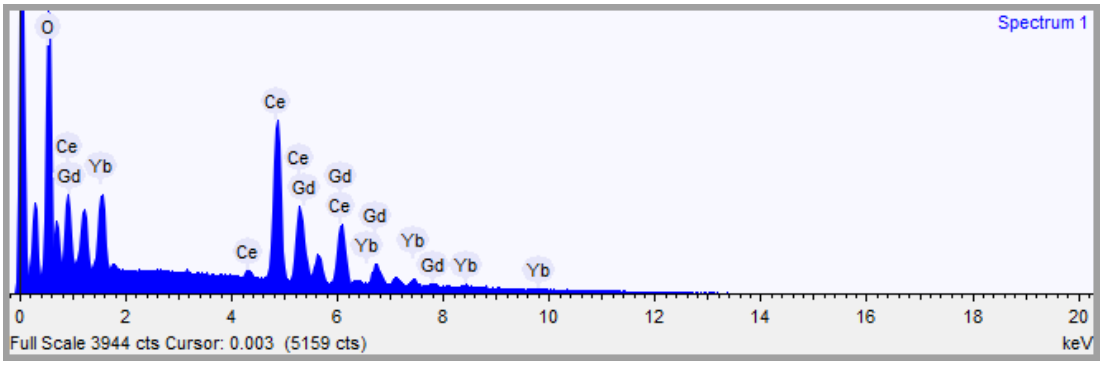

Figure 3.61 EDX spectrum of 10GDC + 6.0% Yb_2O_3

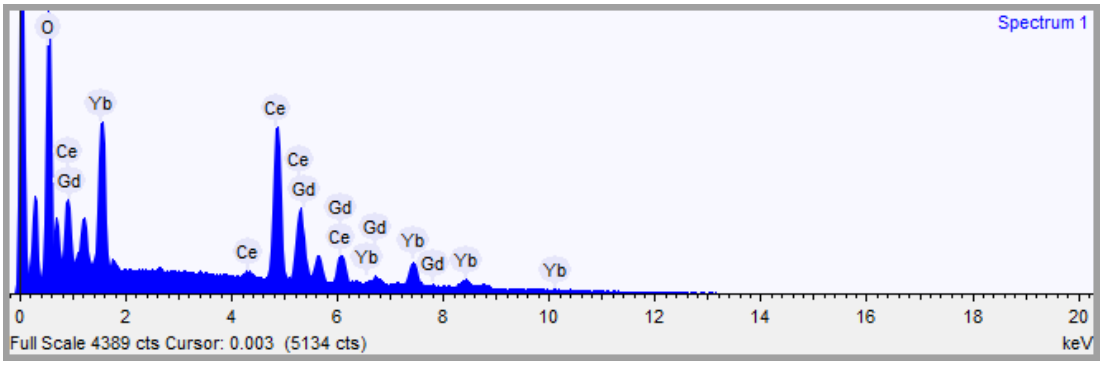

Figure 3.62 EDX spectrum of 10GDC + 12.5% Yb_2O_3

CHAPTER IV

GENERAL REVIEW AND CONCLUSION

This work covers firstly the synthesis of 10% gadolinia doped ceria (10GDC) with additional amounts of CeO_2, and 10GDC composites with Y_2O_3 and Yb_2O_3 via sol-gel combustion synthesis and solid state synthesis techniques, and secondly characterization of the products. Studying of XRD, IR, EDX and SEM of the products obtained in this study led to the following conclusions.

The XRD studies showed that single-phase crystals were obtained with sol-gel combustion synthesis independent on the amount of CeO_2, Y_2O_3 or Yb_2O_3. However, additional Gd_2O_3, Y_2O_3 and Yb_2O_3 phase lines were seen in XRD results of Solid State Synthesis Route products.

From the IR studies it is seen that initially there are bands of organic parts from ethylene glycol and NO_3^- from nitrates of metals. As the temperature rise, only the characteristic bands of GDC and metal oxide bonds remain, leading to the fact that the final products has no organic impurity after heating at 800 ^oC. Moreover, the IR spectra of sol-gel GDC products after heating at 800 ^oC and solid state synthesis products are identical.

SEM results showed that the morphology of particles does not depend on the heating temperature, nature and amount of metal oxide added. Products of sol-gel combustion route have mostly powder grains, concentrated in groups. Solid state

route products are mostly sharp-edged and mixtures of oxides. EDX results were in a good agreement with nominal compositions of elements.

REFERENCES

[1] Callister W. D., 1994, Material Science and Engineering: and introduction, Callister W. Jr., 3rd Ed.

[2] Askeland D.R., 2013, Essentials of Materials Science & Engineering, SI Edition, Cengage Learning

[3] Davis J.R., 1992, ASM Materials Engineering Dictionary, ASM International, 555, 69

[4] Bovey F., 2012, Macromolecules: An Introduction to Polymer Science, Elsevier, 566, 2

[5] Campbell F.C., 2010, Structural Composite Materials

[6] Weissbart J., Ruka R., 1962, "A Solid Electrolyte Fuel Cell," Journal of the Electrochemical Society, 109, 723

[7] Kordesch K.V., Oliveira J.C.T., 1989, Ullmann's Encyclopedia of Industrial Chemistry, 5th Edition, VCH, Vol. A 12, 55

[8] http://www.fz-juelich.de

[9] Aparicio M., Jitianu A., Klein L.C., 2012, Sol-Gel Processing for Conventional and Alternative Energy, 2, 20

[10] Besikiotis V., 2008, Master of Science Thesis, Development of Gadolinia Doped Ceria Electrolyte for IT-SOFC

[11] Winter M., Brodd R.J., 2004, What are batteries, fuel cells, and supercapacitors?, Chemical Reviews, 104, 4260

[12] Ehsani M., Gao Y., Gay S.E., Emadi A., 2005, Modern Electric, Hybrid Electric and Fuel Cell Vehicles, Fundamentals, Theory and Design. CRC Press

[13] Minh N.Q., 1991, High Temperature Fuel Cells, Part 2: The Fuel Cells, Chemtech, 21, 120

[14] Minh N.Q., 1993, Ceramic Fuel Cells, Journal of American Ceramic Society, 76, 563

[15] Spivey B. and Edgar T.F., 2010 Dynamic Modeling of Reliability Indicators in Solid Oxide Fuel Cells and Implications for Advanced Control, AIChE Fall Annual Meeting, Salt Lake City, Utah

[16] Boukamp B.A., 2003, Nature Materials, 2, 294

[17] Rorh F.J., Hagenmuller P., Van Gool W. (Eds.), 1978, Solid Electrolytes, Academic Press, New York, 431

[18] Rohr F.J., Isaacs H.S., Srinivasan S., Harry I.L. (Eds.), 1978, Proceedings of the Workshop on High Temperature Solid Oxide Fuel Cells, Brookhaven National Laboratory, NY, 122

[19] Burkin A.R., Saricimen H., Steele B.C.H., 1980, Preparation of Yttria Stabilized Zirconia (YSZ) Powders by High Temperature Hydrolysis (Hth), Transactions and Journal of the British Ceramic Society, 79, 105

[20] Clearfield A., Serrette G.P.D., Khazi-Syed A.H., 1994, Nature of hydrous zirconia and sulfated hydrous zirconia, Catalysis Today, 20, 295

[21] Agarwal V., Liu M., 1996, Colloidal Processing of $BaCeO_3$-Based Electrolyte Films, Journal of the Electrochemical Society 143, 3239

[22] Lin H.L., Chiang R.K., Kuo C.L., Chang C.W., 2007, Synthesis of BaCeO3 powders by a fast aqueous citrate-nitrate process, Journal of Non-Crystalline Solids, 353, 1188

[23] Takahashi T., Iwahara H., 1978, Oxide ion conductors based on bismuthsesquioxide, Materials Research Bulletin, 13, 1447

[24] Tuller H.L., Nowick A.S., 1979, Defect Structure and Electrical Properties of Nonstoichiometric CeO_2 Single Crystals, Journal of the Electrochemical Society, 126, 209

[25] Hung W., Shuk P., Greenblatt M., 1997, Properties of sol-gel prepared $Ce_{1-x}Sm_xO_{2-x/2}$ solid electrolytes, Solid State Ionics, 100, 23

[26] Chang E.K., Blumenthal R.N., 1988, The nonstoichiometric defect structure and transport properties of CeO_{2-x} in the near-stoichiometric composition range, Journal of Solid State Chemistry, 72, 330

[27] Ruiz-Trejo E., Santoyo-Salazar J., Vilchis-Morales R., Benitez-Rico A., Gomez-Garcia F., Flores-Morales C., Chavez-Carvayar J., Tavizon G., 2007, Microstructure

and electrical transport in nano-grain sized $Ce_{0.9}Gd_{0.1}O_{2-\delta}$ ceramics, Journal of Solid State Chemistry, 180, 3093

[28] Etsell T.H., Flengas S.N., 1970, Electrical Properties of Solid Oxide Electrolytes, Chemical Reviews, 70, 339

[29] Dirstine R.T., Blumenthal R.N., Kuech T.F., 1979, Ionic Conductivity of Calcia, Yttria, and Rare Earth-Doped Cerium Dioxide, Journal of the Electrochemical Society, 126, 264

[30] Steele B.C.H., 2000, Appraisal of $Ce_{1-y}Gd_yO_{2-y/2}$ electrolytes for IT-SOFC operation at 500 ^oC. Solid State Ionics, 129, 95

[31] Kingsley J.J., Pederson L.R., 1993, Energetic Materials in Ceramics Synthesis, Materials Research Society Symposium, 296, 361

[32] Smart L.E., Moore E.A., 2005, Solid State Chemistry "An Introduction", 3rd Edition, CRC Taylor and Francis Group

[33] McKittrick J., Shea L.E., Bacalski C.F., Bosze E.J., 1999, The influence of processing parameters on luminescent oxides produced by combustion synthesis, Displays, 19, 169

[34] Garzon F.H., Mukundan R., Brosha E.L., 2000, Solid-state mixed potential gas sensors: theory, experiments and challenges, Solid State Ionics, 13, 6–137 633-638

[35] Trovarelli A., 2002, Catalysis by Ceria and Related Materials, Catalytic Science Series, Imperial College Press: London, Vol. 2

[36] Tye L., El-Masry N.A., Chikyow T., McLarty P., Bedair S.M., 1994, Electrical characteristics of epitaxial CeO_2 on Si (1 1 1), Applied Physics Letters, 65, 3081

[37] Van Herle J. et al., 1996, Low temperature fabrication of (Y, Gd, Sm)-doped ceria electrolyte, Solid State Ionics, 86–88, 1255

[38] Desroches M.J., Castillo I.A., Munz R.J., 2005, Determination of particle size distribution by laser diffraction of doped-CeO2 powder suspensions: effect of suspension stability and sonication, The Particle and Particle Systems Characterization Journal, 22, 310

[39] Chung D.Y., E.H. Lee, 2004, Microwave-induced combustion synthesis of $Ce_{1-x}Sm_xO_{2-x/2}$ powder and its characterization, Journal of Alloys and Compounds, 374, 69

[40] Mogensen M., Sammes N.M., Tompsett G.A., 2000, Physical, chemical and electrochemical properties of pure and doped ceria, Solid State Ionics, 129, 63

[41] Minh N.Q., 1993, Ceramic fuel cells, Journal of American Ceramic Society, 76, 563

[42] Chourashiya M., Patil J., Pawar S., Jadhav L., 2008, Studies on structural, morphological and electrical properties of $Ce_{1-x}Gd_xO_{2-(x/2)}$, Materials Chemistry and Physics, 109, 39

[43] Zha S., Xia C., and Meng G., 2003, Effect of Gd (Sm) doping on properties of ceria electrolyte for solid oxide fuel cells, Journal of Power Sources, 115, 44

[44] Wang F.Y., Wan B.Z., Cheng S., 2005, Study on Gd^{3+} and Sm^{3+} co-doped ceria based electrolytes, Journal of Solid State Electrochemistry, 9, 168

[45] Guan X., Zhou H., Liu Z., Wang Y., Zhang J., 2008, High performance Gd^{3+} and Y^{3+} co-doped ceria-based electrolytes for intermediate temperature solid oxide fuel cells, Materials Research Bulletin, 43, 1046

[46] Ivanov V., Khrustov V., Kotov Y., Medvedev A., Murzakaev A., Shkerin S., and Nikonov A., 2007, Conductivity and structure features of $Ce_{1-x}Gd_xO_{2-x/2}$ solid electrolytes fabricated by compaction and sintering of weakly agglomerated nanopowders, Journal of the European Ceramic Society, 27, 1041

[47] Kudo T., Obayashi H., 1976, Mixed electrical conduction in the fluorite-type $Ce_{1-x}Gd_xO_{2-x/2}$, Journal of The Electrochemical Society, 123, 415

[48] Peng C., Zhang Z., 2007, Nitrate-citrate combustion synthesis of $Ce_{1-x}Gd_xO_{2-x/2}$ powder and its characterization, Ceramics International, 33, 1133

[49] Tianshu Z., Hing P., Huang H., Kilner J., 2002, Ionic conductivity in the CeO_2/Gd_2O_3 system ($0.05 \leq Gd/Ce \leq 0.4$) prepared by oxalate coprecipitation, Solid State Ionics, 148, 567

[50] Zhang T.S., Ma J., Kong L.B., Chan S.H., Kilner J., 2004, Aging behavior and ionic conductivity of ceria-based ceramics: a comparative study, Solid State Ionics, 170, 209

[51] Fu Y.P., Chang Y.S., and Wen S.B., 2006, Microwave-induced combustion synthesis and electrical conductivity of $Ce_{1-x}Gd_xO_{2-1/2x}$ ceramics, Materials Research Bulletin 41, 2260

[52] Kharton V.V., Figueiredo F.M., Navaro L., Naumovich E.N., Kovalevsky V., Yaremchenko A.A., Viskup A.P., Carneiro A., Marques F.M.B., Frade J.R., 2001, Ceria-based materials for solid oxide fuel cells, Journal of Materials Science, 36, 1105

[53] Ding C., Lin H., Sato K., Hashida T., 2009, Synthesis of NiO–$Ce_{0.9}Gd_{0.1}O_{1.95}$ nanocomposite powders, Scripta Materialia, 60, 254

[54] Li B., X Wei., Pan W., 2009, Synthesis of doped ceria–zirconia core–shell nanocomposites via sol–gel process, Journal of Power Sources, 193, 598

[55] Van Herle J., Horita T., Kawada T., Sakai N., Yokokawa H., Dokiya M., 1998, Oxalate Coprecipitation of Doped Ceria Powder for Tape Casting for low-temperature solid oxide fuel cell anodes by co-precipitation, Ceramics International, 24, 229

[56] Tok A.I.Y., Luo L.H., Boey F.Y.C., 2004, Carbonate co-precipitation of Gd_2O_3 doped CeO_2 solid solution nano-particles, Materials Science and Engineering, 383, 229

[57] Fu Y.P., Wen S.B., Lu C.H., 2008, Preparation and characterization of Samaria-doped Ceria Electrolyte materials for solid oxide fuel cells, Journal of the American Ceramic Society, 91, 127

[58] Higashi K., Sonoda K., Ono H., Sameshima S., Hirata Y., 1999, Synthesis and sintering of rare-earth-doped ceria powder by the oxalate coprecipitation method, Journal of Materials Research, 14, 957

[59] Dikmen S., Shuk P., Greenblatt M., Gocmez H., 2002, Hydrothermal synthesis and properties of $Ce_{1-x}Gd_xO_{2-\delta}$ solid solutions, Solid State Sciences, 4, 585

[60] Yamashita K., Ramanujachary K.V., Greenblatt M., 1995, Hydrothermal synthesis and low temperature conduction properties of substituted ceria ceramics, Solid State Ionics, 81, 60

[61] Sin A., Dubitsky Y., Zaopo A., Aricò A.S., Gullo L., La Rosa D., Siracusano S., Antonucci V., Oliva C., Ballabio O., 2004, Preparation and sintering of $Ce_{1-x}Gd_xO_{2-x/2}$ nanopowders and their electrochemical and EPR characterization, Solid State Ionics, 175, 361

[62] Prasad D. H., Son J.W., Kim B.K., Lee H.W., Lee J.H., 2008, Synthesis of nano-crystalline $Ce_{0.9}Gd_{0.1}O_{1.95}$ electrolyte by novel sol–gel thermolysis process for IT-SOFCs, Journal of the European Ceramic Society, 28, 3107

[63] Jadhav L.D., Chourashiya M.G., Subhedar K.M., Tyagi A.K., Patil J.Y., 2009, Synthesis of nanocrystalline Gd doped ceria by combustion technique, Journal of Alloys and Compounds, 470, 383

[64] Xia C., Liu M., 2002, Microstructures, conductivities, and electrochemical properties of $Ce_{0.9}Gd_{0.1}O_2$ and GDC–Ni anodes for low-temperature SOFCs, Solid State Ionics, 152– 153, 423– 430

[65] Akbari-Fakhrabadi A., Avila R. E., Carrasco H. E., Ananthakumar S., Mangalaraja R.V., 2012, Combustion synthesis of NiO–$Ce_{0.9}Gd_{0.1}O_{1.95}$ nanocomposite anode and its electrical characteristics of semi-cell configured SOFC assembly, Journal of Alloys and Compounds, 541, 1

[66] Mahata T., Das G., Mishra R.K., Sharma B.P., 2005, Combustion synthesis of gadolinia doped ceria, Journal of Alloys and Compounds, 391, 129

[67] Arabacı A., Öksüzömer M.F., 2012, Preparation and characterization of 10mol% Gd doped CeO_2 (GDC) electrolyte for SOFC applications, Ceramics International, 38, 6509

[68] Xia C., Chen F., Liu M., 2001, Electrochemical and Solid-State Letters, Reduced-Temperature Solid Oxide Fuel Cells Fabricated by Screen Printing, 4, A52

[69] Xia C., Liu M., 2001, Low-temperature SOFCs based on $Gd_{0.1}Ce_{0.9}O_{1.95}$ fabricated by dry pressing, Solid State Ionics, 144, 249

[70] Xia C., Liu M., 2001, Journal of the American Ceramic Society, A Simple and Cost-Effective Approach to Fabrication of Dense Ceramic Membranes on Porous Substrates, 84, 1903

[71] Wandekar R.V., Basu M.A., Wani B.N., Bharadwaj S.R., 2006, Physicochemical studies of NiO–GDC composites, Materials Chemistry and Physics, 99, 289

[72] Zha S., Rauch W., Liu M., 2004, Ni-$Ce_{0.9}Gd_{0.1}O_{1.95}$ anode for GDC electrolyte-based low-temperature SOFCs, Solid State Ionics, 166, 241

[73] Ayawanna J., Wattanasiriwech D., Wattanasiriwech S., Sato K., 2013, Electrochemical Performance of $Ni_{1-x}Co_x$-GDC Cermet Anodes for SOFCs, Energy Procedia, 34, 439

[74] Liang B., Suzuki T., Hamamoto K., Yamaguchi T., Sumi H., Fujishiro Y., Ingram B.J., Carter J.D., 2012, Performance of Ni–Fe/gadolinium-doped CeO_2 anode

supported tubular solid oxide fuel cells using steam reforming of methane, Journal of Power Sources, 202, 225

[75] Gansor P., Sabolsky K., Zondlo J.W., Sabolsky E.M., 2013, $Sr_2MgMoO_{6-\delta}/Gd_{0.1}Ce_{0.9}O_{1.95}$ composite anode-supported solid oxide fuel cell (SOFC), Materials Letters, 105, 80

[76] Liu Y., Wang F., Chi B., Pu J., Jian L., Jiang S. P., 2013, A stability study of impregnated LSCF–GDC composite cathodes of solid oxide fuel cells, Journal of Alloys and Compounds, 578, 37

[77] Ko H.J., Myung J., Hyun S., Chung J.S., 2012, Synthesis of LSM–YSZ–GDC dual composite SOFC cathodes for high-performance power-generation systems, Journal of Applied Electrochemistry, 42, 209

[78] Yang S., Jang K., Kim W., Choi H., 2012, The Evaluation of Ca Doped GDC Electrolyte Thin Film for Solid Oxide Fuel Cells by Electron Beam Deposition, Molecular Crystals and Liquid Crystals, 568, 145

[79] Li B., Liu S., Liu X., Hao G., Wang H., Su W., 2013, Study on GDC-LSGM composite electrolytes for intermediate-temperature solid oxide fuel cells, International Journal of Hydrogen Energy, 38, 11392

[80] Su Q., Yoon D., Chen A., Khatkhatay F., Manthiram A., Wang H., 2013, Vertically aligned nanocomposite electrolytes with superior out-of-plane ionic conductivity for solid oxide fuel cells, Journal of Power Sources, 242, 455

[81] Banwell C.N., 1966, Fundamentals of Molecular Spectroscopy, Ch 3

[82] Shastri V.P., Altankov G., 2010, Advances in Regenerative Medicine: Role of Nanotechnology, and Engineering Principles, 329

[83] Coates J., 2000, Interpretation of Infrared Spectra, A Practical Approach, in Encyclopedia of Analytical Chemistry, 10815

[84] Sheibley D.W., Fowler M.H., 1966, Infrared Spectra of Various Metal Oxides in the Region of 2 to 26 Microns